SYNTHESIS OF AND CONFORMATIONAL STUDIES ON PROLINE-CONTAINING PEPTIDES: ION-BINDING BY LINEAR TETRAPEPTIDES

PETER HUGO REHSE

Synthesis of and Conformational Studies on Proline-Containing Peptides:

Ion-Binding by Linear Tetrapeptides

BY

© Peter Hugo Rehse, B.Sc.(Hons.)

A thesis submitted to the School of Graduate Studies in partial fulfillment of the requirements for the degree of Master of Science

Department of Biochemistry
Memorial University of Newfoundland

December 1985

St. John's Newfoundland

ISBN 0-315-33627-7

Abstract

The relationship between peptide backbone topology and ion-binding was investigated through proton and carbon-13 NMR, CD and IR spectroscopy. A literature review on calcium-binding proteins and peptides indicated that a structure characterized by two overlapping β-turns may be involved. To test this hypothesis two peptides which could potentially form the above structure were synthesized.

The peptides N^{α}*t*BocProDAlaAlaNHCH$_3$ and its glycine analogue N^{α}*t*BocProGlyAlaNHCH$_3$ were characterized in the uncomplexed state by all of the above mentioned techniques in a variety of solvents. Proton NMR temperature-dependence studies in DMSO-d$_6$ and NH coupling constants, along with CD and IR spectroscopy indicated that both peptides in solution were made up of a Type II β-turn followed by an overlapping Type I' β-turn. Carbon-13 NMR, IR and CD spectroscopy indicated that the DAla-peptide was, as expected, more stable than the Gly-peptide.

The binding of metal ions to the peptides was monitored using CD spectroscopy. Both peptides were found to be ion-specific. While both were capable of binding calcium ion and incapable of binding sodium and lithium to any significant extent, they differed in their ability to bind magnesium. While the N^{α}*t*BocProDAlaAlaNHCH$_3$ peptide bound magnesium weakly at a level comparable to its binding to the monovalent ions, the glycine analogue bound magnesium to a significant extent. The Gly-peptide also required a lower concentration of calcium ion to reach binding saturation. This was attributed to the greater flexibilty of glycine and hence, its enhanced ability to "fit" the metal ion.

The conformational change of the peptides upon calcium ion titration was followed by proton and carbon-13 NMR. The changes in chemical shifts of the carbonyl resonances and the amide proton resonances indicated that all four peptide carbonyls coordinated to the calcium ion resulting in a breaking of the *intra*molecular hydrogen bonds of the uncomplexed species. Analyses of the CD binding-curves indicated that at low concentrations of calcium to peptide a 2:1 peptide:ion complex was formed, while at higher concentrations a 1:1 complex was predominant. The 2:1 peptide:ion complex is able to fill all eight calcium coordination sites with the peptide carbonyls while the 1:1 complex requires either the perchlorate anion or water molecule to fill the remaining coordination sites.

Acknowledgements

Special thanks to my supervisor, Professor V.S. Ananthanarayanan; the other members of my supervisory committee, Drs. William S. Davidson and Brian Gregory; and also to Dr. Samual K. Attah-Poku for his patient instruction in peptide synthesis and NMR interpretation. Their assistance and friendship provided an ideal environment for the pursuit of a graduate degree.

I would like to extend my appreciation to Dr. Hooper and Bruce McDonald of the Atlantic Region Magnetic Resonance Centre, Halifax, Nova Scotia, for running the NMR analysis and also to Dr. Sastri for performining the Binding Constant analysis.

Many thanks to Mr. Lorne Taylor for his critical perusal of the thesis during production.

This research was supported by a grant from the Medical Research Council of Canada.

"Conformation is Information"

Table of Contents

List of Tables

List of Figures

Abbreviations

Acn	acetonitrile
Aib	α-aminoisobutyric acid
Ala	alanine
Asn	asparagine
Asp	aspartic acid
Bu	butyl
$CHCl_3$	chloroform
CD	Circular Dichroism
$CDCl_3$	deuterated chloroform
Cys	cysteine
DAla	D-alanine
DCC	dicyclohexylcarbodimide
DCU	dicyclohexylurea
DMSO	dimethylsulphoxide
DPhe	D-phenylalanine
EDTA	ethylenediaminetetraacetic acid
Gly	glycine
GuHCl	guanidine hydrochloride
Hz	hertz
Ile	isoleucine
ipr	isopropyl
HPLC	High Performance Liquid Chromatography
IR	Infrared
Leu	leucine
MCBP	Muscle Calcium-Binding Parvalbumin
MeOH	methanol
Nle	norleucine
NMR	Nuclear Magnetic Resonance
NSU	N-hydroxy succinimide
OEt	OCH_2CH_3
Phe	phenylalanine
Piv	pivotyl
Pro	proline
Sar	N-methylglycine
tBoc	*tertiary*-Butoxycarbonyl

TFE	trifluoroethanol
THF	tetrahydrofuran
Trp	tryptophan
Tyr	tyrosine
UV	Ultraviolet

Chapter 1

Introduction

As an increasing number of protein three-dimensional structures are solved by X-ray crystallography, a strong correlation between function and the overall topology of the protein molecule is becoming obvious. The topology is dependent on the folding patterns of the molecule and can be classified in terms of different types of sub-structure. The simplest structural arrangements beyond the covalent interaction of the primary structure (or amino acid sequence) are the so-called secondary structures such as the α-helix, β-structure and the β-turn. The specific arrangement of these structures within a functional domain of a protein (supersecondary structure) correlates very well with the functional role of that domain. For example, the heme binding domain is characterized by four α-helices folded back on themselves. The relationship between structure and function continues to manifest itself at the level of the completely folded (tertiary) structure and the association of individual protein subunits in the quaternary structure (Creighton, 1983).

The β-turn is a secondary strucural feature pervasive throughout globular proteins. On an average, about 30 percent of the secondary structure of all globular proteins is made up of the β-turn. The β-turn is characterized by a

reversal of nearly 180° in the direction of a peptide chain and is stabilized by an *intra*molecular hydrogen bond between the carbonyl (C=O) of residue (*i*) and the amide (N-H) of residue (*i*+3) (Zimmerman and Scheraga, 1977; Crawford *et al.*, 1973; Smith and Pease, 1980). By reversing the direction of the polypeptide chain, the β-turn provides a useful device which enables the more periodic and repetitive secondary structures to fold into their final supersecondary and tertiary structures (Sibanda and Thornton, 1985). Although this effect can be achieved by a "random coil", the ability of the β-turn to form a hydrogen bond acts as a "driving force". The β-turn has been implicated as a site of nucleation in protein folding (Ptitsyn, 1981). Since its formal definition by Venkatachalam in 1968, a considerable amount of effort has been expended to determine the structural characteristics of the various β-turn types in both proteins and peptides. In recent years, several functional roles have been investigated. I will summarize below the relevant data on β-turns and related areas which would form a useful basis for the studies described in this thesis.

1.1. Structural Characteristics of the Beta-Turn

1.1.1. Definitions and Nomenclature

The β-turn, like other secondary structures, can be defined by a set of dihedral angles that describe the conformation of the peptide backbone. A dihedral angle is defined as follows: if a system of four atoms A-B-C-D is projected onto a plane normal to bond B-C, the angle between the projection of A-B and the projection of C-D is described as the dihedral angle. The dihedral angle is considered positive or negative according to whether, when the system is viewed along the

central bond B → C (or C → B), the bond to the front atom A (or D) is rotated to the right or to the left, respectively, in order that it may eclipse the bond to the rear atom D (or A) (CRC Handbook of Biochemistry and Molecular Biology, 1976). Figure 1-1 defines the dihedral angle and demonstrates the 0° and 180° positions of both the Φ and the Ψ angles which correspond, respectively, to the rotations about the N-C^{α} and C^{α}-C' bonds. The dihedral angle ω refers to the rotation about the peptide (N-C') bond which is given a value of 180° (*trans* conformation) in defining the various β-turn types although slight deviations from planarity do occur (Ramachandran *et al.*, 1973).

The β-turn was originally classified into three main types (I, II and III) and their mirror images (I', II' and III') based on the Φ,Ψ angles of the corner residues $(i+1)$ and $(i+2)$ (see Table 1-1) (Venkatachalam, 1968). Venkatachalam's (1968) classification system was derived from theoretical calculations based on a linked three-peptide unit (C_1^{α} to C_4^{α} and the ability to form a 4 → 1 hydrogen bond. The peptide bond between residues $(i+1)$ and $(i+2)$ of Types I and II differ by approximately 180°. The Type III is similar to the conformation of the Type I, the former being the beginning of a 3_{10}-helix. The mirror images refered to by the prime (') differ from their roots by a sign change. Hence the $\Phi_{(i+1)}$ of a Type I β-turn is -60° while that of Type I' is +60°. A diagram of the β-turn (in the Type I and Type II forms) is shown in Figure 1-2 along with the notations used for Φ,Ψ angles of the respective amino acid residues.

In 1973, Chandrasekaran *et al.* correlated theoretical studies with experimental data and produced a range notation (see Table 1-2). The experimental data

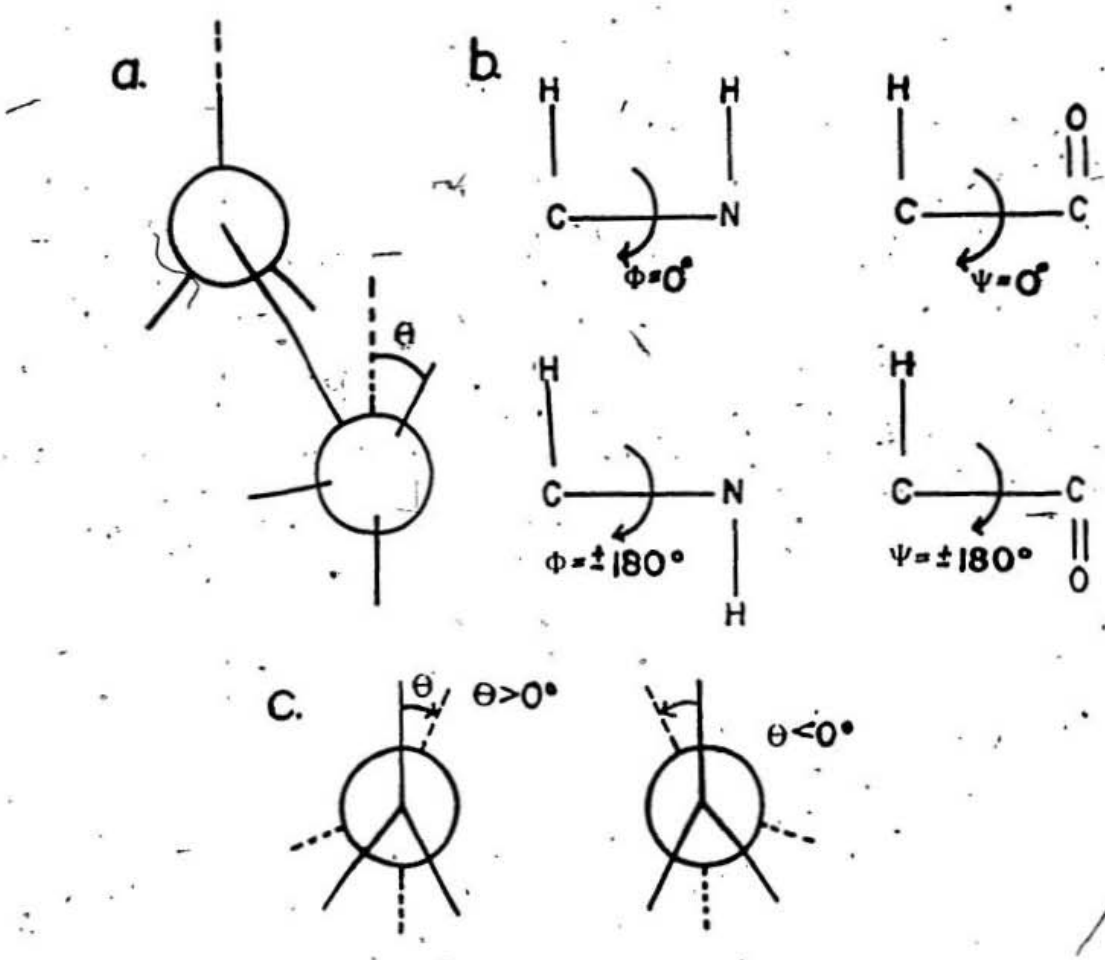

Figure 1-1: Dihedral Angles

Table 1-1: β-Turn Types as Defined by Venkatachalam (1968) and Lewis *et al.* (1973)

Type	$\Phi_{(i+1)}$	$\Psi_{(i+1)}$	$\Phi_{(i+2)}$	$\Psi_{(i+2)}$
I	-60°	-30°	-90°	0°
I'	60°	30°	90°	0°
II	-60°	120°	80°	0°
II'	60°	-120°	-80°	0°
III	-60°	-30°	-60°	-30°
III'	60°	30°	60°	30°
IV	exists when two or more of the angles of Types I through III' differ by at least 40° from any of the values listed above.			
V	-80°	80°	80°	-80°
V'	80°	-80°	-80°	80°
VI	contains a *cis* proline at position $(i+2)$			
VII	a kink in the protein chain created by $\Psi_{(i+1)} \approx 180°$ and $\lvert\Phi_{(i+2)}\rvert < 60°$ or $\lvert\Psi_{(i+1)}\rvert < 60°$ and $\Phi_{(i+2)} \approx 180°$			

Types IV through VII are from the expanded definition of Lewis *et al.*, 1973.

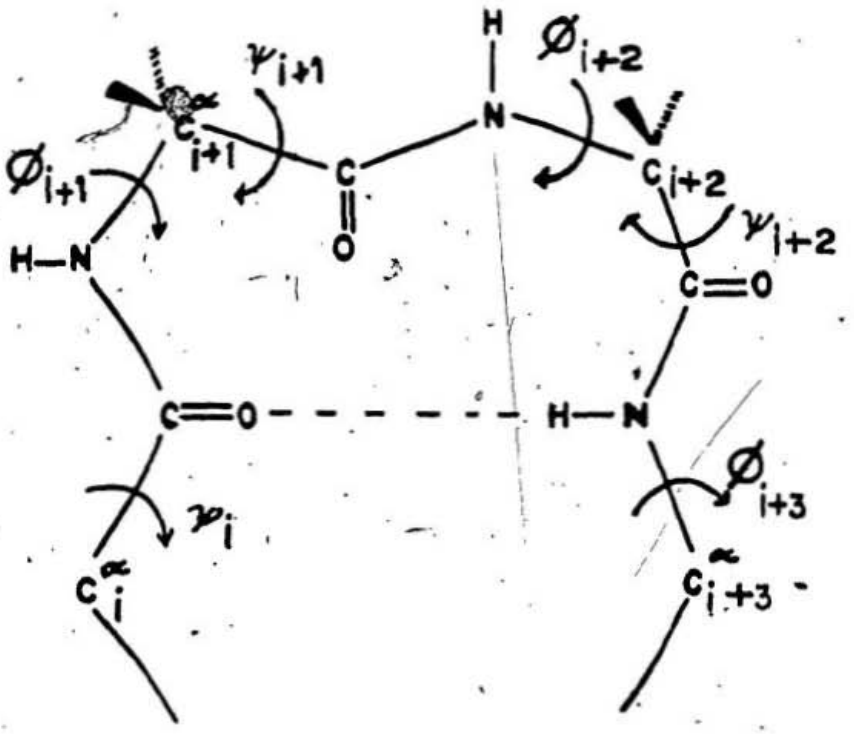

Figure 1-2: Geometry of the β-Turn

Table 1-2: ϕ,ψ Ranges of β-Turns as Defined by Chandrasekaran *et al.* (1973)

A	B	$\phi_{(i+1)}$	ψ_{i+1}	$\phi_{(i+2)}$	$\psi_{(i+2)}$
Ia	I	(-80)-(-20)°	(-90)-(-10)°	(-150)-(70)°	10-80°
Ib	II	(-80)-(-30)°	80-140°	20-80°	10-70°
IIa	I′	20-80°	10-90°	70-150°	(-80)-(-10)°
IIb	II′	30-80°	(-160)-(-70)°	(-80)-(-20)°	(-70)-(-10)°
III	II	(-90)-(-30)°	70-160°	30-170°	(-70)-80°
IV	II′	30-90°	(-160)-(-70)°	(-170)-(-30)°	(-80)-70°

A = Type as notated by Chandrasekaran *et al.*
B = Corresponding Type as defined by Venkatachalam

were based on the crystallographic structures of lysozyme, chymotrypsin and a series of peptides, and on the NMR profiles of several cyclic peptides. The following month, in the same journal, Lewis *et al.* (1973) produced a more extensive list of β-turns occurring in proteins. They examined the crystal structure of eight proteins and identified "β-bends" as structures where the distance between the α-carbons of the ith and $(i+3)$th residues was $\leq$ 7 Å. Since the definitions are based upon distance rather than on the existence of a hydrogen bond, the term "bend" was used by these authors rather than "turn". They differentiated the β-bends from α-helices by requiring the α-helices to have four or more consecutive $R_{i,(i+3)}$ α-carbon distances of $<$ 6 Å. Using the above criteria, they identified 135 β-bends. From the above data and the energy minimization calculations on a number of peptides, they expanded the β-turn notation of Venkatachalam (1968) from six to eleven (see Table 1-1). The dihedral angles of Types I through III' as originally proposed by Venkatachalam (1968) were retained. These "bends" were allowed to have one dihedral angle differing from the "ideal" value by up to 50° and still maintain its designation even if there was no *intra*molecular hydrogen-bonding. A Type IV bend occurred if two or more of the dihedral angles used to define β-turn types I through III' differed by more than 40° from the ideal. Type V was representative of a C_7 conformer or γ-turn (with an $i+2 \rightarrow i$ or $3 \rightarrow 1$ hydrogen bond) as opposed to the C_{10} β-turn which has an $i+3 \rightarrow i$ or $4 \rightarrow 1$ hydrogen bond. The C_x notation refers to the number of atoms involved in the ring formed by the hydrogen-bonded reverse turn. Type V' was not observed by Lewis *et al.* (1973) however, they stated that it could theoretically exist. Type VI is produced by a *cis* proline

in position (i+2) and Type VII is effectively a "kink" in the protein chain. In addition to the C_7 and C_{10} conformers mentioned above, Lewis *et al.* (1973) refer to the existence of a C_5 conformer (2 → 1 hydrogen bond). The existence was based on the results of energy minimization calculations of N-acetyl,N'-methyl,AlaAlaAlaAlaAmide. The major consideration of the work of Lewis *et al.* (1973) and Chandrasekaran *et al.* (1973) is that there is a range of ϕ,ψ values for each of the various β-turn types.

In this thesis, the original ϕ,ψ angles and hydrogen-bonding requirement of Venkatachalam (1968) will be used. The notations of Lewis *et al.* (1973) and Chandrasekaran *et al.* (1973) along with the C_x notation will be referred to on occasion.

1.2. Positional Preference of Amino Acids in Beta-Turns

The β-turn, unlike more uniform structures such as α-helices and β-sheets, demonstrates a marked positional preference of amino acids adding another dimension to the maker/breaker approach used in the prediction of protein and peptide secondary structures. This preference was first recognized by Venkatachalam (1968) who pointed out that because of steric requirements the Type I β-turn tends to prefer the "LL" sequence and the Type II prefers the "LD" sequence. The notation refers to the particular amino acid enantiomers in positions (i+1) and (i+2) of the β-turn, respectively. This chiral preference would later be used to advantage in the synthesis of β-turn models (see section 1.3). Crawford *et al.* (1973), after a study of the crystal structure of 11 proteins, observed that aspartic acid seemed to be preferred in the first position, proline in

the second, asparagine in the third, and tryptophan in the fourth. They stated that the limited data pool (125 turns) was not enough for a definitive study. They also pointed out what appeared to be a variance of positional preference based on β-turn type.

In 1977, Chou and Fasman completed a much more extensive study using the atomic coordinates, as determined by x-ray crystallography, of 29 proteins. They discovered 459 β-turns as described by Lewis *et al.* (1973). The percent frequency of occurrence of each particular type is: Type I, 41.8; Type II, 15.2; Type III, 18.3, with the other types (I' through VII) occurring with much smaller frequencies. Type I is thus seen to be by far the most common followed by Type III and then Type II. The remaining β-turn types are relatively rare. As did Crawford *et al.* (1973), Chou and Fasman (1977) noticed a variation in the positional preference of amino acids based on β-turn type, but because of a limited data pool, they grouped the β-turns together. The most common amino acids were; position *i*, Asn (17%), Cys (17%), Asp (16%); position (*i*+1), Pro (33%), Ser (14%), Lys (13%); position (*i*+2), Asn (21%), Asp (20%), Gly (20%); and at position (*i*+3), Trp (19%), Gly (17%), Tyr (15%). Steric considerations are an important factor but it appears that there is also an inverse relationship between hydrophobicity and turn-forming potential. Chou and Fasman (1977) also examined the regions ± 4 residues to each side of the β-turn forming tetrapeptide and still noted positional preferences. It must be remembered that the above values are weighted towards what occurs for the most common β-turn type. By looking at the data on an individual β-turn basis certain statements can be made. The most common

(i+1),(i+2) sequence of the β-turn is ProGly. This sequence occurs most often for Type II followed by Type I and then III but never for any of the mirror images. This is most likely due to the sterically restrictive proline. Glycine with no side chain could act as either a D or L amino acid and therefore fit the LD configuration requirement of the Type II β-turn (Venkatachalam, 1968; Chandrasekaran, 1973). An interesting point is that several L-amino acids can also be found at the (i+2)th position of the Type II β-turn. Although these Type II β-turns are probably not ideal, the LD requirement is obviously an oversimplification. The LD requirement was based on the so-called Ramachandran plot of D and L alanine peptides (Ramachandran and Sasisekharan, 1968).

The positional preference of an amino acid depends upon the neighbouring residues. This was demonstrated by Ananthanarayanan *et al.* (1984) who searched the sequences of 34 globular proteins of known crystal structure for the tetrapeptide sequence Z-Pro-Y-X, which fixes proline as the (i+1)th residue. They compared their results with those of Chou and Fasman (1977) and noted that there were some major differences. For example, aromatic hydrophobic residues such as tryptophan and phenylalanine were found to have a relatively high occurrence at position i when proline was in position (i+1), while such hydrophobic residues are generally not preferred in this position in the Chou-Fasman (1977) analysis. Glycine, although one of the top three in overall occurrence at position (i+2) in the analysis of Chou and Fasman (1977), becomes by far the most predominant residue at this position when proline is at position

(*i*+1). The cause of many of these effects can be explained through the results of Schimmel and Flory (1968) who observed that the proline ring restricts the conformational space available to its immediate N-terminal neighbour. Further examination of β-turns with more than one residue fixed becomes difficult because of the limited pool of protein structural data.

1.3. Peptide Models for the Beta-Turn

The examination of β-turns in proteins has its limitations (see section 1.2). The use of peptide models can provide much more fundamental information since not only can one look at a simpler isolated system but the potential data pool can be increased over that available in proteins. A synthetic approach also has the added advantage of the possible addition of groups which do not normally occur in proteins. Amino acids such as β-alanine, N-methylglycine (Sar), α-aminobutyryl (Aib) and the D-enantiomeric amino acids provide unique steric restrictions which can be very useful in the study of peptide conformation.

1.3.1. Cyclic Peptides

Cyclic peptides have been widely used in the study of β-turns. These include oxytocin (Urry and Walter, 1971), its analogue [Pro^3,Gly^4]-oxytocin (Ballardin *et al.*, 1978) and wholly synthetic peptides (Torchia *et al.*, 1972; Blaha and Budesinsky, 1973; Kopple *et al.*, 1978; Pease and Watson, 1978; Nemethy *et al.*, 1981; Maxfield *et al.*, 1981). The major advantage of using cyclic peptides is also their major disadvantage. Cyclization restricts the conformational mobility of the peptide. Hence a β-turn would tend to remain in a particular definable configuration. Because of this, the cyclic peptide is not the best system for the

study of the relative stabilities of β-turns and the effect of neighbouring residues on that stability. Linear peptides are much more conducive to this type of study.

1.3.2. Linear Peptides

The proline-containing linear peptides have aroused the most interest in the study of β-turns for two reasons. Proline was found to be the most abundant residue at position (*i*+1) of the β-turn in proteins (Chou and Fasman, 1977, 1978) (see section 1.2) and through conformational energy calculations (Zimmerman and Scheraga, 1977; Zimmerman *et al.*, 1977) was shown to be limited to a small number of conformations because of the restricted rotation around the N-C^{α} bond in the pyrrolidine ring ($\phi \approx -60°$). In 1979, Boussard *et al.* investigated a series of proline-containing tripeptides. The β-turns were stabilized by hydrogen-bonding between the carbonyl of the N-terminal protecting group RCO and the C-terminal protecting group NHR where R in both cases was either a methyl, isopropyl or a *tert*-butyl group. The use of protecting groups to provide the carbonyl and NH required for hydrogen bond formation and hence β-turn stabilization is a theme which occurs again and again with synthetic linear peptide models. Boussard *et al.* (1979) investigated Pro-X and X-Pro containing sequences using proton NMR and infrared methods. They found that the Type II β-turn was the most favoured conformation with ProDAla and ProGly containing sequences while ProAla contained semi-opened C_7C_5 and C_5C_7 conformers in addition to the expected Type I β-turn. Aubry *et al.*, (1977) also found the RroAla sequence forms a Type I β-turn in solution, however, in crystal they found that N^{α}*t*BuProAlaNHipr prefers the Type II β-turn conformation. This is a

strong reminder that the crystal structure does not always reflect the conformation in solution. In this instance, they blamed the formation of *inter*molecular hydrogen-bonds in crystal for the difference. The X-Pro sequences seemed to prefer the mirror image β-turns as defined by Venkatachalam (1968) and were generally less stable.

The effect of the X residue on the β-turn forming ability of the sequence N-acetylProGly-X-OH was investigated by Brahmachari *et al.* (1982). They found, using proton NMR, CD and IR spectroscopy that the X residue affected the relative stability of the β-turn in the order: Leu>Ala>Ile>Gly>Phe. The tripeptide N-acetylProGlyLeuOH had been previously shown to be nearly 100% Type II β-turn in TFE at -40° C, using vacuum ultraviolet CD measurements (Brahmachari *et al.*, 1979). The peptide N-acetylProGlyPheOH was shown by X-ray crystallography to form a Type II β-turn (Brahmachari *et al.*, 1981). The formation of the $4 \rightarrow 1$ hydrogen bond is very important in defining the conformation of the β-turn. The crystal structure of the dipeptide $N^{\alpha}t$BocProGlyOH, which cannot form a C_{10} hydrogen-bonded structure was shown to contain ϕ,ψ angles for the Pro and Gly residues similar to those found in a Type I β-turn (Benedetti, 1977). This is in sharp contrast to the Type II β-turn formed by ProGly sequences in the tripeptides that are capable of forming a hydrogen-bonded β-turn (see preceeding paragraph). It may be mentioned here that although the ProGly sequence is the most commonly found for β-turns in proteins, the conformational flexibility of the glycine residue might be expected to lead to other "random" structures, particularily in solution.

The effect of the (i+2)th residue on the stability of the β-turn was demonstrated by Tamburro *et al.* (1984). They investigated, through CD and IR spectroscopy, the effect of the X residue in the sequence $N^{\alpha}t$BocPro-X-GlyOEt on the stability of the β-turn. They found that in TFE at room temperature, the molar fraction of β-turn conformation (hence stability) was Val>Ile>Nle>Pro,Leu. In a similar study, Boussard and Marraud (1985) found that when proline was in position (i+1) of the β-turn there was an increase in the percentage β-turn in CH_2Cl_2 going from L-alanine to glycine to D-alanine as the (i+2)th residue. These data, together with the theoretical calculations of Venkatachalam (1968) combine to give an interesting insight into the relative stabilities of Type I and Type II β-turns. According to Venkatachalam (1968) the Type II β-turn prefers the "LL" sequence whereas the Type II β-turn prefers the "LD" sequence. Hence, the ProDAla sequence containing peptides would be expected to take on a Type II β-turn conformation while the ProAla sequence containing peptides would be expected to take on a Type I β-turn conformation. The steric restrictions placed upon both the L- and the D-alanines are the same, yet a significantly greater percentage of the peptide containing the ProDAla sequence forms a β-turn. This indicates a lower stability of the Type I β-turn as compared to the Type II β-turn when proline is in the (i+1)th position. This statement is further supported by the observation that ProGly containing β-turns are almost invariably Type II even though glycine can be considered either a D or a L amino acid (Boussard, 1979; Brahmachari *et al.*, 1981, 1982; see chapter 3). Both crystal and solution studies have shown that β-turn forming peptides with the ProDAla sequence take on a Type II conformation (Aubry *et al*, 1977; Ananthanarayanan and Shyamasundar,

1981; Rao *et al.*, 1983; Crisma *et al.*, 1984). This taken in conjunction with the data of Boussard and Marraud (1985) indicate that the substitution of the glycine with D-alanine would stabilize the Type II β-turn conformation. Therefore, the inclusion of sterically restrictive amino acids at position (i+2) of the β-turn to "lock" the conformation into a limited potential range becomes attractive.

Other amino acid residues, besides D-alanine, which do not normally occur in peptides, have been used to produce conformationally restricted β-turn-forming linear peptides. These include other D amino acids such as D-serine and D-proline (Nair *et al.*, 1979; Boussard and Marraud, 1985) and α-aminoisobutyric acid (Aib) (Nagaraj and Balaram, 1979, 1981; Rao *et al.*, 1980; Smith *et al.*, 1981; Prasad *et al.*, 1982; Jung *et al.*, 1983; Van Roey *et al.*, 1983; Bonora *et al.*, 1984; Crisma *et al.*, 1984). The peptides containing D-serine and D-proline at position (i+2) of a β-turn with proline at position (i+1) were found to be 100% β-turn as opposed to the 90% β-turn achieved with D-alanine in that position (Boussard *et al.*, 1985). This would be expected since the D-proline and D-serine side chain groups are much bulkier than the methyl group of D-alanine. Hence they are much more conformationally restrictive. The Aib group is characterized by two mothyls on the α-carbon as opposed to the one found with alanine. The preferred conformation, whether proline is its neighbour or not, appears to be a 3_{10}-helix or a Type III(I) β-turn variation even though Prasad *et al.* (1982) reported a Type II β-turn with PivProAibNHCH$_3$ in crystal and solution. Theoretical conformational analysis performed by Prasad *et al.* (1982) indicated that the Type II β-turn conformer was 2 kcal mol^{-1} more stable than the Type III. They attributed the

3_{10}-helix observed by others to long range factors. The Aib-containing sequences previously studied were oligopeptides.

The three points that reveal themselves after an examination of the literature are that:

- Cyclic peptides are not required to obtain a stable β-turn structure. A linear peptide with an appropriately chosen sequence could form this structure.
- The stability and type of β-turn formed depends on residues i through $(i+3)$.
- The Type I β-turn is intrinsically less stable than the Type II β-turn.

The above considerations will become important during the design of a double β-turn forming tetrapeptide. A study analogous to those performed by Chou and Fasman (1977, 1978) and Ananthanarayanan *et al.* (1984) on the occurrence of β-turns in proteins was performed by Isogai *et al.* (1980). They examined the crystal strucures of 23 proteins for multiple bends. A double bend was defined as a sequence in which two successive distances between C^{α}_{i} and $C^{\alpha}_{(i+3)}$ (R_3) and $C^{\alpha}_{(i+1)}$ and $C^{\alpha}_{(i+4)}$ (R_3) meet the requirements of Lewis *et al.* (1973) for a β-bend. In other words, they are sequences with two overlapping $4 \rightarrow 1$ hydrogen bonds which are not part of a helix. They found that 5.4% of all residues occur in multiple bends. Of these, thirty eight percent have a distance between C^{α}_{i} and C^{α}_{i+4} (R_4) of less than 5.6 Å. These structures are folded more tightly than α-helices and those double β-bends which are merely distorted helices. The formation of these tightly wound structures is aided by the frequent occurrence of glycine.

There are several peptides which have been proposed to take on a double β-turn structure. Apart from the Aib containing peptides which, as expected, take on a 3_{10}-helix conformation (Nagaraj *et al.*, 1979; Van Roey *et al.*, 1983), there are several peptides which produce double β-turns but do not contain Type III β-turns. As pointed out in section 1.1, the Type III β-turn can be considered the beginning of a 3_{10}-helix. An example of a double β-turn which does not contain a Type III β-turn is PivProProAlaNHCH$_3$ which in the crystalline state exists as a Type II' β-turn followed by an overlapping Type I β-turn (Nair *et al.*, 1979). The above structure has also been proposed for the gramicidin S analogue, di-N-methyl-leucine gramicidin S (Kumar *et al.*, 1975). Through solution spectroscopic studies, Venkatachalapathi and Balaram (1979) described PivProProAlaNHCH$_3$ as an incipient 3_{10}-helix although it is likely that that the structure may actually prove to be made up of a polyproline-II-like extended structure followed by a Type II β-turn (Ananthanarayanan, personal communication).

With two overlapping β-turns, the $(i+2)$th residue of the first β-turn is also the $(i+1)$th residue of the second. To be sterically "compatible", their allowed ϕ,ψ angles must be very close. Figure 1-3 plots the ϕ,ψ angles of the $(i+1)$th and $(i+2)$th residues of β-turn types I, I', II, II' as defined by Venkatachalam (1968) on a Ramachandran plot (Ramachandran and Sasisekharan, 1968). As seen in Figure 1-3, a Type II β-turn can only be followed by a Type I' or III'. Although not shown in the figure, the ϕ,ψ angles of the $(i+1)$th residue of a Type III' β-turn are identical to that of the Type I' β-turn (Venkatachalam, 1968). The ϕ,ψ angles corresponding to the $(i+1)$th residue of all the other β-turn types are not close

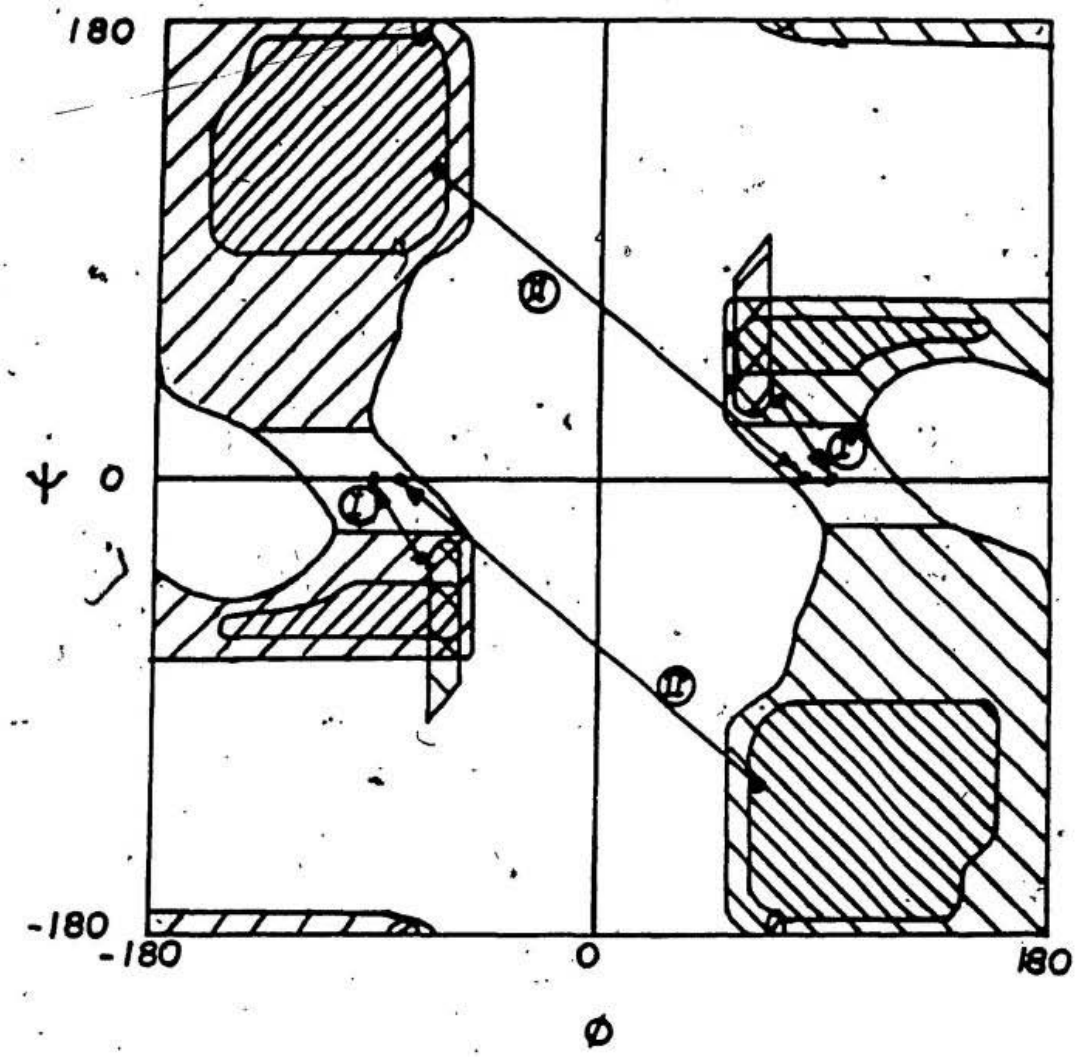

Figure 1-3: ϕ,ψ map showing sterically allowed regions for both L and D amino acids. ▨, fully allowed for L-residue; ▨, allowed for L-alanine; ▨, fully allowed for D-residue; ▨, allowed for D-alanine. β-turn Types I, I', II and II' are indicated by arrows beginning at the ϕ,ψ angles of residue $i+1$ and ending at the ϕ,ψ angles of residue $i+2$.

enough to the ϕ,ψ angles of the $(i+2)$th residue of the Type II β-turn. Also, the $(i+2)$th residue ϕ,ψ angles of types I and I' are quite different from those of the $(i+1)$th residue of any of the β-turn types. Hence it would be difficult for a Type I or Type I' β-turn to be followed by any type of β-turn. The non-3_{10}-helix double β-turn would therefore be either a Type II β-turn followed by either a Type I' or III' or a Type II' followed by a Type I or III β-turn. The above considerations become very important in designing a double β-turn-forming tetrapeptide which can potentially bind calcium ion. (see section 1.5).

1.4. Functional Role of Beta-Turns

The high occurrence of β-turns, especially at the surface of proteins (Kuntz, 1975), led to the postulation of a number of functional roles in addition to its structural usefulness. These include the β-turn serving as recognition sites for enzymatic phosphorylation (Small *et al.*, 1977), glycosylation (Aubert *et al.*, 1976) and proline hydroxylation (Brahmachari and Ananthanarayanan, 1978, 1979).

In 1979, Vogt *et al.* examined the loop region of a series of homologous calcium-binding proteins for β-turn forming potential based on the secondary structure prediction methods of Chou and Fasman (1975). They found a strong correlation between the ability to bind calcium ion and the position and linear density of β-turn forming residues. A brief description of the structural data on the calcium-binding regions of these proteins is presented below.

The solution of the X-ray crystallographic structure of the carp muscle calcium-binding parvalbumin (MCBP) indicated the involvement of an α-helix-loop-α-helix

structure in calcium-binding and suggested that the twelve-residue long loop segment was responsible for the actual complexing to the calcium ion (Kretsinger and Nockolds, 1973). This segment contains regularly spaced carbonyl, carboxyl and hydroxyl ligands which could coordinate to the positively charged calcium ion. There were three such structures found in parvalbumin but only two, referred to as CD hand and EF hand respectively, were capable of binding calcium ion. The third, referred to as AB hand, was characterized by a ten-residue loop segment instead of the twelve residues found in those loops capable of binding. Of greater interest was the discovery of a Type I β-turn at the very beginning of the loop segments capable of binding calcium ion and the absence of this structure in the loop segment which could not bind (Moews and Kretsinger, 1975). The two deletions in the latter loop segment correspond to positions 6 and 8 of the twelve-residue loop segments. It was generally accepted that the lack of binding was due to the deletions (Kretsinger, 1980). These deletions would not be expected to affect the β-turn structure. A number of other calcium-binding proteins showed a good homology in the α-helix-loop-α-helix region even though the relationship between the entire sequences was often fairly weak. The homologous regions of proteins such as heart troponin C, T4 lysozyme, modulator protein, vitamin-D induced calcium-binding protein, the alkali-extractable (ALC) and dithionitrobenzoate-extractable (DLC) light chain of muscle myosin, the EDTA-extractable light chain (ELC) from mollusc myosin, and smooth muscle light chain myosin (SLC) were deemed to have the same structure as that of parvalbumin (Kretsinger, 1976, 1980). The solution of the X-ray structures of other calcium-binding proteins such as bovine intestinal calcium-binding protein

(Szebenyi *et al.*, 1981) and, more recently, troponin C (Herzberg and James, 1985; Sundaralingam *et al.*, 1985) and calmodulin (Babu *et al.*, 1985), showed that the previous structural correlations based on homology were essentially correct. The lack of calcium-binding activity exhibited by some of the homologous sequences could not be explained by the number and position of the ligands and the number of residues in the loop segment (Weeds and McLachlin, 1974; Tufty and Kretsinger, 1975).

Vogt *et al.* (1979) examined the loop segments of the 9 calcium-binding proteins listed above. Because of a multitude of homologous regions in some proteins, they were left with 26 data sets with some sequences capable of binding calcium ion while others were not. They examined all possible tetrapeptides within the loop segments and calculated their β-turn forming potential in terms of the probability parameter P_t as defined by Lewis *et al.* (1971):

$$P_t = f_i f_{(i+1)} f_{(i+2)} f_{(i+3)}$$

Where f_i, etc. are the frequencies of residues in the four successive positions of the β-turn as observed in known protein structures. The values used by Vogt *et al.* (1979) were obtained by Chou *et al.* (1975) from a survey of the X-ray crystal structures of 17 proteins (298 β-turns). Local stretches of high P_t values indicate a series of overlapping tetrapeptides each with a high β-turn potential (Lewis *et al.*, 1971). In the 26 homologous sequences examined by Vogt *et al.* (1979) two consecutive peaks with P_t values greater than or equal to the value of 3.0×10^{-4} were found to occur precisely at the first residue of each loop region that binds

calcium ion. These "doublets" would be expected for two overlapping β-turns (Vogt *et al.*, 1979). The start of the doublet obtained from the loop sequence of the calcium-binding region of MCBP aligned precisely with the start of the MCBP Type I β-turns. Very interestingly, there were no such doublets found in the homologous loop sequences which did not bind calcium ion, and neither were comparable doublets found in any other part of the sequences of calcium-binding proteins. In rabbit skeletal Troponin C no tetrapeptide, apart from those involved in the doublets, had P_t values greater than or equal to the value of 3.0×10^{-4}.

Vogt *et al.* (1979) also examined the sequences of several non-homologous calcium-binding proteins. These included *Staphylococcus* nuclease, thermolysin, concanavalin A and trypsin. Although doublets do occur at calcium-binding sites they are not the rule as with the homologous proteins. However, in the majority of cases one finds at least one tetrapeptide with a high P_t value near a calcium-binding site. There is therefore a strong suggestion that a β-turn is involved in calcium-binding. It should be noted that the above data relied on prediction methods based on non-calcium-binding regions. Hence the β-turn predictions refer to uncomplexed sequences and do not pertain to the conformation after calcium has complexed to the loop segment. Until now, the above observations remained one of mere interest. The laboratory in which the results presented in this thesis were obtained has been interested in delineating the conformational features of the β-turn by spectral methods and elucidating its involvement in functions such as proline-hydroxylation (Ananthanarayanan, 1983;

Ananthanarayanan *et al.*, 1984; Brahmachari and Ananthanarayanan, 1978; Brahmachari *et al.*, 1979, 1981, 1982; Chopra and Ananthanarayanan, 1982). It was therefore logical to examine the role of β-turns in metal ion-binding. The final catalyst for the project came from an examination of cyclic peptides.

Many cyclic peptides, both synthetic and natural, are capable of selectively complexing with calcium ion or other alkali or alkali earth metal ions. Two features that these ionophores have in common are the presence of β-turns in the uncomplexed species and the coordination of the peptide carbonyl groups to the metal ion in the complexed species. Both valinomycin (Degelaen *et al.*, 1984) and its analogue cyclo-(AlaGlyDPhePro)$_3$ (Vishwanath and Easwaran, 1982) were shown to contain six $4 \rightarrow 1$ hydrogen bonds. The carbonyls were coordinated to calcium ion upon binding and this involved the breaking of *intra*molecular hydrogen bonds. Another example is found in a paper by Pease and Watson (1978). They designed the pentapeptide cyclo-(GlyProDAlaPro) with the intent of having both a β-turn and a γ-turn ($3 \rightarrow 1$ hydrogen bond) present. Again, as with the valinomycins, the hydrogen bonds were broken as the carbonyls coordinated to the metal ion. This particular peptide was subjected to a molecular mechanical study by Lynn and Kushick (1984) which provides a set of excellent stereodiagrams of the peptide in both its uncomplexed and lithium-complexed form. A similar set of diagrams can be found in a paper by Duax and Smith (1981) who were interested in detailing a sequence of steps involved in the complexing of the metal ion to valinomycin. The diagrams relate a progressive coordination of carbonyls to metal ion and breaking of *intra*molecular hydrogen

bonds. In addition to the uncomplexed and complexed forms there are a series of intermediates. Several other cyclic-peptides are also capable of complexing metal ions including cyclo-(DPheProGlyDAlaPro) (Karle, 1984), cyclo-$(SarSarGly)_2$, cyclo-$(Sar)_6$ (Sughihara *et al.*, 1976) and cyclo-$(ProSar)_n$ (n=3,4) (Shimizu and Fujishige, 1980). The paper by Karle (1984) compares the crystal structures of the uncomplexed and magnesium-complexed species. The carbonyls involved in the formation of *intra*molecular hydrogen bonds in the uncomplexed species (β- and γ-turns) are coordinated to the magnesium ion in the complexed species. The latter two papers indicate the presence of *intra*molecular hydrogen bonds in the uncomplexed states and the required carbonyl coordination to the metal ion for binding but go no further except to say there was a possibility of multiple conformers. Other examples of cyclic metal ion-binding peptides include cyclo-$(X\text{-}Pro)_4$, where X= Phe, Leu or Lys(N^{ϵ}-protected) (Kimura and Imanishi, 1983) and the bicyclic S,S'-Bis-cyclo-(GlyhemiCysGlyGlyPro) (Schwyzer *et al.*, 1970). The latter two papers do not talk about the conformation of the peptides in the uncomplexed state but do point out that the complexed state is achieved through the coordination of the peptides' carbonyls to the metal ion. The above papers are very useful not only in presenting a possible relationship between ion-binding and the β-turn but also for their technical merit. The methods used in the above papers to determine and follow ion-binding, especially those by Vishwanath and Easwaran (1982) and Pease and Watson (1978), were used as a basis for the calcium-binding studies presented in this thesis. These authors characterized the uncomplexed species and followed ion-binding using both carbon-13 and proton NMR and CD spectroscopy. The peptides studied by Pease

and Watson (1978) and Vishwanath and Easwaran (1982) were, like the peptides studied in this thesis, too small to be studied by many of the techniques generally used for studying calcium-binding proteins.

The β-turn-forming doublet pattern observed by Vogt *et al.* (1979) in the loop segment of homologous calcium-binding protein sequences along with the results of the cyclic ion-binding peptides led to the belief that the β-turn is a favourable conformational prerequisite for ion-binding. To test this postulated role, linear peptides, which could mimic the overlapping β-turns seen with the homologous calcium-binding proteins, were synthesized and their interactions with calcium and other metal ions were studied and compared to single β-turn and non-β-turn forming peptides.

1.5. Design of Postulated Calcium-Binding Peptides

Two considerations in the design of peptides capable of forming two overlapping β-turns and potentially binding calcium ion have to be made especially if one wishes to examine the relationship between structure and function. First, the peptide conformation must be stable in solution and secondly, since the binding of calcium ion probably involves a conformational change, the peptide must maintain a certain degree of flexibility. Therefore, the amount of conformational restriction provided by the amino acids incorporated into the peptide must reflect a balance between the two needs. The peptide $N^{\alpha}t$BocProDAlaAlaNHCH$_3$ and its potentially more flexible analogue $N^{\alpha}t$BocProGlyAlaNHCH$_3$ were considered capable of striking the balance. The peptides are theoretically capable of forming two overlapping β-turns. The first β-turn is stabilized by a hydrogen bond

between the carbonyl of the *t*Boc group and the NH of the alanyl residue; the second is stabilized by a hydrogen bond between the carbonyl of the prolyl residue and the NH of the $NHCH_3$. The *t*Boc and the $NHCH_3$ groups each act as half a residue contributing a carbonyl and an amide group, respectively. The peptides are therefore three and two halves long and are referred to as tetrapeptides.

Proline-containing peptides were used since much of the work done on linear peptides models of β-turns uses proline in the $(i+1)$th position. The ProDAla and ProGly sequence-containing peptides were shown to favour Type II β-turns, the former being more stable than the latter, and each more stable than ProAla sequence-containing β-turns. The D-alanine, because of the single methyl group as its side chain, was considered to provide enough steric hindrance to produce a defined structure in solution yet maintain the flexibility of the peptide chain. Although the replacement of D-alanine by D-serine or D-phenylalanine would provide a more stable β-turn, the larger side chains have a greater chance of interfering in any conformational changes that might occur upon ion-binding. The more interference from amino acid side chains, the more difficult the interpretation of the effect of the peptide backbone conformation. The use of alanine at position $(i+3)$ of the first β-turn ($i+2$ of the second) again reflects the need of balance between stability and flexibility. Leucine, although superior at position $(i+3)$ to alanine in stabilizing the β-turn, has a bulkier side group. The DAlaAla and the GlyAla sequences, although not strong β-turn formers, are not expected to act as disrupters. Hence, the ability to form a second β-turn relies

only on the ability to form the second hydrogen bond. The final limitation on the amino acids used in the synthesis of calcium-binding peptides is that only the peptide backbone would be allowed to provide potential ligands for calcium ion coordination. Therefore, amino acids such as serine with its hydroxyl group and glutamic acid with its carboxylate group were not used.

Chapter 2

Experimental

2.1. Materials

Amino acids and derivatives, N-hydroxysuccinimide, isobutylchloroformate, N-methylmorpholine, N,N'-dicyclohexylcarbodiimide, methylamine hydrochloride, calcium chloride, and deuterated solvents were purchased from Sigma Chemical Company. Reagent and HPLC grade solvents were purchased from Fisher Scientific Company as were the perchlorate salts of calcium, magnesium, sodium and potassium. Lithium perchlorate was purchased from Fluka Chemicals. Water was purified to HPLC grade on a Synbron/Barnstead NANOpure II filtration system. Molecular sieves were purchased from Davison Chemical. Peptides and salts were vacuum dried for several hours before use.

2.2. Methods

2.2.1. Purity of Peptides

All peptides used in analysis were crystallized twice. Intermediates used in synthesis were crystallized once. The purity of peptides used in analysis was checked by HPLC with at least two different elution profiles. Further checks of purity by way of proton NMR, elemental analysis and amino acid analysis were performed on the two major peptides, N^{α}tBocProDAlaAlaNHCH$_3$ and its analogue N^{α}tBocProGlyAlaNHCH$_3$.

2.2.2. Crystallization of Peptides

Peptides were dissolved in a minimum of chloroform in an Erlenmeyer flask by heating in a hot water bath. Petroleum ether (40/60) was added drop wise until the solution became cloudy. The solution was reheated until clear and again petroleum ether (40/30) was added dropwise to the solution until it became cloudy. The solution was reheated until clear and set aside to cool. After about an hour the top of the flask was covered with parafilm perforated with small holes. After a minimum of six hours the flask was then cooled to 0-5 ° C for a minimum of four hours and further cooled to -20 ° C for two hours. The crystals were filtered on Whatman filter paper (#1) and washed with petroleum ether (40/60). The Buchner funnel, filter paper and petroleum ether were cooled to -20 ° C before use.

2.2.3. Melting Point

The melting points were recorded on a Thomas Hoover melting point apparatus made available to us by the MUN Chemistry Department and are uncorrected. The reported values are the average of at least three runs.

2.2.4. Elemental Analysis

The peptides were analyzed for carbon, hydrogen and nitrogen by Canadian Microanalytical Service Ltd., Vancouver, B.C. after extensive drying. The percent oxygen was determined by subtraction.

2.2.5. Amino Acid Analysis

The amino acid content of the peptides was determined by D. Hall of the Biochemistry Department on a Beckman model 121 automated analyzer. The samples were hydrolyzed with 6M HCl in sealed evacuated tubes at 110° C for 24 hours.

2.2.6. HPLC

The HPLC of peptides was performed on a Perkin-Elmer (Series 4LC) liquid chromatograph with a HP-5 ODS C-18 reverse phase column using HPLC grade acetonitrile, water and methanol as the mobile phase. The samples were prepared for injection by dissolving in methanol (1-2 mg ml^{-1}). Peaks were detected by UV at 225 nm on a Perkin-Elmer model LC-85B spectrophotometric absorbance detector.

2.2.7. Infrared Spectroscopy

Infrared (IR) spectra were recorded at room temperature on a Perkin-Elmer model 983G spectrophotometer with 1.0 mm BaF_2 cells (Buck Scientific). Wavelength calibration was checked using a 0.05 mm polystyrene film. The peptides were dissolved in $CHCl_3$ which was freshly distilled over calcium chloride. A spectrum was obtained by electronically subtracting a spectrum of $CHCl_3$ in both the sample and reference cells from a spectrum with the peptide dissolved in $CHCl_3$ in the sample cell and $CHCl_3$ in the reference cell. In this way, the effect of minute differences between cells was removed.

2.2.8. Circular Dichroism Spectroscopy

CD spectra from 260 to 185 nm were recorded at room temperature on a Jasco J-500A spectropolarimeter equipped with a DP-500N data processor. Wavelength was calibrated with neodymium glass and amplitude was calibrated using 0.6% D-10-camphor sulphonic acid in H_2O. Unless otherwise stated, peptide concentrations of 0.5 mg ml^{-1} were used in a 0.5 cm quartz cell (Jasco). HPLC grade organic solvents were dried over molecular sieves for at least 24 hours and then filtered before use. The spectra were averaged after eight accumulations at 50 nm/min and a time constant of 0.5. Spectra were obtained by electronically subtracting the spectrum of solvent from the spectrum of peptide in solvent. Values are reported as mean residue ellipticity ($[\theta]_{res}$). For a detailed description of the term $[\theta]_{res}$ see section 4.1.1.

2.2.9. Nuclear Magnetic Resonance

Proton noise-decoupled Fourier transformed carbon-13 and proton NMR spectra were recorded on a Nicolet NB 360 MHz spectrometer at the Atlantic Region Magnetic Resonance Centre, Halifax, Nova Scotia. Tetramethylsilane was used as an internal reference. Unless otherwise indicated, peptide concentrations of 10 mg ml^{-1} and 25 mg ml^{-1} in the appropriate solvent were used for the proton and carbon-13 NMR, respectively. Deuterated solvents were stored over molecular sieves and filtered before use. Tube sizes of 5 mm and 10 mm were used for proton and carbon-13 NMR, respectively. All spectra, unless otherwise specified, were obtained at 24 $\pm$ 1 ° C.

2.2.10. Binding Studies by Circular Dichroism

The binding of cation to peptide was followed by CD in both water and acetonitrile. Calcium chloride was used in the titration in water while perchlorate salts were used when acetonitrile was used as the solvent. Final peptide concentrations were equimolar to 0.5 mg ml^{-1} $N^{\alpha}t$BocProDAlaAlaNHCH$_3$. Peptide stock solutions were prepared 9.75 times the concentration used in the final measurement. An initial stock solution of salt was diluted to a series of secondary stock solutions in 10 ml volumetric flasks. Using Lambda pipets (H.E. Pedersen), 1750 μl of secondary stock solution was added to 200 μl of the peptide stock solution resulting in a series of ion/peptide ratios. A parallel set of solvent solutions was prepared by replacing the 200 μl of peptide stock with 200 μl of solvent. Solutions were thoroughly mixed using a rotor mixer and allowed to incubate for a minimum of 30 minutes before use. Only glass and teflon were allowed to come in contact with the solutions.

2.2.11. Binding Studies by NMR

$N^{\alpha}t$BocProDAlaAlaNHCH$_3$ and $N^{\alpha}t$BocProGlyAlaNHCH$_3$ were titrated with calcium perchlorate in acetone-d_6 and acetonitrile-d_3, respectively. Peptide concentrations of 20 mg ml^{-1} for proton NMR and 25 mg ml^{-1} for carbon-13 NMR were used. Lamda pipets (H.E. Pedersen) were used to add μl increments of a concentrated salt stock solution so that at a salt to peptide ratio of 1, the dilution of the peptide was no more than 1:1. Solutions were mixed thorougly using a rotor mixer before measurement.

2.3. Peptide Synthesis

2.3.1. Introduction

The N^{α}*t*BocProDAlaAlaNHCH$_3$ peptide was elongated from *t*BocPro by an activated ester method using NSU. The addition of the N-methylamide to the C-terminal was accomplished by mixed anhydride coupling. The outline of synthesis is given in Figure 2-1. Both the activated ester method and the mixed anhydride method are well established solution techniques and are described in a monograph on peptide synthesis by Bodanszky *et al.* (1976). Although coupling by the mixed anhydride method requires fewer steps than coupling by the activated ester method, unless care is taken it can cause racemization of the amino acid residue on the N-terminal side of the bond being formed. The activated ester method requires the initial synthesis of a NSU derivative before coupling can occur, but racemization is not a problem (Bodanszky *et al.*, 1976). The activated ester method cannot be used to couple N-methylamine to the C-terminal end of the sequence. Standard precautions to minimize racemization were taken during the addition of the N-methylamide. It was therefore assumed that no racemization had taken place during synthesis.

The N^{α}*t*BocProGlyAlaNHCH$_3$ peptide was synthesized by Dr. S.K. Attah-Poku. The peptide was recrystallized and checked for purity, as outlined in the methods section. The final peptide was synthesized by coupling N^{α}*t*BocProGlyOH and AlaNHCH$_3$ by the mixed anhydride method. Because glycine has two α-carbon hydrogens, there is no problem with racemization. Dr. S.K. Attah-Poku was also responsible for the synthesis of N^{α}*t*BocProDAlaNHCH$_3$ and N^{α}*t*BocProDAlaAlaOCH$_3$.

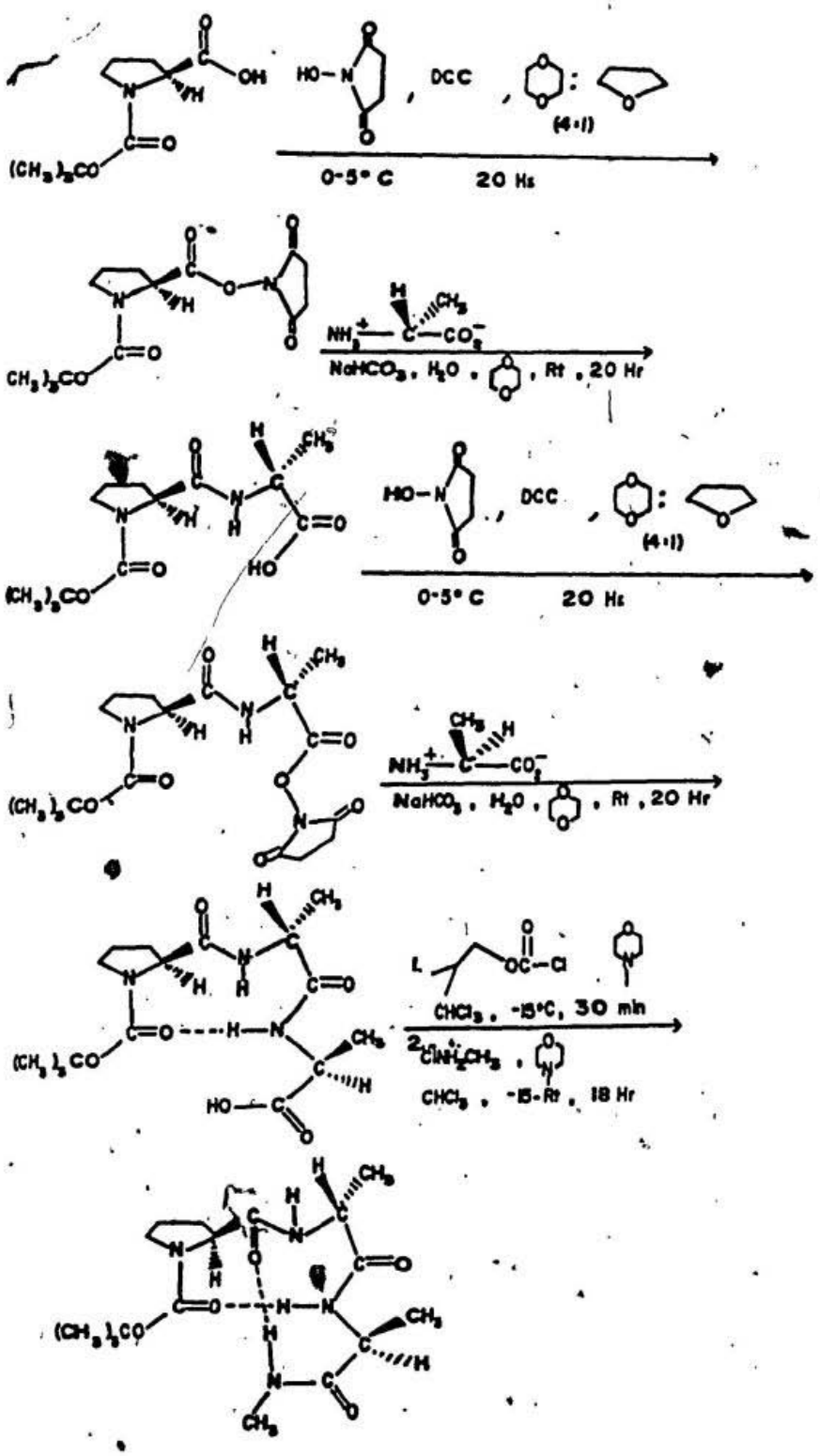

Figure 2-1: Outline of Synthesis of N^{α}*t*BocProDAlaAlaNHCH$_3$

2.3.2. N^{α}tBocProDAlaAlaNHCH$_3$

The synthesis of $N^{\alpha}t$BocProDAlaAlaNHCH$_3$ is given below. The description is representative since more than one synthesis run was made. (The complete synthesis of this peptide including its intermediates was done by the writer.)

2.3.2.1. N^{α}tBocProONSU

A solution containing equimolar amounts of $N^{\alpha}t$BocProOH (9.63g, 44.8 1.60mmole) and NSU (5.15g, 44.8 mmole) in dioxane:THF (1:1, v:v) was cooled to 0° C in an ice-bath. The mixture was stirred for 20 hours at 0-5° C after the addition of 1.1 molar equivalents of DCC (10.15g, 49.2 mmole). The reaction mixture was filtered to remove the DCU byproduct and the solvent removed on a rotary evaporator. The product was crystallized from a chloroform-petroleum ether mixture (12.09g, 38.8 mmole, 86.6%).

2.3.2.2. N^{α}tBocProDAlaOH

$N^{\alpha}t$BocProONSU (10.69g, 34.3 mmole) was dissolved in 200 ml dioxane and stirred. A 1 molar equivalent of DAlaOH (3.42g, 38.4 mmole) was dissolved in a minimum amount of water with 2 molar equivalents of $NaHCO_3$ (6.45g, 76.8 mmole) ($\approx$ 20 ml). The second solution was added to the first and 1 ml of dioxane was added for every ml of water required for the second solution. The reaction mixture was stirred for 20 hours at room temperature, cooled to 0° C and filtered after 10-15 minutes. The solvent was removed to dryness and the residue extracted with ethyl acetate. The aqueous layer was concentrated to 40 mls, adjusted to pH 2 and then brought back up to 100 mls with water. The solution was slowly saturated with NaCl and then extracted 3 times with

chloroform. The chloroform layers were dried with Na_2SO_4, filtered and concentrated on a rotary evaporator. The product was crystallized from a chloroform-petroleum ether mixture (6.67g, 23.3 mmole, 67.9%)

2.3.2.3. N^{α}tBocProDAlaONSU

A solution containing equimolar amounts of N^{α}tBocProDAlaOH (6.67g, 23.3 mmole) and NSU (2.68g, 23.3 mmole) in dioxane:THF (4:1, v:v) was cooled to 0° C in an ice-bath. The mixture was stirred for 20 hours at 0-5° C after the addition of 1.1 molar equivalents of DCC (5.29g, 25.6 mmole). The reaction mixture was filtered to remove the DCU byproduct and the solvent removed on a rotary evaporator. The product was crystallized from a chloroform-petroleum ether mixture (5.01g, 13.1 mmole, 56.2%).

2.3.2.4. N^{α}tBocProDAlaAlaOH

N^{α}tBocProDAlaONSU (5.00g, 13.1 mmole) was dissolved in 100 ml dioxane and stirred. A 1 molar equivalent of AlaOH (1.16g, 13.1 mmole) was dissolved in water with 2 molar equivalents of $NaHCO_3$ (2.19g, 26.1 mmole). The second solution was added to the first and 1 ml of dioxane was added for every ml of water required for the second solution. The reaction mixture was stirred for 20 hours at room temperature, cooled to 0° C and filtered after 10-15 minutes. The solvent was removed to dryness and the residue extracted with ethyl acetate. The aqueous layer was concentrated to 40 mls, adjusted to pH 2 and then brought back up to 100 mls with water. The solution was slowly saturated with NaCl and then extracted 3 times with chloroform. The chloroform layers were dried with Na_2SO_4, filtered and concentrated on a rotary evaporator. The product was

crystallized from a chloroform-petroleum ether mixture (3.68g, 10.3 mmole, 78.6%)

2.3.2.5. N^{α}tBocProDAlaAlaNHCH$_3$

N^{α}tBocProDAlaAlaOH (3.68g, 10.3 mmole) was dissolved in a minimum amount of chloroform and placed in a salt-ice mixture while stirring. One molar equivalent of N-methylmorpholine (1.13 ml) was added and the solution stirred for 30 minutes. A 1 molar equivalent of N-methylamide hydrochloride (0.69g, 10.3 mmole) and N-methylmorpholine (1.13 mls) was added and the solution was allowed to come to room temperature in the salt/ice bath while stirring for a minimum of 18 hours. The solvent was removed to dryness, the residue redissolved in chloroform and washed successively with cold 1M HCl, saturated bicarbonate solution and saturated NaCl solution. The organic phase was dried with anhydrous Na_2SO_4, filtered and concentrated on a rotary evaporator. The product was crystallized from a chloroform-petroleum ether mixture (1.60g, 4.31 mmole, 41.8%). The overall yield of the synthesis from N^{α}tBocPro to final peptide was 9.6%.

The melting point was determined to be 216-217° C. Amino acid analysis yielded a 2:1 ratio of alanine to proline. The D and L enantiomers of alanine could not be distinguished. The elemental analysis indicated a percent weight distribution as follows: 55.11% carbon, 8.13% hydrogen, 21.75% oxygen and 15.01% nitrogen. The calculated values for $C_{17}H_{30}O_5N_4$ were 55.12% carbon, 8.15% hydrogen, 21.59% oxygen and 15.12% nitrogen. The results of a former elemental analysis differed from the calculated values by an unacceptable amount.

However, when one water molecule was introduced into the calculation the discrepancy vanished. Subsequent samples were accompanied with instructions to thoroughly dry and there was no further problem. Each sample yielded a single peak on HPLC.

2.3.3. N^{α}tBocProGlyAlaNHCH$_3$

The melting point of N^{α}*t*BocProGlyAlaNHCH$_3$ was determined to be 167-168° C. Amino acid analysis revealed a 1:1:1 ratio of proline to glycine to alanine. The elemental analysis indicated a percent weight distribution as follows: 53.79% carbon, 7.97% hydrogen, 22.65% oxygen and 15.59% nitrogen. The calculated values for $C_{16}H_{28}O_5N_4$ were 53.91% carbon, 7.92% hydrogen, 22.44% oxygen and 15.72% nitrogen. The sample gave a single peak on HPLC.

Chapter 3

NMR Characterization

3.1. Introduction to NMR

As described in the introductory chapter, nuclear magnetic resonance has been an extremely useful tool in the study of the molecular structure of both linear and cyclic calcium-binding peptides in either the complexed or uncomplexed states. What follows is a detailed study on the conformation of the uncomplexed tetrapeptides N^{α}*t*BocProGlyAlaNHCH$_3$ and its D-alanine analogue N^{α}*t*BocProDAlaAlaNHCH$_3$ along with the assignment of resonances which are used to monitor the effect of calcium ion on the conformation of the peptides. The Ca^{2+}-induced conformational changes will be dealt with in Chapter 5. Both carbon-13 and proton NMR of the two peptides were run in DMSO-d_6, acetonitrile-d_3 (used for the Gly-peptide only) and acetone-d_6 (used for the DAla-peptide only). Proton NMR of both peptides in $CDCl_3$ and the carbon-13 NMR spectrum of N^{α}*t*BocProDAlaAlaNHCH$_3$ in $CHCl_3$ were also run. The choice of the solvents used was based upon the following considerations. Acetonitrile-d_3 and acetone-d_6 were used primarily because they were useful in the studies on calcium-binding by the peptides (see Chapter 5). Acetone-d_6 was used for the DAla-peptide since it was only sparingly soluble in acetonitrile-d_3. These solvents, as well as $CHCl_3$ and its deuterated form $CDCl_3$, were used since they are

relatively non-polar and hence would not be expected to disrupt the *intra*molecular hydrogen bonds within the peptide (Bayley, 1980). This is not the case with DMSO-d_6 which, being relatively polar, could interact with the polar peptide bonds. In fact, one usually observes two isomers of peptides containing the sequence X-Pro in this solvent (Thomas and Williams, 1972; Wuthrich *et al.*, 1972; Dorman and Bovey, 1973; Smith *et al.*, 1973; Young and Deber, 1975). With the N^{α}*t*BocPro-containing peptides, the rotation about the urethane bond results in a *cis* isomer (or rotamer) and a *trans* isomer. The *cis* isomer is normally rare except in the case of proline-containing peptides (Ramachandran and Mitra, 1976). The *cis* and *trans* conformers of proline-containing peptides have been extensively characterized by both carbon-13 and proton NMR (Stimson *et al.*, 1977; Higashijima *et al.*, 1977). When proline is in the $(i+1)$th position of the β-turn, only the *trans* isomer is capable of forming the required $4 \rightarrow 1$ hydrogen bond (Brahmachari *et al.*, 1982; Ramaprasad *et al.*, 1981; Boussard *et al.*, 1979). Data on the *cis* and *trans* populations, usually obtained from carbon-13 NMR data, would therefore give an estimate of the population of the hydrogen-bonded form *versus* the non-bonded form of the peptides (see section 3.2.2.1).

3.2. Carbon-13 NMR

3.2.1. Introduction to Carbon-13 NMR Studies

The assignment of the carbon-13 resonances of small peptides can be accomplished relatively easily through off-resonance proton-decoupling experiments and the comparison of peptide analogues and precursors run under the same conditions (Howarth and Lilley, 1978). Although sequence effects are generally small (Grathwohl and Wuthrich, 1974; Christl and Roberts, 1972), they do occur. These shifts, along with those due to secondary structural effects such as hydrogen-bonding, make direct application of resonances determined from standard random-coil peptides inappropriate (Bovey, 1969). The latter peptides were obtained by Grathwohl and Wuthrich (1974) by substituting X in the sequence TFAGlyGly-X-AlaOCH$_3$ with various amino acids. They used this particular sequence because, with the possible exception of the bulkier amino acids, it seemed to be representative of an extended random-coil. The random-coil values were used for the assignment of the resonances of the initial precursor which, in the case of the two peptides studied here, was N$^{\alpha}$*t*BocProOH. Excellent discussions on the theory and application of carbon-13 NMR are available (Howarth and Lilley, 1978; Wuthrich, 1976; Levy, 1976).

3.2.2. Carbon-13 NMR of N^{α}tBocProGlyAlaNHCH$_3$

3.2.2.1. Studies Using DMSO-d_6 as Solvent

The assignment of the carbon-13 resonances of the peptide N^{α}*t*BocProGlyAlaNHCH$_3$ in DMSO-d_6 was made through a direct comparison with the previously assigned carbon-13 spectrum of N^{α}*t*BocProGlyAlaOH in DMSO-d_6 (Attah-Poku and Ananthanarayanan, to be published). Their assignments were built up from the carbon-13 spectra of N^{α}*t*BocProOH and N^{α}*t*BocProGlyOH in DMSO-d_6. The spectrum of N^{α}*t*BocProGlyAlaNHCH$_3$ is shown in Figure 3-1, and the expanded spectrum is shown in Figure 3-2. Tables 3-1 and 3-2 list the peak assignments of N^{α}*t*BocProGlyAlaNHCH$_3$ and its precursor N^{α}*t*BocProGlyAlaOH, respectively. The two spectra correlate very well, there were no ambiguous peaks; the peak at 25.58 ppm, which did not correspond to any of the resonances assigned to the carbons of the peptide N^{α}*t*BocProGlyAlaOH, was assigned to the NH<u>C</u>H$_3$.

The differentiation of signals due to the *cis* and *trans* isomers of the peptide relied on other considerations besides position. Earlier studies by others have shown that the best method for determining the *cis* or *trans* isomer populations is by the analysis of the proline ring β- and γ-carbon resonances (Dorman and Bovey, 1973; Somorjai and Deslauriers, 1976; Deslauriers *et al.*, 1976; Deber *et al.*, 1975). The *cis* and *trans* resonances of these atoms are well resolved and are therefore useful in the detection and initial estimation of the relative populations of the two isomers. In the peptide containing the methylamide group considered here, the proline β-carbon resonances were found at 30.93 and 29.91 ppm for the

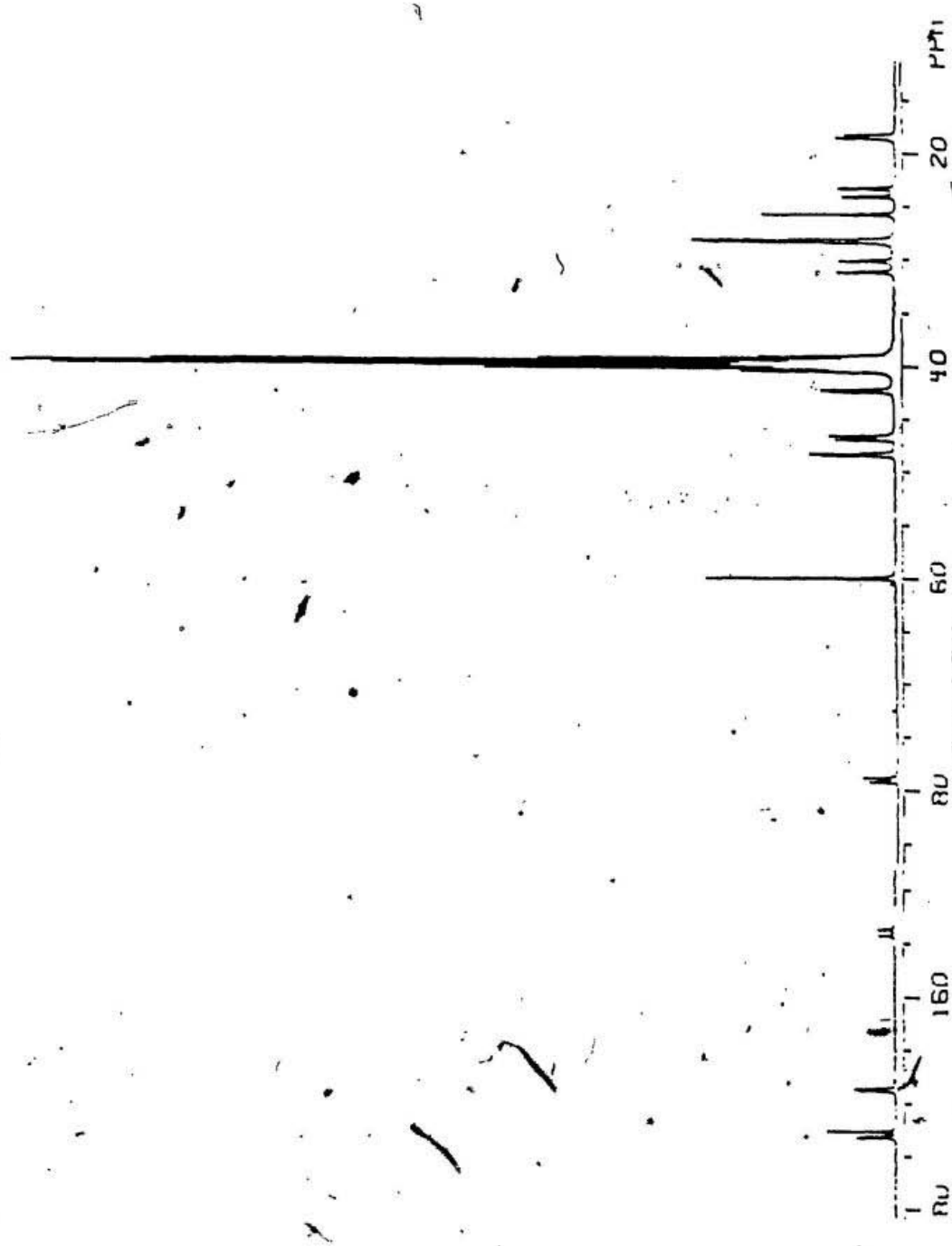

Figure 3-1: Carbon-13 NMR Spectrum of N^{α}*t*BocProGlyAlaNHCH$_3$ in DMSO-d_6

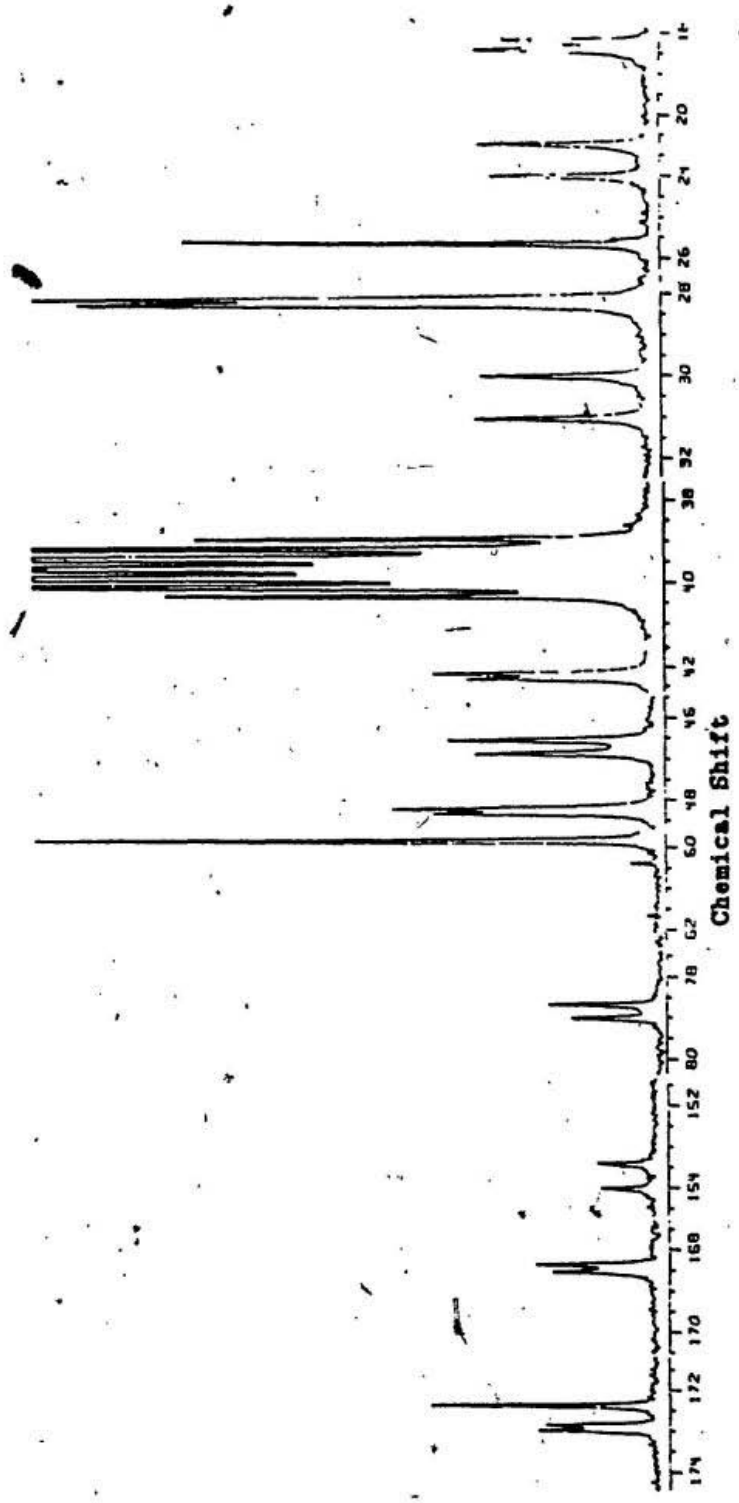

Figure 3-2: Expanded Carbon-13 NMR Spectrum of N^{α}*t*BocProGlyAlaNHCH$_3$ in DMSO-d$_6$

Table 3-1: Carbon-13 NMR Peak Assignments of N^{α}*t*BocProGlyAlaNHCH$_3$ in DMSO-d$_6$

Resonance	*t*Boc	Pro	Gly	Ala	$NHCH_3$
$(\underline{C}H_3)_3$-C-O	28.15^t 28.02^c	---	---	---	---
$(CH_3)_3$-$\underline{C}$-O	78.91^t 78.56$_c$	---	---	---	---
C=O	153.92^t 153.33^c	172.31	168.45^t 168.28^c	172.78^t 172.91^c	---
α-C	---	59.75	46.79^t 46.46^c	48.24^t 48.14^c	---
β-C	---	29.91^t 30.93^c	---	18.12^t 18.35^c	---
γ-C	---	23.93^t 23.14^c	---	---	---
δ-C	---	42.23^t 42.10^c	---	---	---
$NH\underline{C}H_3$	---	---	---	---	25.58

chemical shift values in ppm, t = *trans* isomer, c = *cis* isomer

Table 3-2: Carbon-13 NMR Peak Assignments of N^{α}*t*BocProGlyAlaOH in DMSO-d_6

Resonance(ppm)	*t*Boc	Pro	Gly	Ala
$(\underline{C}H_3)_3$-C-O	28.05^{t} 28.21^{c}	---	---	---
$(\overline{C}H_3)_3$-$\underline{C}$-O	78.51^{t} 78.82^{c}	---	---	---
C=O	154.38^{t} 153.34^{c}	172.39^{t} 172.72^{c}	168.54^{t} 168.35^{c}	173.97^{t} 173.83^{c}
α-C	---	59.60^{t} 59.69^{c}	46.84^{t} 46.49^{c}	47.52
β-C	---	29.96^{t} 30.98^{c}	---	17.37^{t} 17.45^{c}
γ-C	---	23.97^{t} 23.90^{c}	---	---
δ-C	---	41.62^{t} 41.77^{c}	---	---

t = *trans* isomer, c = *cis* isomer

cis and *trans* isomers, respectively. The *cis* and *trans* resonances of the proline ring γ-carbon were found at 23.14 and 23.93 ppm respectively (see Table 3-1). These values correspond closely to those found in other proline-containing peptides (Young and Deber, 1975; Richarz and Wuthrich, 1978; London *et al.*, 1978). With both the proline ring β- and γ-carbons of the N^{α}*t*BocProGlyAlaNHCH$_3$ peptide, the *cis* resonances were found to be significantly more dominant. Based on this, the *cis* isomer resonances of other carbons (besides the proline ring β and γ) were distinguished from their respective *trans* isomer resonances through the measurement of peak heights. Most of the resonances were resolved into *cis* and *trans* isomers, the exceptions being the prolyl α-carbon, the prolyl carbonyl and the NH$\underline{C}$H$_3$. In the case of the precursor peptide N^{α}*t*BocProGlyAlaOH, all carbons except the alanyl α-carbon, were resolved in terms of the *cis* and *trans* resonances. The *cis* isomer was the major conformer for both N^{α}*t*BocProGlyAlaNHCH$_3$ and its precursor N^{α}*t*BocProGlyAlaOH. The relative positions of the *cis* and *trans* resonances were the same in both the peptides with the exception of the *t*Boc carbons, the alanyl carbonyl and the proline ring δ-carbon whose *trans* isomer resonances with N^{α}*t*BocProGlyAlaNHCH$_3$ were upfield from their respective *cis* isomer resonances in contrast to their downfield positions with N^{α}*t*BocProGlyAlaOH.

Although it has been common practice to quantitate the *cis*/*trans* ratio through the measurement of the relative intensities (heights) of the respective signals of single carbon atoms such as the proline ring β or γ (Young and Deber, 1975; London *et al.*, 1978), this involves the assumption that the nuclear Overhauser

enhancements and the spin-lattice relaxation times are equal in all the carbon atoms for *cis* and *trans* isomers. This is not necessarily true. Minor differences have been observed in several peptides (Deslauriers *et al.*, 1974; Fermandijan *et al.*, 1975). To correct for these potential differences, all *cis/trans* assignable line intensities of the title peptide were taken into account and the mean value for the relative intensities of the two rotamer signals was calculated. By this method, the peptide N^{α}*t*BocProGlyAlaNHCH$_3$ was found to be 53.0 ± 3.2 % *cis* and 47.0 ± 3.2 % *trans*. Table 3-3 lists the individual *cis/trans* ratios. Note that the *cis/trans* ratios range from 1.06 to 1.20 with a mean of 1.13 ± 0.07.

The majority of the chemical shifts in the carbon-13 spectrum of the title peptide was very close to those obtained with the random coil peptides (see Figure 3-1). The exceptions are a) the glycine α-carbon which gave a value of 42.10 ppm for the random-coil peptide (Grathwohl and Wuthrich, 1974) as compared to the observed ones for the Gly-peptide at 46.79 ppm (*trans*) and 46.46 ppm (*cis*) and b) the proline ring δ-carbon resonances which gave values of 42.23 ppm (*trans*) and 42.10 ppm (*cis*) as compared to the literature values of 45.8 ppm (*trans*) and 46.8 ppm (*cis*). The peaks seen in Figure 3-1 between 38.54 and 40.25 ppm were due to the solvent DMSO-d$_6$.

3.2.2.2. Studies Using Acetonitrile-d$_3$ as Solvent

The carbon-13 spectrum of N^{α}*t*BocProGlyAlaNHCH$_3$ in acetonitrile-d$_3$ is shown in Figure 3-3. The peak assignments are listed in Table 3-4. Unlike the carbon-13 NMR spectrum of the title peptide in DMSO-d$_6$, there were no spectra of precursors run under the same conditions from which to build up the

Table 3-3: *Cis/Trans* Ratios of N^{α}*t*BocProGlyAlaNHCH$_3$ in DMSO-d_6 as Determined by Carbon-13 NMR

Resonance	*t*Boc	Pro	Gly	Ala
$(\underline{C}H_3)_3$-C-O	1.06	---	---	---
$(CH_3)_3$-$\underline{C}$-O	1.20	---	---	---
C=O	1.17	UR.	1.09	1.13
α-C	---	UR.	1.14	1.15
β-C	---	1.10	---	1.13
γ-C	---	1.13	---	---
δ-C	---	1.12	---	---

UR. = unresolved

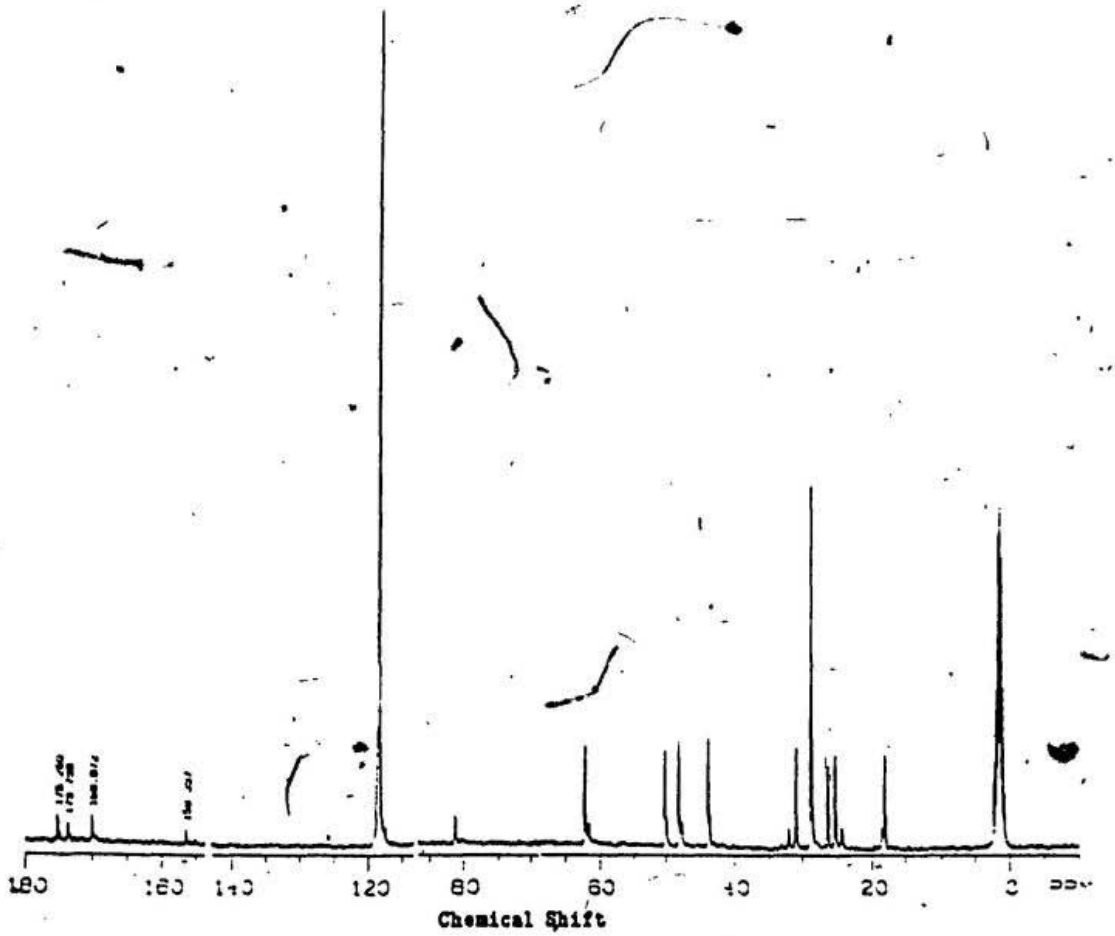

Figure 3-3: Carbon-13 NMR Spectrum of N^{α}-tBocProGlyAlaNHCH$_3$ in Acetonitrile-d_3

Table 3-4: Carbon-13 NMR Peak Assignments of N^{α}*t*BocProGlyAlaNHCH$_3$ in Acetonitrile-d$_3$

Resonance	*t*Boc	Pro	Gly	Ala	$NHCH_3$
$(\underline{C}H_3)_3$-C-O	28.60	---	---	---	---
$(CH_3)_3$-$\underline{C}$-O	81.04	---	---	---	---
C=O	156.34	169.97	173.74	175.25	---
α-C	---	62.18^t 61.62^c	48.01^t 47.56^c	50.09^t 49.88^c	---
β-C	---	30.82^t 31.93^c	---	18.01^t 18.46^c	---
γ-C	---	25.26^t 24.32^c	---	---	---
[illegible]	---	43.83^t 43.64^c	---	---	---
$NH\underline{C}H_3$	---	---	---	---	26.29

chemical shift values in ppm, t = *trans* isomer, c = *cis* isomer

assignment of resonances. However, the spectrum was similar enough to that of the peptide in DMSO-d_6 to allow general assignments to be made even though, due to solvent effects, specific assignments were not always identical.

The carbonyl resonances were found in the region 155 ppm to 175 ppm. The chemical shift of the *t*Boc carbonyl was expected, as with the peptide in DMSO-d_6, to be highly upfield from the other carbonyls. Therefore the peak at 156.34 ppm was assigned to the *t*Boc carbonyl. Of the remaining three carbonyl resonances, two were found grouped close together. The grouped resonances at 173.74 ppm and 175.25 ppm, were assigned to the glycyl and alanyl residues, respectively. This distinction was made on the basis of the carbon-13 spectrum of the peptide in DMSO-d_6. In that case, the glycyl carbonyl resonance was upfield from the alanyl carbonyl resonance. The resonance at 169.97 ppm was attributed to the prolyl carbonyl; the difference from the other amino acid carbonyl resonances was attributed to the effect of the proline ring. None of the carbonyl resonances was resolved into *cis* and *trans* isomers. This was probably a function of the number of accumulations since their peaks were not very intense.

The remaining assignments followed closely the model provided by the peptide in DMSO-d_6. Only the peptide's α-carbon resonances and the resonances due to the carbons of the proline ring were resolved into *cis* and *trans* isomers. The distinction between the resonances due to the *cis* isomer and those due to the *trans* isomer relied, as with the peptide in DMSO-d_6, on the β- and γ-carbons of the proline ring. The proline ring β-carbon resonances were found at 31.93 ppm and 30.82 ppm for the *cis* and *trans* isomers respectively. The *cis* and *trans*

resonances of the proline ring γ-carbon were found at 25.26 ppm and 24.32 ppm, respectively (see Table 3-4 and Figure 3-3). With both the β and γ-carbons, the *trans* form was significantly more populated. This is in marked contrast to the situation prevailing in DMSO-d_6 described in section 3.2.2.1. The *cis/trans* assignments of the remaining resolved resonances proceeded on the basis of peak height.

The determination of the *cis/trans* ratios was described in section 3.2.2.1. The N^{α}tBocProGlyAlaNHCH$_3$ peptide in acetonitrile-d_3 was found to be 16.2 $\pm$ 4.5 percent *cis* and 83.8 $\pm$ 4.5 percent *trans*. Table 3-5 lists the individual *cis/trans* ratios. The *cis* ratio ranges from 0.14 to 0.26 with a mean of 0.19 $\pm$ 0.06. The hydrogen-bonded form (*trans* isomer) predominates in acetonitrile-d_3.

3.2.3. Carbon-13 NMR of N^{α}tBocProDAlaAlaNHCH$_3$

3.2.3.1. Studies Using DMSO-d_6 as Solvent

The assignment of carbon-13 NMR resonances, the differentiation of *cis* and *trans* isomer peaks, and the determination of *cis/trans* ratios followed the procedure described in the previous sections on the carbon-13 NMR data on N^{α}tBocProGlyAlaNHCH$_3$ in DMSO-d_6.

The assignment of carbon-13 NMR resonances of the peptide N^{α}tBocProDAlaAlaNHCH$_3$ in DMSO-d_6 proceeded through a direct comparison with the previously assigned carbon-13 NMR spectrum of N^{α}tBocProDalaOH in DMSO-d_6 (Ananthanarayanan and Attah-Poku, to be published). Figure 3-4 shows the carbon-13 NMR spectrum of N^{α}tBocProDAlaAlaNHCH$_3$ in DMSO-d_6.

Table 3-5: *Cis/Trans* Ratios of N^{α}*t*BocProGlyAlaNHCH$_3$ in Acetonitrile-d_3 by Carbon-13 NMR

Resonance	Proline	Glycine	Alanine
α-Carbon	0.19	0.19	0.25
β-Carbon	0.14	---	0.17
γ-Carbon	0.16	---	---
δ-Carbon	0.26	---	---

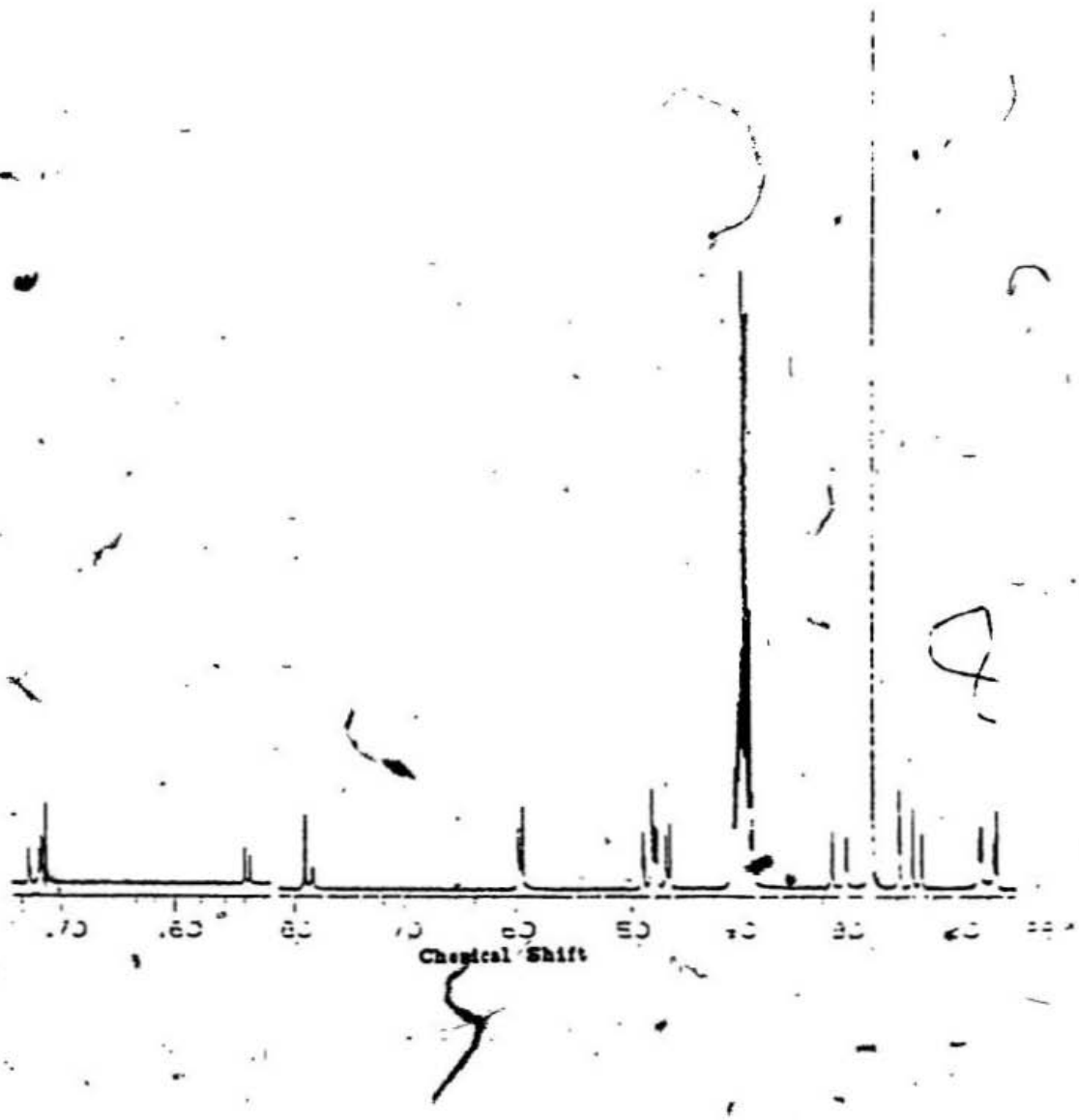

Figure 3-4: Carbon-13 NMR Spectrum of N^{α}tBocProDAlaAlaNHCH$_3$ in DMSO-d$_6$

Table 3-6 and Table 3-7 list the peak assignments for N^{α}*t*BocProDAlaOH and N^{α}*t*BocProDAlaAlaNHCH$_3$, respectively. Their assignments correlate well with the carbon-13 NMR assignments of N^{α}AcProDAlaNHCH$_3$ (Ramaprasad *et al.*, 1981). The assignment of the carbon-13 NMR resonances of N^{α}*t*BocProDAlaAlaNHCH$_3$ was not as straight forward as those of the Gly-peptide in DMSO-d_6. The problem arose because of the presence of two enantiomers of alanine in this peptide. It is reasonable to expect their resonances to be close to each other.

The relative intensities of the *cis* and *trans* isomer resonances were determined through the β- and γ-carbons of the proline ring. The proline ring β-carbons resonances were found at 31.01 ppm for the *cis* isomer and 29.84 ppm for the *trans* isomer. The resonances of the proline ring γ-carbons were found at 23.18 ppm and 24.18 ppm for the *cis* and *trans* isomers, respectively. There was little deviation of the above resonances from the respective resonances of the precursor, N^{α}*t*BocProDAlaOH. In both cases, there is signifigantly more of the *trans* isomer than the *cis* isomer. The differentiation of the remaining peaks into *cis* and *trans* isomers proceeded on the basis of peak intensity.

The carbonyl of the *t*Boc group exhibited a resonance, as expected, far upfield from the other carbonyls. The peaks at 153.92 ppm and 153.64 ppm were assigned to the *t*Boc carbonyls of the *trans* and *cis* isomers, respectively. The proline and alanine carbonyl assignments were a problem due to the similarity between the two alanine enantiomers and a general crowding of the resonances. With the carbon-13 NMR spectrum of N^{α}*t*BocProDAlaOH in DMSO-d_6 the D-

Table 3-6: Carbon-13 NMR Peak Assignments of N^{α}*t*BocProDAlaOH in DMSO-d_6

Resonance(ppm)	*t*Boc	Proline	D-Alanine
$(\underline{C}H_3)_3$-C-O	27.87	---	---
$(CH_3)_3$-$\underline{C}$-O	78.35	---	---
C=O	153.21	171.51^{t} 171.91^{c}	173.59^{t} 173.72^{c}
α-C	---	59.40	47.43^{t} 47.17^{c}
β-C	---	29.87^{t} 30.93^{c}	17.41^{t} 17.27^{c}
γ-C	---	23.70^{t} 22.94^{c}	---
δ-C	---	46.63^{t} 46.33^{c}	---

t = *trans* isomer, c = *cis* isomer

Table 3-7: Carbon-13 NMR Peak Assignments of N^{α}*t*BocProDAlaAlaNHCH$_3$ in DMSO-d$_6$

Resonance	*t*Boc	Pro	DAla	Ala	$NHCH_3$
$(\underline{C}H_3)_3$-C-O	28.02^t 28.11^c	---	---	---	---
$(CH_3)_3$-$\underline{C}$-O	79.10^t 78.50^c	---	---	---	---
C=O	153.92^t 153.64^c	171.55	173.26^t 172.26^c	171.89^t 172.00^c	---
α-C	---	59.43^t 59.73^c	49.06^t 48.09^c	48.33^t 47.88^c	---
β-C	---	29.84^t 31.01^c	17.42^t 17.14^c	18.57^t 18.42^c	---
γ-C	---	24.18^t 23.18^c	---	---	---
δ-C	---	46.97^t 46.55^c	---	---	---
$NH\underline{C}H_3$	---	---	---	---	25.70^t 25.59^c

chemical shift values in ppm, t = *trans* isomer, c = *cis* isomer

alanine carbonyls resonated fairly far downfield at 174 ppm while the proline carbonyls resonated relatively far upfield at 172 ppm. Hence, with the peptide N^{α}*t*BocProDAlaAlaNHCH$_3$, the single large resonance at 171.55 ppm was assigned to the proline carbonyl and the resonances at 173.26 ppm and 172.26 ppm were assigned to the D-alanine carbonyls of the *trans* and *cis* isomers respectively. The intermediately placed resonances, at 172.00 and 171.89 ppm were assigned to the *cis* and *trans* isomers of the title peptide's L-alanine carbonyls respectively.

The peaks between 47 ppm and 60 ppm were assigned to the α-carbon resonances. The resonances at 59.43 ppm and 59.73 ppm were assigned to the proline α-carbons of the *trans* and *cis* isomers, respectively. They compare well with the proline α-carbon resonances of the precursor and the Gly-peptide. The assignment of the two alanine α-carbons was made more difficult by spurious side peaks that can be associated with the large solvent peaks found around 40 ppm. The use of the *cis/trans* ratio of the proline α-carbon resonances (0.821) as a reference was useful in separating out the peaks. The alanyl α-carbon resonances of the Gly-peptide and the D-alanine α-carbon resonances of the N^{α}*t*BocProDAlaOH peptide indicate that the α-carbon resonances belonging to the D-alanine are downfield from those of the L-alanine. By using expected peak heights and *cis/trans* ratios, the resonances at 48.09 ppm and 49.06 ppm were assigned to the *cis* and *trans* isomers of D-alanine respectively. The resonance at 48.33 ppm and 47.88 ppm were then assigned to the L-alanine α-carbon resonances of the *trans* and *cis* isomers, respectively. Because of the still possible

uncertainty in the assignment of the D- and L-alanine α-carbon resonances due to their overlap, they were not used in the final calculation of the *cis/trans* ratio.

The D-alanine β-carbon of the precursor peptide N^{α}*t*BocProDAlaOH resonates at 17.41 ppm (*trans*) and 17.27 ppm (*cis*). The alanine β-carbon of the glycine analogue resonates at 18.12 (*trans*) ppm and 18.35 ppm (*cis*). Hence, the resonances at 17.14 ppm and 17.42 ppm were assigned to the D-alanyl β-carbon resonances of the N^{α}*t*BocProDAlaAlaNHCH$_3$ peptide, *cis* and *trans* isomers respectively, and the peaks at 18.57 ppm and 18.42 ppm were assigned to the L-alanyl residue β-carbon resonances, *cis* and *trans* respectively.

The remaining peak assignments correlated well with the precursor peptide and the glycine analogue. The peak at 25.70 ppm was assigned to the NHCH$_3$ methyl carbon of the *trans* isomer and the resonance at 25.79 ppm was assigned to the corresponding *cis* isomer. Unlike the precursor, the *cis/trans* peaks of the *t*Boc carbons and the proline α-carbon were resolved while the proline carbonyl resonances were not. The series of peaks centred around 40 ppm, as stated previously, are due to the DMSO-d$_6$ solvent. The carbon-13 NMR spectrum of the DAla-peptide is very similar to its glycine analogue.

The *cis/trans* ratios of the individual carbons of N^{α}*t*BocProDAlaAlaNHCH$_3$ are shown in Table 3-8. Although the methyl carbons of the *t*Boc could be resolved into *cis* and *trans* isomers, the peaks were broad and overlapped. Hence, the *cis/trans* ratios could not be accurately calculated. As mentioned above, the α-carbons of the alanines were not used in the calculation because of some doubt

Table 3-8: *Cis/Trans* Ratios of N^{α}*t*BocProDAlaAlaNHCH$_3$ in DMSO-d_6 by Carbon-13 NMR

Resonance	*t*Boc	Pro	DAla	Ala	$NHCH_3$
$(CH_3)_3$-C-O	0.63	---	---	---	---
C=O	0.75	UR.	0.74	0.82	---
α-C	---	0.82	0.74	0.55	---
β-C	---	0.68	0.90	0.89	---
γ-C	---	0.64	---	---	---
δ-C	---	0.66	---	---	---
$NHCH_3$	---	---	---	---	0.70

UR. = unresolved

with their assignment. In DMSO-d_6, the peptide N^{α}tBocProDAlaAlaNHCH$_3$ was found to be 47.6 ± 4.9 percent *cis* and 52.4 ± 4.9 percent *trans*. The *cis/trans* ratios ranged from 0.83 to 0.90 with a mean of 0.75 ± 0.08. When compared to the glycine analogue, two observations stand out. First, the range of error was greater with the D-alanine analogue (± 4.9 %) than with the glycine analogue (± 3.2 %) and second, more importantly, the percent *cis* was significantly lower. The amount of peptide in the *cis* conformation decreases by 10.4 percentage points upon the substitution of a glycine with a D-alanine. This would indicate that the D-alanine in position (i+2) of a sequence has a somewhat different effect on the rotation around the urethane-proline bond between residues i and (i+1) of the same sequence as compared to glycine in the (i+2)th position. The conformationally restrained nature of the ProDAla sequence could force the peptide into a position more favourable for hydrogen-bonding than is possible with the glycine. I am unable to explain the increased range of *cis/trans* ratios seen with the DAla-peptide in DMSO-d_6 as compared to the glycine analogue in DMSO-d_6 and can only refer back to statements made earlier on the involvement of unequal nuclear Overhauser enhancements and spin-lattice relaxation times (see section 3.2.2.1). The phenomenon is probably not just a function of sequence since with the Gly-peptide a change to a more non-polar solvent resulted in an increased range of *cis/trans* ratios along with an increased proportion of *trans* isomer (see sections 3.2.2.1 and 3.2.2.2).

3.2.3.2. Studies Using $CHCl_3$ as Solvent

The carbon-13 NMR spectrum of N^{α}*t*BocProDAlaAlaNHCH$_3$ in $CHCl_3$ is shown in Figure 3-5. The assignments were carried out through a direct comparison with the carbon-13 NMR spectrum of N^{α}*t*BocProDAlaOH in $CHCl_3$ (Attah-Poku and Ananthanarayanan, to be published) whose peak assignments are listed in Table 3-9. They built up the resonance assignment from the carbon-13 NMR spectrum of N^{α}*t*BocProOH in $CHCl_3$. Their assignments are very similar to those by Ramaprasad *et al.* (1981) of N^{α}AcProDAlaNHCH$_3$ in $CDCl_3$. The carbon-13 NMR peak assignments of N^{α}*t*BocProDAlaAlaNHCH$_3$ in $CHCl_3$ are listed in Table 3-10. Only one isomer appears to exist. Since the majority of the DAla-peptide exists as the *trans* isomer in the more polar solvent DMSO-d_6, it is extremely likely that the peptide in $CHCl_3$ is all *trans* rather than all *cis*. Chloroform, unlike DMSO-d_6, tends to stabilize *intra*molecular hydrogen bonds and hence the *trans* form (Bayley, 1980). In contrast, the major isomer of the peptide N^{α}*t*BocProDAlaOH in $CHCl_3$ is the *cis* form. In that case, there are not enough residues to form a hydrogen-bonded β-turn. The addition of the AlaNHCH$_3$ group to the C-terminal end of the sequence allows the formation of such hydrogen bonds and hence stabilizes the *trans* isomer. The peak assignments were relatively straight forward with only one point of additional interest. The β-carbons of both alanine enantiomers do not resolve. This becomes more interesting once the peaks are assigned to the D-Ala peptide in acetone-d_6 (see section 3.2.3.3). Solvent peaks are expected and found around 77 ppm.

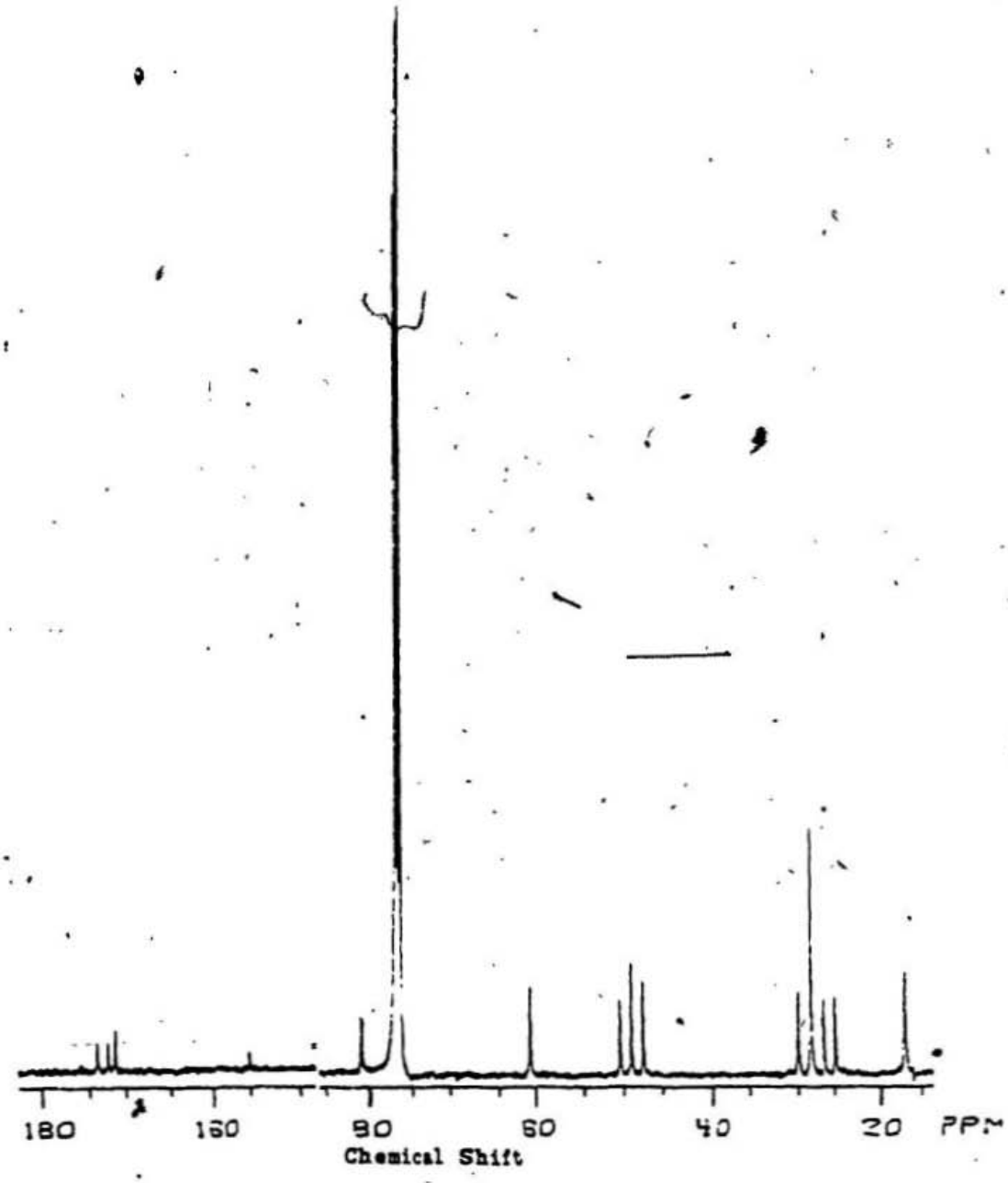

Figure 3-5: Carbon-13 NMR Spectrum of N^{α}*t*BocProDAlaAlaNHCH$_3$ in $CHCl_3$

Table 3-9: Carbon-13 NMR Peak Assignments of N^{α}tBocProDAlaOH in $CHCl_3$

Resonance(ppm)	tBoc	Proline	D-Alanine
$(\underline{C}H_3)_3$-C-O	28.36	---	---
$(CH_3)_3$-$\underline{C}$-O	81.25^t 81.88$_c$	---	---
C=O	155.47^t 155.94^c	172.36^t 171.98^c	175.42^t 175.02^c
α-C	---	59.58^t 61.26^c	47.67
β-C	---	29.53^t 31.21^c	18.24
γ-C	---	24.15^t 23.50^c	---
δ-C	---	47.08	---

chemical shift values in ppm, t = *trans* isomer, c = *cis* isomer

Table 3-10: Carbon-13 NMR Peak Assignments of N^{α}*t*BocProDAlaAlaNHCH$_3$ in $CHCl_3$

Resonance	*t*Boc	Pro	DAla	Ala	$NHCH_3$
$(\underline{C}H_3)_3$-C-O	28.14	---	---	---	---
$(CH_3)_3$-$\underline{C}$-O	80.83	---	---	---	---
C=O	155.04	171.33	173.91	172.40	---
α-C	---	60.53	50.34	48.77	---
β-C	---	29.85	17.03*	17.03*	---
γ-C	---	24.67	---	---	---
δ-C	---	47.21	---	---	---
$NH\underline{C}H_3$	---	---	---	---	26.21

chemical shift values in ppm
*The two peaks were unresolved.

3.2.3.3. Studies Using Acetone-d_6 as Solvent

The assignments of the carbon-13 NMR resonances of N^{α}*t*BocProDAlaAlaNHCH$_3$ in acetone-d_6 are shown in Table 3-11. The spectrum is shown in Figure 3-6. Acetone-d_6 was used since the D-Ala peptide was only sparingly soluble in acetonitrile-d_3 at the concentrations required for carbon-13 NMR (25 mg ml^{-1}). However, acetone-d_6 is not the best solvent for carbon-13 NMR, especially if one is concerned with the *cis* and *trans* isomer populations. Solvent peaks occur at and around 30 ppm, an area useful for determining whether the *cis* or *trans* isomer is the most populated. The spectrum was fairly noisy and although there were some indications of the presence of a minor species, the level was too low to quantitate. Since the D-alanine peptide is mostly *trans* in the more polar solvent, DMSO-d_6, it was considered unlikely that the major species is the *cis* isomer. Also, the γ-carbon of the proline ring resonates at 25.31 ppm which is in the area expected for a signal corresponding to the *trans* isomer. In some respects, the spectrum was very similar to the ones with the peptide in DMSO-d_6 and $CHCl_3$ and therefore one can feel fairly confident with general assignments. One would, because of solvent effects, feel less confident with the more specific assignments.

The *t*Boc carbonyl resonates highly upfield in relation to other carbonyls with a variety of peptides in a variety of solvents (see above). Therefore, the resonance at 155.45 ppm was assigned to the *t*Boc carbonyl. Of the remaining three resonances, two were grouped relatively close together. The two closer resonances at 172.87 and 172.33 ppm were assigned to the two alanine (D and L) carbonyls

Table 3-11: Carbon-13 NMR Peak Assignments of N^{α}tBocProDAlaAlaNHCH$_3$ in Acetone-d$_6$

Resonance	tBoc	Pro	DAla	Ala	$NHCH_3$
$(\underline{C}H_3)_3$-C-O	28.53	---	---	---	---
$(CH_3)_3$-$\underline{C}$-O	80.28	---	---	---	---
C=O	155.45	175.27	172.87	172.33	---
α-C	---	60.92	51.16	49.57	---
β-C	---	UR.	17.06	17.48	---
γ-C	---	25.31	---	---	---
δ-C	---	48.05	---	---	---
$NH\underline{C}H_3$	---	---	---	---	26.18

chemical shift values in ppm.
UR. = unresolved.

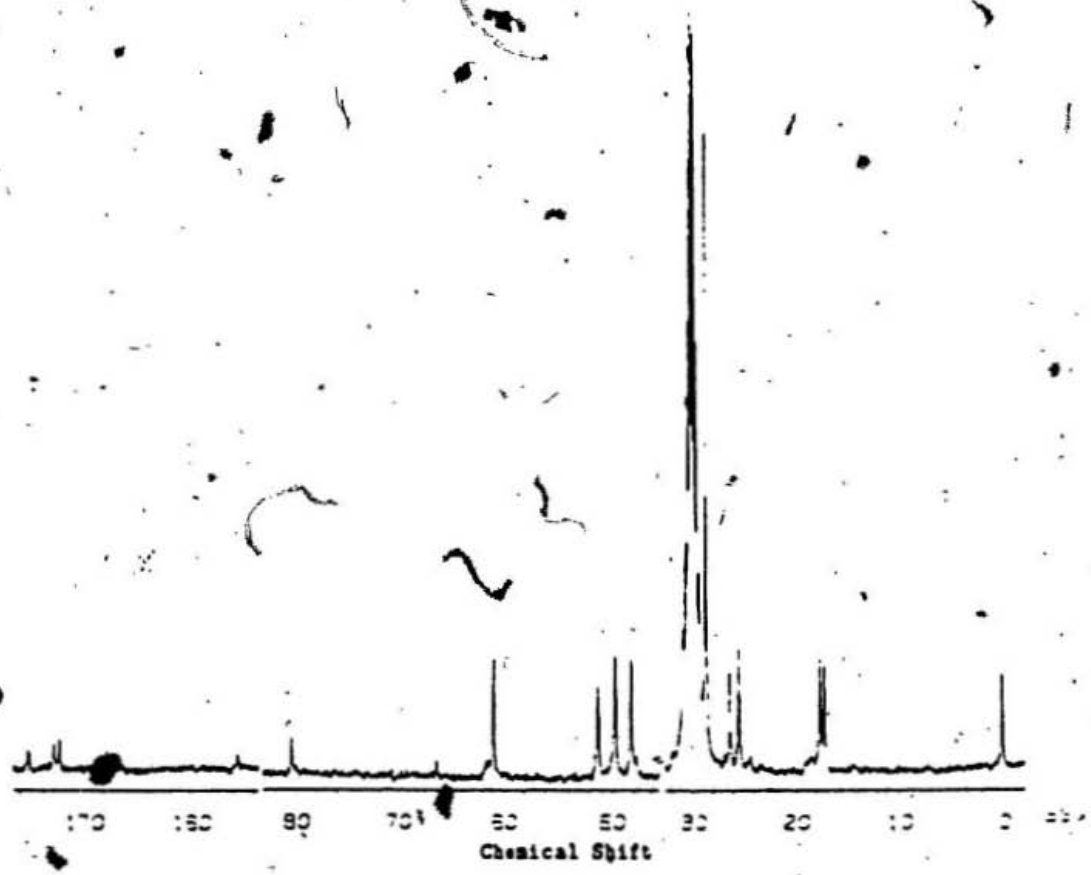

Figure 3-6: Carbon-13 NMR Spectrum of N^{α}tBocProDAlaAlaNHCH$_3$ in Acetone-d_6

based upon their similarity. In both $CHCl_3$ and DMSO-d_6 the D-alanine carbonyl resonance is downfield from the corresponding L-alanine resonance. Therefore the resonance at 172.87 ppm was assigned to the D-alanine carbonyl and that at 172.33 ppm was assigned to the L-alanine carbonyl. The peak at 175.27 ppm was assigned to the proline carbonyl, in this case downfield with respect to the alanine carbonyls as observed in the peptide in $CHCl_3$ and DMSO-d_6.

The alanyl β-carbon resonances are much closer to each other than in DMSO-d_6. The distance between the two seems to be a function of solvent polarity (see 3.2.3.2). The D-alanine β-carbon was assigned to the more upfield resonance at 17.06 ppm and the β-carbon of the L enantiomer to 17.48 ppm, on the basis of the relative position of the two resonances in DMSO-d_6. The exact effect of the solvent was unknown and therefore one cannot be sure of the validity of the assignment.

The remaining resonance peak assignments were relatively straight forward and followed the patterns observed with both the Gly-peptide and the DAla-peptide in a variety of solvents (see above).

3.2.4. Solvent-Dependence of Carbonyl Resonances

3.2.4.1. Introduction

By changing the solvent one may be able to alter the chemical shifts of the carbon-13 resonances (Howarth and Lilley, 1978). The change in chemical shift ($\Delta\delta$) arises through alterations in solute charge distribution, space shielding and conformation (Lyerla *et al.*, 1973; Moon and Richards, 1972). The extent to

which a particular carbonyl is affected by a change in solvent depends, in part, to whether or not that carbonyl is hydrogen-bonded. A series of papers by Urry and co-workers have shown that in the case of tetra-, penta- and hexapeptide models of elastin, the $\Delta\delta$ value of hydrogen-bonded carbonyls upon changing the solvent from DMSO-d_6 to either water, methanol or trifluoroacetic acid is less than half when compared to those carbonyls which are not hydrogen-bonded (Urry and Mitchell, 1976; Urry *et al.*, 1974[a,b,c]; Khaled *et al.*, 1976; Okamoto and Urry, 1976; Urry *et al.*, 1975[a,b]). The amount a particular carbonyl resonance shifts with a change in solvent depends on other factors besides hydrogen-bonding and therefore a direct comparison between two solvents has only a limited use. The studies cited above used a solvent-titration which is the method of choice. What follows is a comparison of carbonyl chemical shifts of the *trans* isomers of N^{α}*t*BocProGlyAlaNHCH$_3$ and N^{α}*t*BocProDAlaAlaCH$_3$ in various solvents. The *trans* isomers are expected to be the hydrogen-bonded form (see section 3.1) (Boussard *et al.*, 1979; Brahmachari *et al.*, 1982).

3.2.4.2. N^{α}*t*BocProGlyAlaNHCH$_3$

The chemical shifts of the carbonyl resonances corresponding to the *trans* isomer of N^{α}*t*BocProGlyAlaNHCH$_3$ in the relatively polar DMSO-d_6 and the relatively non-polar acetonitrile-d_3 were compared. The differences in terms of $\Delta\delta$ were as follows: *t*Boc 2.42 ppm, proline 2.34 ppm, glycine 5.20 ppm and alanine 2.47 ppm. The carbonyl of the glycyl residue, which was not expected to hydrogen bond, is found to show the largest shift. The two carbonyls which were expected to hydrogen bond (*t*Boc and Proline) showed a change in shift of approximately half that seen with the glycine carbonyl. The above results are in

line with the observations of Urry and co-workers (see Introduction). However, the alanyl carbonyl raises an anomaly. Its $\Delta\delta$ value was not signifigantly greater than that of the *t*Boc. Does this mean that it was hydrogen-bonded or was it less affected by the solvent change for some reason other than hydrogen-bonding? The distinction between these two possibilities cannot be made on the carbon-13 solvent-dependence data alone.

3.2.4.3. N^{α}*t*BocProDAlaAlaNHCH$_3$

The chemical shifts due to the carbonyls of N^{α}*t*BocProDAlaAlaNHCH$_3$ in DMSO-d_6, acetone-d_6 and $CHCl_3$ were compared. The results were found to be conflicting and could not be used to delineate hydrogen-bonding patterns. They do, however, emphasize the different interactions the peptide has with the various solvents. Although both $CHCl_3$ and acetone-d_3 are considered less polar than DMSO-d_6, their effects on the carbonyl chemical shifts were found to be dissimilar.

3.3. Proton NMR

3.3.1. Introduction to Proton NMR Studies

Proton NMR is a useful technique in the determination of peptide conformation and hydrogen-bonding patterns. Once the assignment of the individual proton resonances is completed, the hydrogen-bonding patterns can be elucidated by following the temperature-dependencies of the NH resonances. The characteristic splitting patterns observed for individual NH protons can yield coupling constants which are related to the dihedral angle of the N-C^{α} bond (ϕ angle) and can be used for an estimation of the peptide's conformation. The assignment of the

resonances of a proton NMR spectrum rely on the intensity, location and splitting patterns of the proton peaks as well as on the results of decoupling experiments. The proton(s) on one atom affect(s) the resonance pattern of the proton(s) on a neighbouring atom. The splitting pattern expected can be determined by the following formula:

$$(2n_A I+1)(2n_B I+1)$$

where I is the spin number of the particular nucleus being examined and n_A and n_B refer to the number of magnetically equivalent nuclei. Since the spin number of hydrogen is $\frac{1}{2}$ the above formula can be simplified to $(n_A+1)(n_B+1)$ (Jackman and Sternhell, 1969). Hence the NH proton of an alanyl residue yields a doublet since the neighbouring α-carbon has a single proton while with a glycyl residue, whose α-carbon has two protons, the NH would be expected to give rise to a triplet. The neighbouring carbonyl group has no protons so $n_B = 0$ in this instance. The patterns described above relate to first order conditions. The two α-carbon protons of the glycyl residue produce an ABX system which can produce secondary splitting patterns. Instances where secondary splitting patterns effect the interpretation of a proton NMR spectrum will be pointed out in the course of the discusion. Decoupling of a proton resonance would tend to affect those protons of the same molecule closest to it causing either a collapse of the peak or removal of the coupling effect (i.e. a triplet becomes a singlet). The location of peaks follows a general pattern with minor variations. These patterns along with an excellent discussion on the theory and practice of proton NMR are found in a monograph by Wuthrich (1976).

3.3.2. Proton NMR of N^{α}tBocProGlyAlaNHCH$_3$

3.3.2.1. Peak Assignments in DMSO-d_6

The proton NMR spectrum of N^{α}*t*BocProGlyAlaNHCH$_3$ in DMSO-d_6 at 24° C is shown in Figure 3-7. The peak assignments are listed in Table 3-12.Through carbon-13 NMR it was determined that, in DMSO-d_6, there exist two isomer populations (*cis* and *trans*) of N^{α}*t*BocProGlyAlaNNHCH$_3$ with the *cis* isomer being the more favoured (see section 3.2.2.1). On the basis of this observation, in instances where the resonances of of the two isomer populations of a particular proton were resolved, the resonance with the greater relative area was assigned to the *cis* isomer.

Peptide N<u>H</u> protons are expected to resonate in the 7-10 ppm region. The expanded spectrum of this region is shown in Figure 3-8. Glycine with two protons on its α-carbon is expected to yield a triplet for its N<u>H</u> proton if the two α-carbon protons are equivalent. With N^{α}*t*BocProGlyAlaNHCH$_3$, two well resolved triplets were found with chemical shifts (δ) of 8.07 and 8.24 ppm. The greater relative area of the former leads to its assignment to the glycyl N<u>H</u> corresponding to the *cis* isomer and that at 8.24 as corresponding to the *trans* isomer. The occurrence of the triplets indicates that the two α-carbon protons are equivalent. The alanyl N<u>H</u> proton resonance was expected to yield a doublet because of the single proton on its α-carbon. The clear doublet centred at 8.01 ppm was therefore assigned to the alanyl N<u>H</u>. The protons of the NHC<u>H</u>$_3$ methyl group are expected to couple to the N<u>H</u>CH$_3$ resonance which would resonate as a quartet. What appeared to be a poorly resolved quartet at 7.70 ppm was assigned

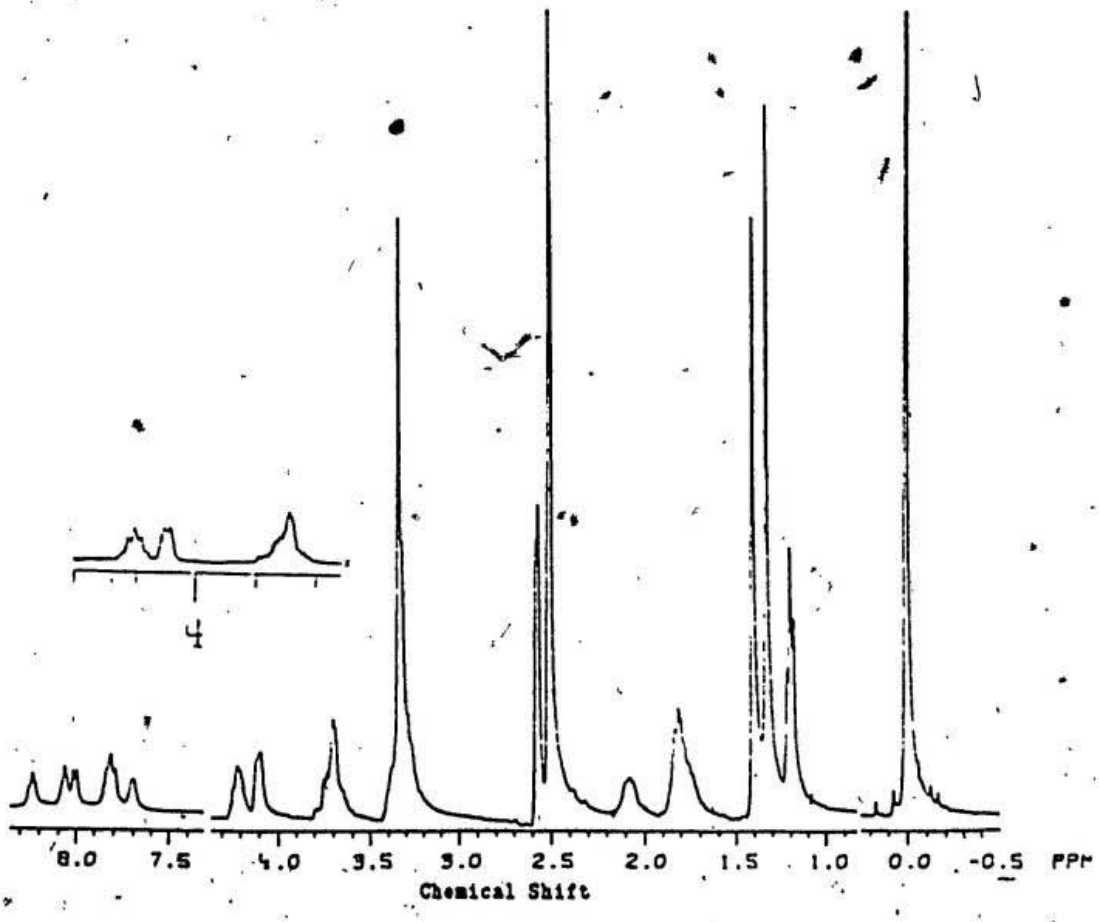

Figure 3-7: Proton NMR Spectrum of N^{α}*t*BocProGlyAlaNHCH$_3$ in DMSO-d$_6$

Table 3-12: Proton NMR Peak Assignments of N^{α}*t*BocProGlyAlaNHCH$_3$ in DMSO-d$_6$

Resonance	*t*Boc	Pro	Gly	Ala	$NHCH_3$
$(C\underline{H}_3)_3$-C-O	1.39^t 1.32^c	---	---	---	---
α-C$\underline{H}$	---	4.21	4.10	3.70	---
β-C$\underline{H}$	---	2.07	---	1.19	---
γ-C$\underline{H}$	---	1.81	---	---	---
δ-C$\underline{H}$	---	3.35	---	---	---
N$\underline{H}$	---	---	8.24^t 8.07^c	8.01^t 7.82^c	7.70^t 7.83^c
$NHC\underline{H}_3$	---	---	---	---	2.56

Chemical shift values in ppm, t = *trans* isomer, c = *cis* isomer

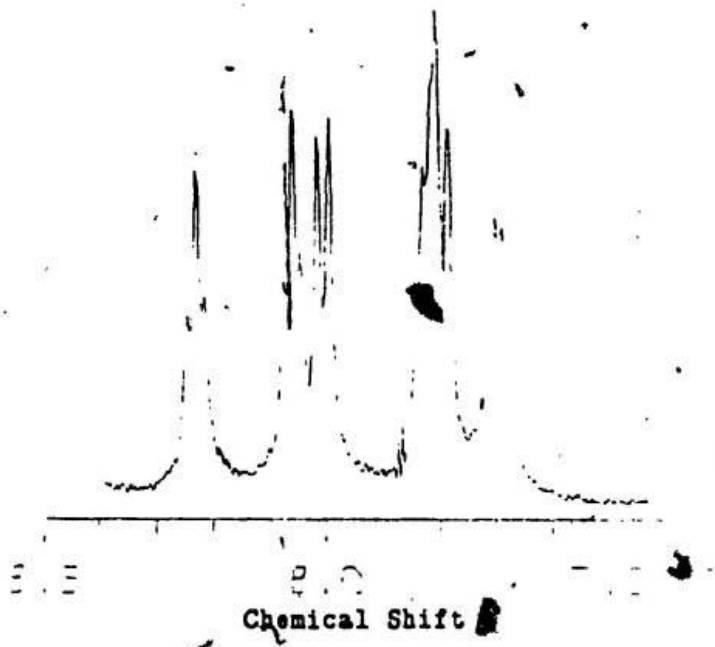

Figure 3-8: Expanded NH Region of the Proton NMR Spectrum of N^{α}*t*BocProGlyAlaNHCH$_3$ in DMSO-d$_6$

to the NH proton of the $NHCH_3$. Unfortunately, the two remaining resonances in the NH region overlapped to some degree. However, it appeared that the peak at 7.80 ppm was part of a doublet centred at 7.82 ppm and the peaks around 7.83 ppm were a composite of a quartet and the other half of the doublet. A comparison of the integrated peak area of the doublet at 7.82 ppm with the doublet at 8.01 ppm allowed the assignment of the former resonance as being due to the alanyl NH of the *trans* isomer and the latter as corresponding to the resonance of the alanyl NH of the *cis* isomer. By an identical process, the quartet at 7.70 ppm was assigned to the $NHCH_3$ resonance of the *trans* resonance while the quartet at 7.83 ppm was assigned to the $NHCH_3$ resonance of the *cis* isomer.

The α-carbon proton resonances are located in the region from 3.6 to 4.4 ppm. The *cis/trans* isomers were found to be unresolved. The individual assignments rely heavily on the peak splitting patterns (see Figure 3-7). The proline α-CH resonance was expected to be a triplet because of the two proline β-carbon protons. The well-resolved triplet at 4.21 ppm was therefore assigned to the proline α-carbon protons. The alanyl α-carbon proton is coupled to three methyl protons and to the NH proton and hence would be expected to resonate as an octet. Therefore, the multiplet at 3.70 ppm was assigned to the alanyl α-CH. Glycyl α-CH resonances may not occur as a doublet if the two α-carbon protons on the glycine are non-equivalent. Non-equivalent protons would be expected to produce a quartet. However, there was a well resolved doublet at 4.10 ppm and it was assigned to the glycyl α-carbon protons.

Electron-withdrawing groups such as oxygen and nitrogen have a deshielding

effect on neighbouring protons as does the proline ring. Deshielded protons tend to be shifted downfield (i.e. to a higher ppm). In addition to the standard methods used above, the following assignments relied on these additional factors. Both the proline ring δ-carbon and $NHC\underline{H}_3$ methyl protons were expected to resonate at a position appropriate to the deshielding effect of the neighbouring nitrogen. The multiplet at 3.35 ppm was therefore assigned to the two proline δ-C<u>H</u>s. The multiplet arose from the coupling effect of the two neighbouring γ-C<u>H</u>s compounded by the non-equivalency of the two δ-carbon protons. The next farthest upfield peak was a doublet centred at 2.56 ppm which was assigned to the $NHC\underline{H}_3$ methyl protons. (The peak at 2.49 ppm was due to non-deuterated DMSO contamination.) The doublet arose from the coupling effect of the N<u>H</u> on the near equivalent methyl protons. The relative area of the doublet indicated that it was composed of the resonance contributions of three protons. The multiplets at 2.07 and 1.81 ppm were assigned to the proline ring β and γ-protons respectively. The β-carbon protons were expected to resonate as a multiplet because of the effect of the two protons on the proline ring γ-carbon, the single proton on the proline ring α-carbon and the non-equivalency of all involved proline ring protons. The same effect was seen with the γ-carbon protons except that these protons were spin-coupled to the two protons of the δ-carbon instead of the single α-carbon resulting in a more complex multiplet. The δ-C<u>H</u>s were differentiated from the γ-C<u>H</u>s on the basis of their greater simplicity and the added effect of the carbonyl whose oxygen acts in a similar way to the nitrogen. Both carbons are the same distance from the proline nitrogen so the protons closest to the deshielding oxygen are expected to be the farthest downfield.

The remaining peak assignments were relatively straight forward. The relative intensity and position allow the assignment of the resonances at 1.32 and 1.39 ppm as belonging to the methyl protons of the *cis* and *trans* isomers of the *t*Boc respectively. The nine *t*Boc methyl protons produce a resonance which dominates the spectrum. The alanine β-carbon proton resonances are found at 1.19 ppm. They are usually the most upfield resonances of all (Wuthrich, 1976).

3.3.2.2. Peak Assignments in $CDCl_3$

The proton NMR spectrum of N^{α}*t*BocProGlyAlaNHCH$_3$ in $CDCl_3$ is shown in Figure 3-9. The peak assignments are listed in Table 3-13. Only one isomer was found to exist. As mentioned in the introduction to this chapter, $CDCl_3$, because it is relatively non-polar, is not expected to disrupt *intra*molecular hydrogen bonds and hence the *trans* isomer is expected to be predominant. The stabilizing effect of chloroform on the *trans* isomer was demonstrated with the carbon-13 data of the DAla-peptide, which in $CHCl_3$, existed nearly 100% as the *trans* isomer. Therefore, it was assumed that in $CDCl_3$, N^{α}*t*BocProGlyAlaNHCH$_3$ exists only as the *trans* isomer. The reasoning behind the assignments was much the same as when DMSO-d_6 was used as the solvent. Expected peak splitting patterns are identical to those described in the section on the title peptide in DMSO-d_6 (see section 3.3.2.1).

The peptide NH protons of the peptide in $CDCl_3$ resonate between 6.8 and 7.5 ppm. The expanded spectrum of the NH region is shown in Figure 3-10. Alanine, with a single α-carbon proton is expected to yield a doublet. The well resolved doublet at 7.45 ppm was therefore assigned to the alanyl NH. The remaining two

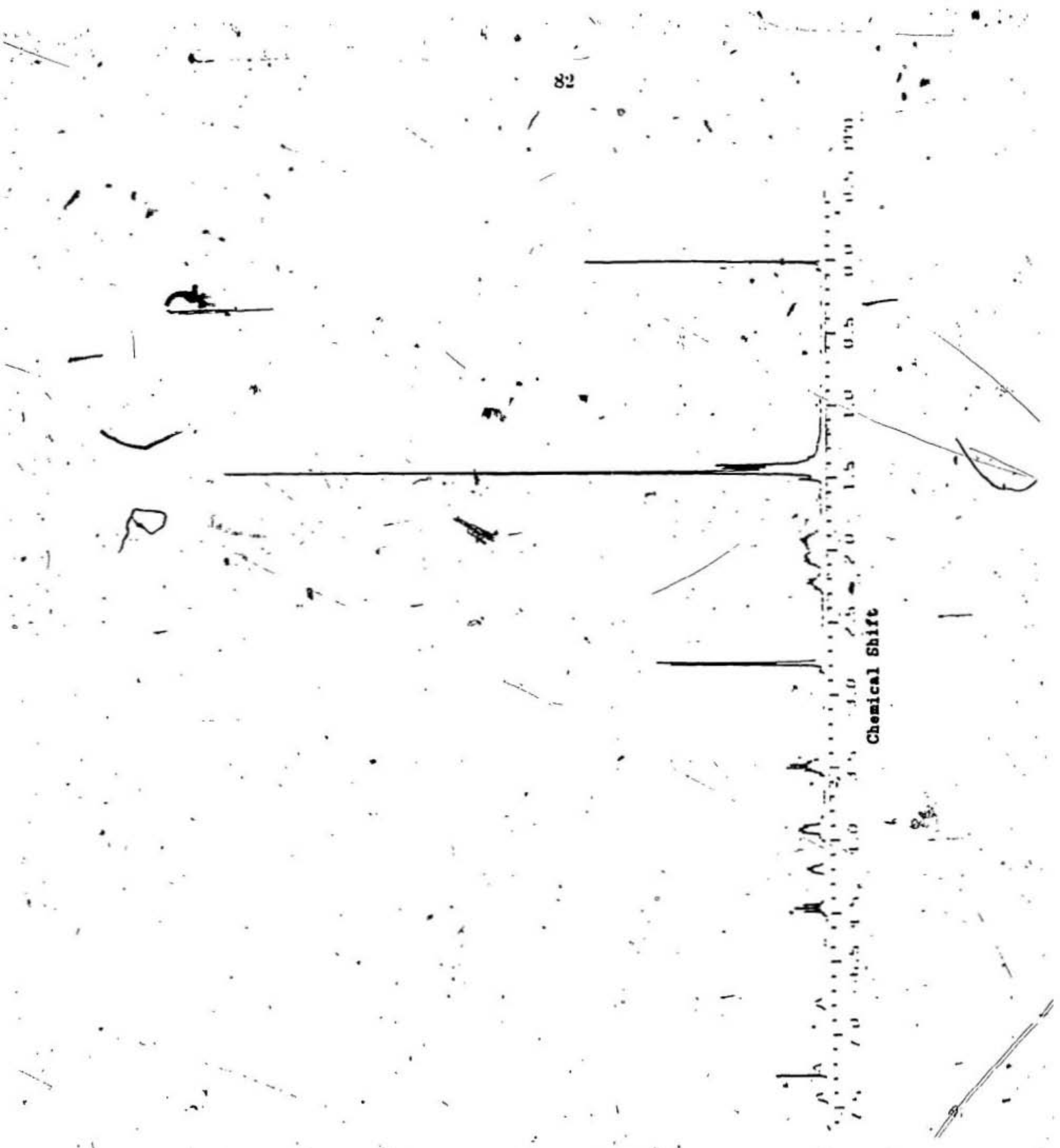

Figure 3-9: Proton NMR Spectrum of N^{α}*t*BocProGlyAlaNHCH$_3$ in CDCl$_3$.

Table 3-13: Proton NMR Peak Assignments of N^{α}*t*BocProGlyAlaNHCH$_3$ in $CDCl_3$

Resonance	*t*Boc	Pro	Gly	Ala	$NHCH_3$
$(CH_3)_3$-C-O	1.46	---	---	---	---
α-CH	---	4.20	3.93	4.46	---
β-CH	---	2.25	---	1.42	---
γ-CH	---	2.07 1.94	---	---	---
δ-CH	---	3.50	---	---	---
NH	---	---	7.26	7.45	6.81
$NHCH_3$	---	---	---	---	2.79

Chemical shift values in ppm

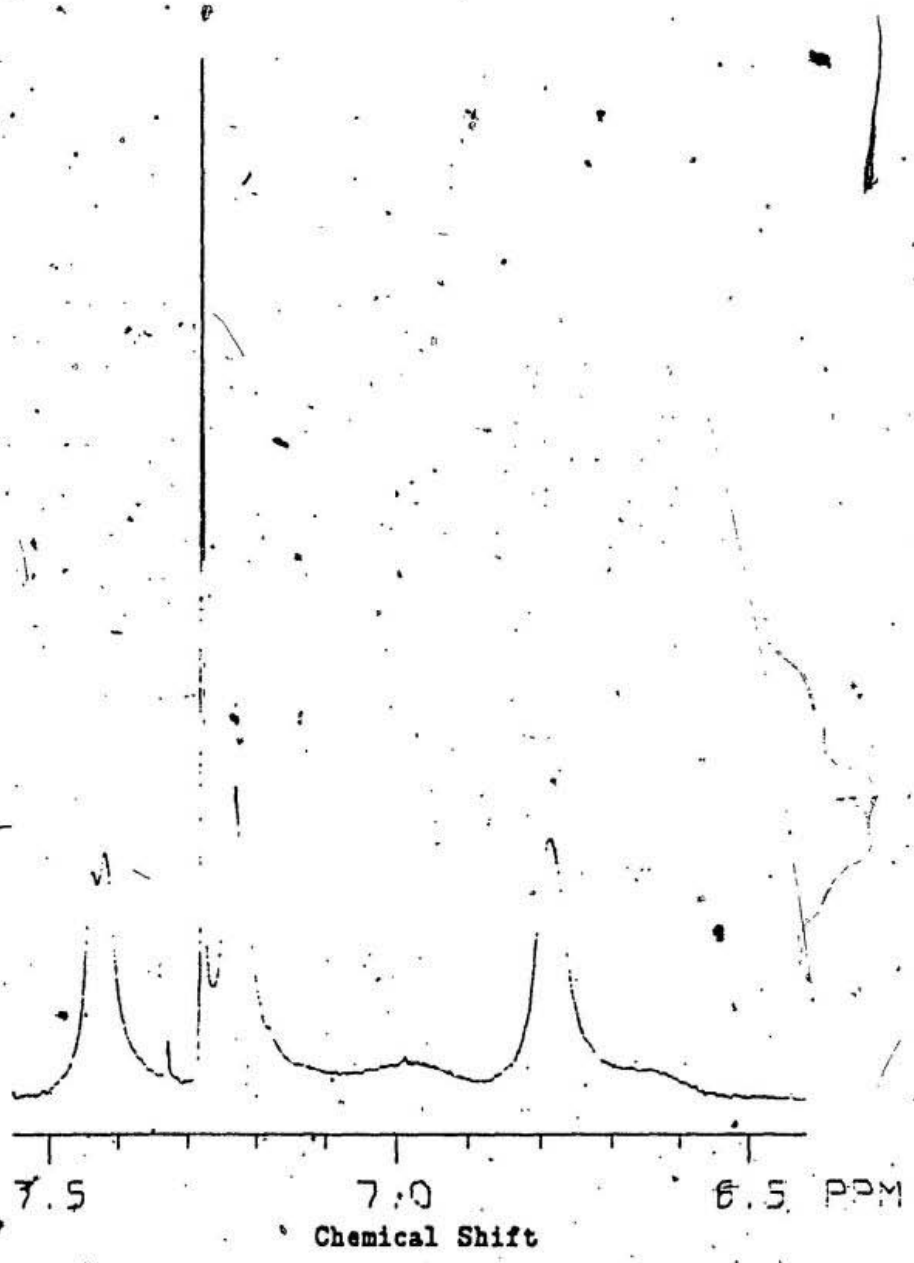

Figure 3-10: Expanded NH Region of the Proton NMR Spectrum of N^{α}*t*BocProGlyAlaNHCH$_3$ in $CDCl_3$

NH resonances at 7.26 ppm and 6.81 ppm were not well resolved. The glycyl NH, because of its two α-carbon protons, was expected to resonate as a triplet. The signal centered at 7.26 ppm could be considered a triplet and was assigned to the NH of the glycine. The NH proton of the $NHCH_3$ is coupled to the three protons of the $NHCH_3$ methyl group. The broad singlet at 6.81 ppm was considered representative of an ill-resolved multiple and was therefore assigned to the $NHCH_3$. The lack of resolution could be due to a weak four bond coupling to the alanine α-carbon proton. In DMSO-d_6 the NH resonance corresponding to the $NHCH_3$ of the title peptide was also not very well resolved (see section 3.3.2.1). The peak at 7.27 ppm is due to non-deuterated $CHCl_3$.

The α-carbon proton resonances are found between 3.9 and 4.5 ppm. The proline α-carbon proton is coupled to the two protons of the proline β-carbon. Hence the triplet at 4.20 ppm was assigned to the proton of the prolyl α-carbon. An octet was expected for the alanyl α-carbon proton and therefore the multiplet at 4.46 ppm was tentatively assigned as being due to the α-carbon proton. Decoupling experiments showed that the alanine α-carbon proton was coupled to both the alanine NH at 7.45 ppm and the alanine β-CH at 1.42 ppm. As in DMSO-d_6, the alanine β-CH was the most upfield resonance. The decoupling observations add further strength to the assignment of all the alanine protons. There was no further information derived from the decoupling experiments. The remaining multiplet, at 3.93 ppm, was easily assigned to glycine if one considers the two α-carbon protons to be slightly non-equivalent. The non-equivalency would give rise to complex second order splitting patterns which would appear as

a multiplet. The slight non-equivalency might also explain the ill-resolved nature of the glycine NH resonance.

The remaining resonances follow a pattern very similar to that seen with the peptide in DMSO-d_6. The δ-CHs of the proline are, as expected, shifted downfield because of the effect of the proline nitrogen and were found as a multiplet at 3.50 ppm. The doublet at 2.79 ppm is representative of the $NHCH_3$ methyl group protons. The peak at 1.46 ppm belongs to the methyl group protons of the *t*Boc. The resonance at 2.25 ppm was assigned to the proline ring β-carbon protons. Those of the proline ring γ-CHs were found as a composite of two broad multiplets at 2.07 and 1.94 ppm. Both the latter peaks are broad, the edges of one contributing to the size of the other. The effect results from the non-equivalency of the proline γ-CHs, and can also be seen in the spectrum of N^{α}tBocProDAlaOH in DMSO-d_6 (Attah-Poku and Ananthanarayanan, to be published). The fact that this type of pattern was seen with both peptide analogues in $CDCl_3$ demonstrates that it is not a function of *cis/trans* isomeration (see section 3.3.3.2). Proline ring puckering cannot be wholly ruled out but one would expect to see an enhanced effect with the CHs closer the the main chain of the peptide.

3.3.2.3. Peak Assignments in Acetonitrile-d_3

The proton NMR spectrum of N^{α}*t*BocProGlyAlaNHCH$_3$ is shown in Figure 3-11. The peak assignments are listed in Table 3-14. The resonance assignments were made through the position and splitting of peaks as outlined in the previous sections on proton NMR (see above). Carbon-13 NMR indicated that

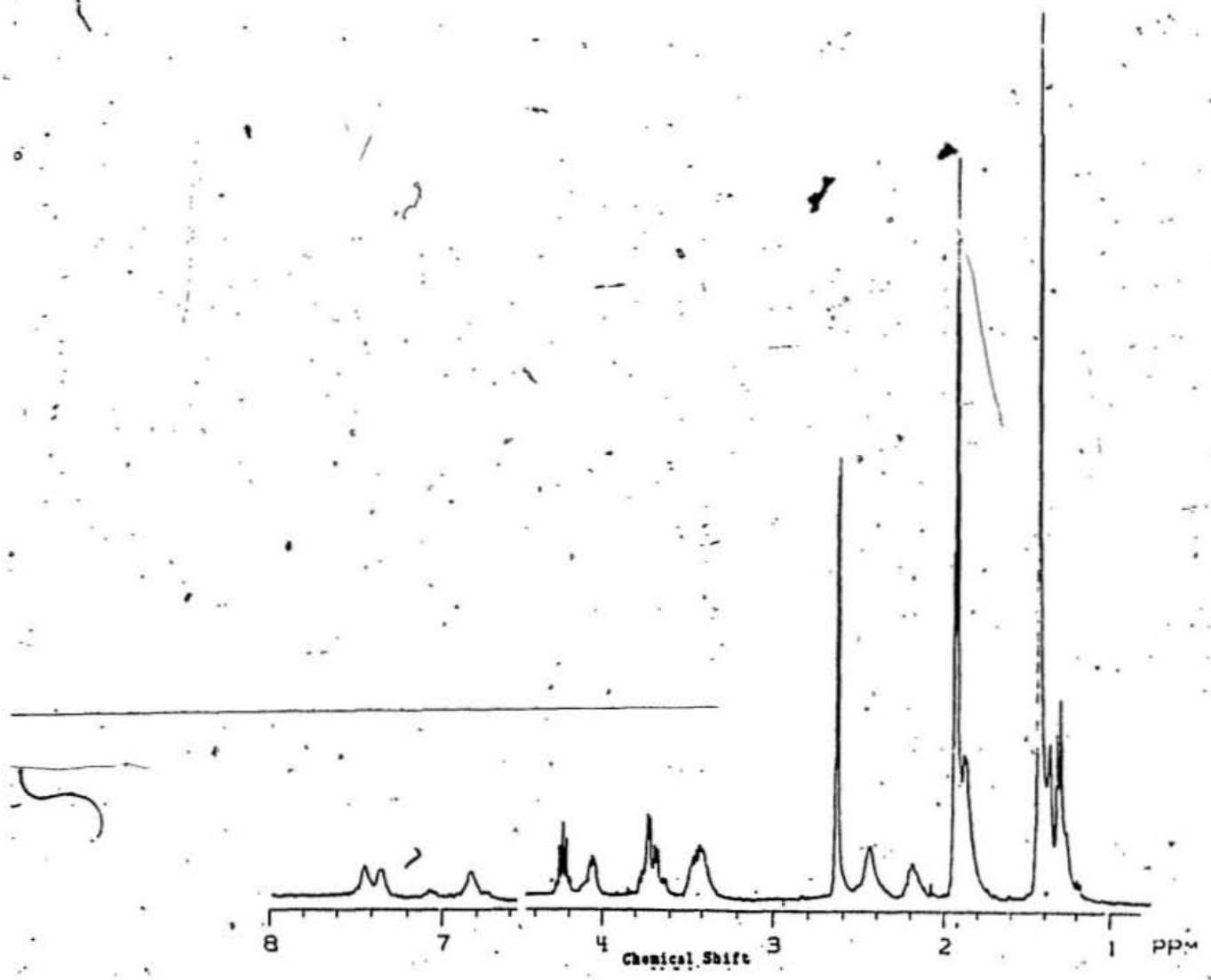

Figure 3-11: Proton NMR Spectrum of $N^{\alpha}t$BocProGlyAla$NHCH_3$ in Acetonitrile-d_3

Table 3-14: Proton NMR Peak Assignments of N^{α}*t*BocProGlyAlaNHCH$_3$ in Acetonitrile-d$_3$

Resonance	*t*Boc	Pro	Gly	Ala	$NHCH_3$
$(C\underline{H}_3)_3$-C-O	1.45	---	---	---	---
α-C$\underline{H}$	---	4.08	3.71* 3.75	4.25	---
β-C$\underline{H}$	---	2.47	---	1.33	---
γ-C$\underline{H}$	---	2.19	---	---	---
δ-C$\underline{H}$	---	3.45	---	---	---
N$\underline{H}$	---	---	7.45	7.37	6.85
$NHC\underline{H}_3$	---	---	---	---	2.66

Chemical shift values in ppm
* due to non-equivalency of the two glycyl α-C$\underline{H}$s

in acetonitrile-d_3 the peptide existed 16.2 ± 4.5 percent in the *cis* form and 83.8 ± 4.5 percent in the *trans* form.

The NH protons resonated between 6.5 and 7.5 ppm. Figure 3-12 shows the expanded spectrum of the NH region. As can be seen, the resonances were not well resolved. However, this situation changed dramatically upon the addition of calcium perchlorate to a $[Ca^{2+}]/[Peptide]$ ratio of 6.5:1, the peaks became extremely well-resolved. The addition of calcium ions would be expected to affect the chemical shift of a resonance but, generally, not its splitting pattern since the number of protons on a neighbouring atom should remain the same. Conformational changes may affect coupling constants which, in extreme cases, may affect splitting patterns. It is, however, highly unlikely for a triplet to occur where there are not at least two protons on the neighbouring atom. The increased resolution may be a result of conformational changes of the peptide and/or a decrease in the number of available conformations. The flexible nature of the glycine residue could allow several peptide conformations even within the restrictions of a hydrogen-bonded *trans* isomer. The titration of calcium ion was originally an experiment in calcium-binding whose results will be described in Chapter 5. Although the chemical shifts of the NH resonances do change upon the addition of calcium ion, they do not cross over and hence the relative order remains the same. Figure 3-13 shows the expanded NH region of the proton NMR spectrum of N^{α}*t*BocProGlyAlaNHCH$_3$ in acetonitrile-d_3 with a $[Ca^{2+}]/[Peptide]$ ratio of 6.5:1. The doublet found at 7.56 ppm on the spectrum of the calcium-perturbed peptide corresponds to the noisy doublet centred at 7.37 ppm on the

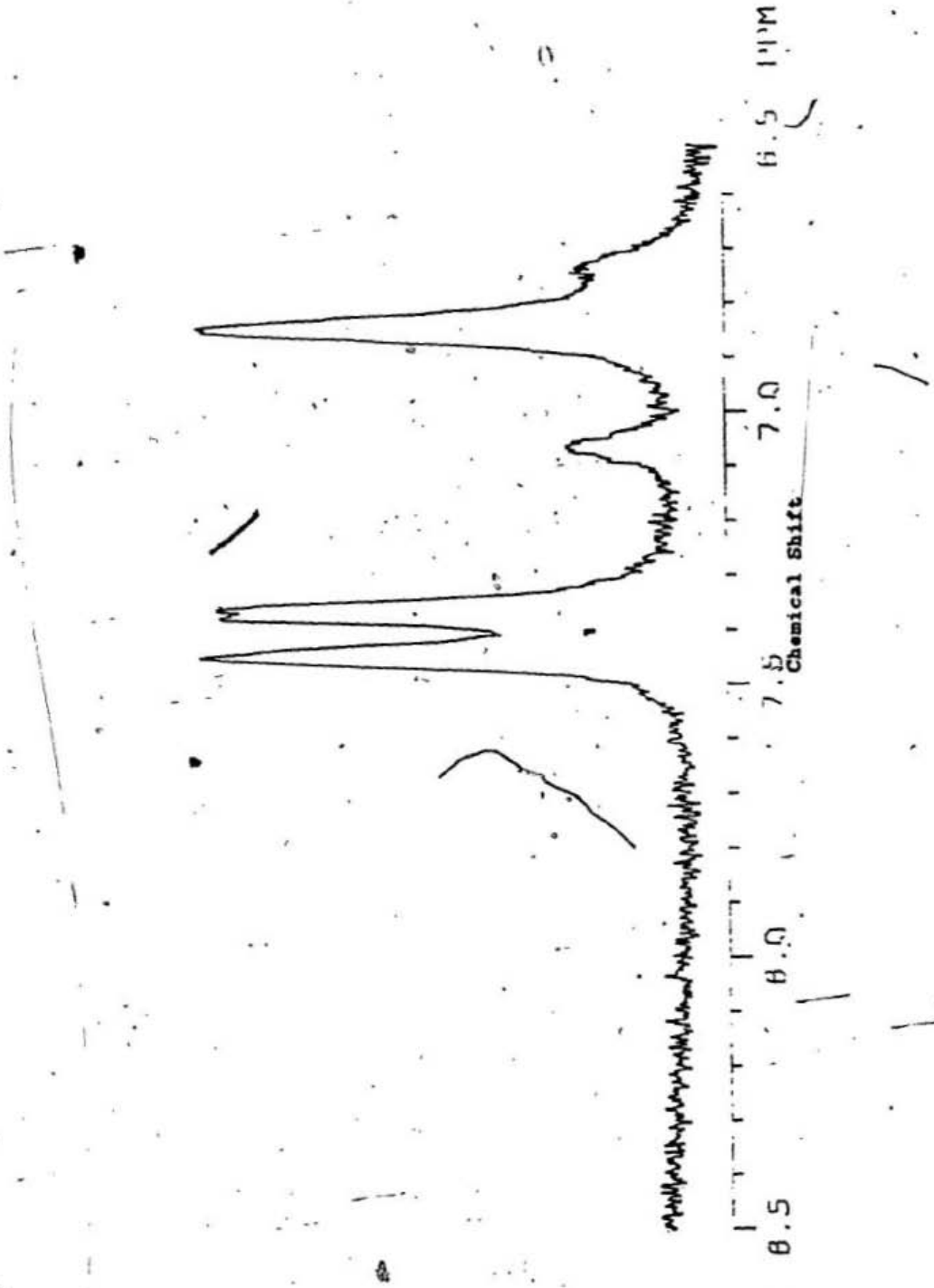

Figure 3-12: Expanded N<u>H</u> Region of the Proton NMR Spectrum of N^{α}*t*BocProGlyAlaNHCH$_3$ in Acetonitrile-d$_3$

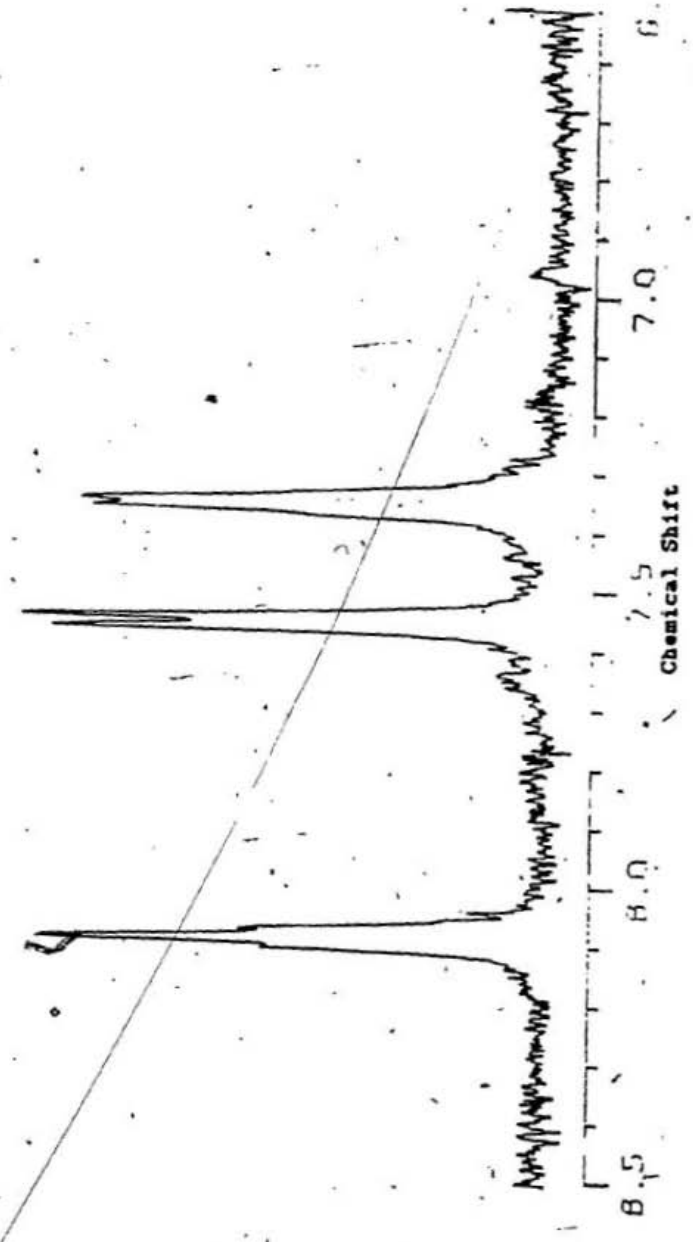

Figure 3-13: Expanded NH Region of the Proton NMR Spectrum of the Calcium-Perturbed N^{α}*t*BocProGlyAlaNHCH$_3$ in Acetonitrile-d$_6$

spectrum of the calcium-free peptide solution. Therefore, since the alanyl NH was expected to resonate as a doublet, the spectrum at 7.37 ppm was assigned to the alanyl NH. The resonance at 7.45 ppm on the spectrum of the peptide in acetonitrile-d_6 alone became a triplet at 8.09 ppm upon the addition of calcium ion. The glycyl NH resonance was expected to occur as a triplet and therefore the peaks at 8.09 ppm and 7.45 ppm were so assigned. The remaining NH resonance, centred at 6.85 ppm on the spectrum of the calcium-free peptide, appears as a poorly resolved quartet centred 7.36 ppm with the addition of calcium ion. Therefore, since the $NHCH_3$ was expected to resonate as a quartet, the resonance at 7.36 ppm on the spectrum of the unperturbed peptide was assigned to the $NHCH_3$. The two small peaks at 7.06 ppm and 6.74 ppm seen with the spectrum of the calcium-free peptide disappeared upon the addition of calcium ion. They were attributed to the *cis* isomer but could not be specifically assigned.

The α-carbon protons resonated between 3.7 and 4.3 ppm. The multiplet at 4.25 ppm was assigned to the alanyl α-CH which was expected to resolve as an octet. The two doublets which occurred close together at 3.71 and 3.75 ppm were assigned to the two glycyl α-CHs. The complex multiplet was attributed to secondary splitting patterns arising through the non-equivalency of the α-carbon protons. The resonance at 4.08 ppm, through the process of elimination, was assigned to the prolyl α-CH.

The remaining resonances followed closely the pattern seen with the proton NMR spectrum of the Gly-peptide in both DMSO-d_6 and $CDCl_3$. The resonance

at 3.45 ppm was assigned to the prolyl δ-carbon proton and the doublet at 2.66 ppm was assigned to the N<u>H</u>CH$_3$. The resonances at 2.47 ppm and 2.19 ppm were assigned to the prolyl β- and γ-carbon protons, respectively. The large resonance at 1.45 ppm was assigned to the methyl protons of the *t*Boc group and the doublet at 1.33 ppm was assigned to the alanyl β-carbon. The resonance at 1.96 ppm was attributed to non-deuterated acetonitrile contamination (Jackman and Sternhell, 1969).

3.3.2.4. Temperature-Dependence of N<u>H</u> Protons

The temperature coefficients of both solvent-shielded and solvent-exposed N<u>H</u> protons have been extensively characterized and documented (Stimson *et al.*, 1977; Urry and Long, 1976; Kopple, 1971; Brahmachari *et al.*, 1982). Based on the arguments of the above authors, temperature coefficients of -2x10^{-3} ppm/° C and -6x10^{-3} ppm/° C are expected for hydrogen-bonded and non-hydrogen-bonded N<u>H</u> protons, respectively. Non-hydrogen-bonded refer to N<u>H</u> protons which are not *intra*moleular hydrogen-bonded and whic may in fact be *inter*molecular hydrogen-bonded to solvent molecules. The results of temperature-dependance experiments on N$^{\alpha}$*t*BocProGlyAlaNHCH$_3$ in DMSO-d$_6$ are plotted in Figure 3-14, the slopes are presented in Table 3-15.Unfortunately, with this particular system the results were not definitive: All the N<u>H</u> peaks of the glycine peptide have slopes above -4x10^{-3} ppm/° C. Only the alanyl N<u>H</u> slopes are close to the -6x10^{-3} value of a non-bonded N<u>H</u> proton. The slope of the N<u>H</u> proton from the alanyl residue of the *trans* isomer may be questioned since it was determined from only three data points as opposed to a larger number (6) used for the other protons.2.88 The peak collapsed into the *trans* isomer's N<u>H</u>CH$_3$

Table 3-15: Temperature-Dependence of NH Protons of N^{α}tBocProGlyAlaNHCH$_3$ in DMSO-d$_6$

Residue	N	Slope (x10^3 ppm/° C)
Glycine-trans	6	-4.38
Glycine-cis	6	-4.15
Alanine-trans	3	-6.09
Alanine-cis	6	-5.62
NHCH$_3$-trans	6	-4.19
NHCH$_3$-cis	6	-4.61

N = the number of values used to determine slope

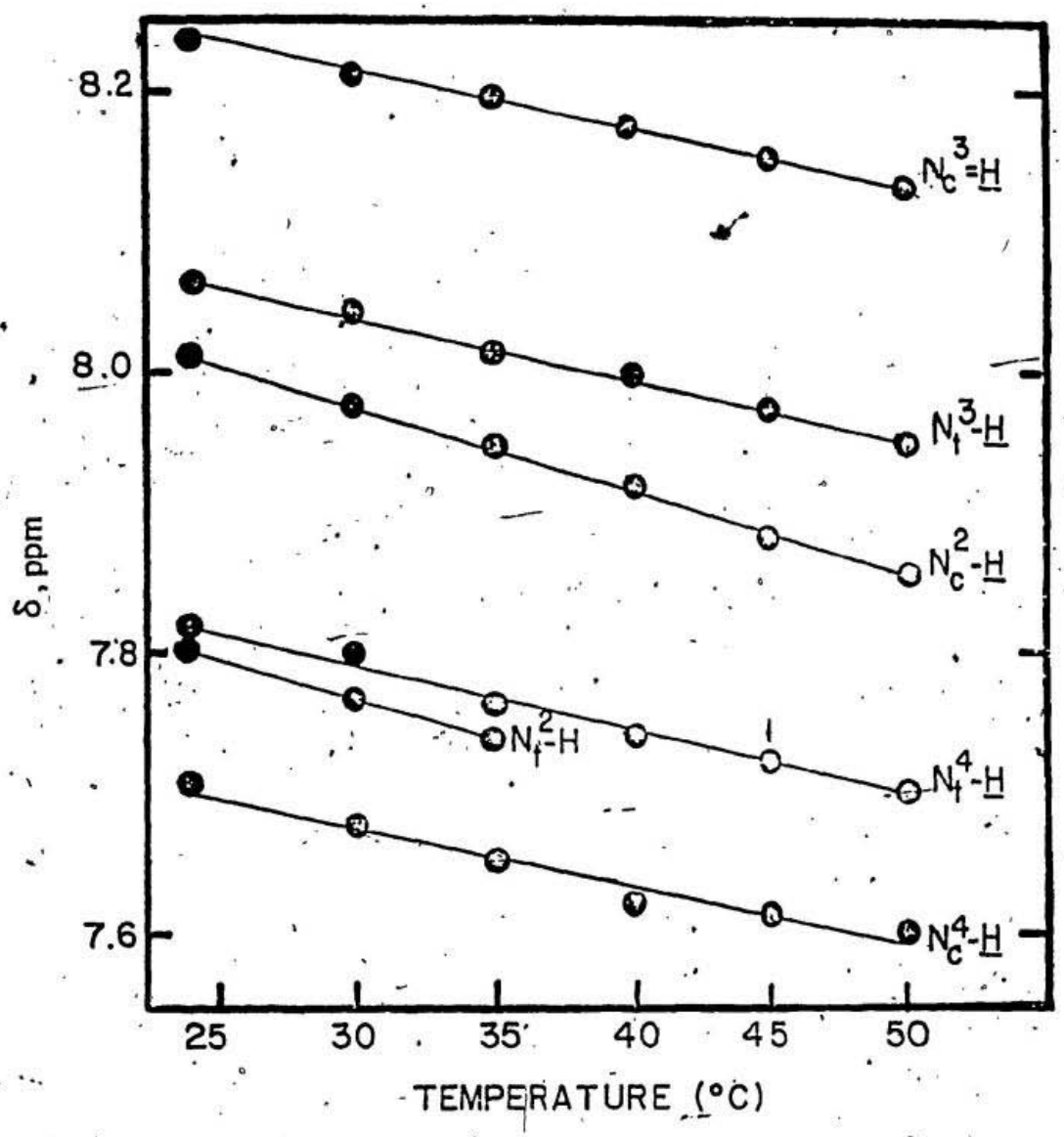

Figure 3-14: Temperature-Dependence of NH Protons of N^{α}tBocProGlyAlaNHCH$_3$ in DMSO-d_6

peak after only two temperature changes. The followed peak was also only one half of the doublet attributed to the *trans* isomer's alanyl NH, the other half being imperfectly resolved from the $N\underline{H}CH_3$ of the *trans* isomer. Hydrogen-bonding does occur as was shown by carbonyl solvent shifts (see section 3.2.4) and infrared data (see section 4.2). There are two possible explanations to why the results are ambiguous. First, the peak assignments could be incorrect. If this were so, there would have been one to three peaks whose temperature shifts would have been substantially lower than the others. This was not the case. The alternative reason revolves around the flexible nature of the glycyl residue. The conformation of the hydrogen-bonded structure may be more "loose" and hence be more subject to the effects of temperature. This would then serve as a contrast to what was observed with the more conformationally restrained DAla-peptide which gave much more definitive results with the temperature-dependance studies (see section 3.3.3.4).

3.3.3. Proton NMR of N^{α}tBocProDAlaAlaNHCH$_3$

3.3.3.1. Peak Assignments in DMSO-d_6

The proton NMR spectrum of N^{α}*t*BocProDAlaAlaNHCH$_3$ in DMSO-d_6 is shown in Figure 3-15. The peak assignments are listed in Table 3-16. The reasoning behind the peak assignments was similar to that employed with the Gly-peptide. Thus, the expected splitting patterns were analyzed as outlined in the section on the proton NMR of the glycine analogue in DMSO-d_6. However, the assignment of peaks based upon splitting patterns was not as successful as with the glycine analogue because of the presence of the two alanine enantiomers in the DAla-

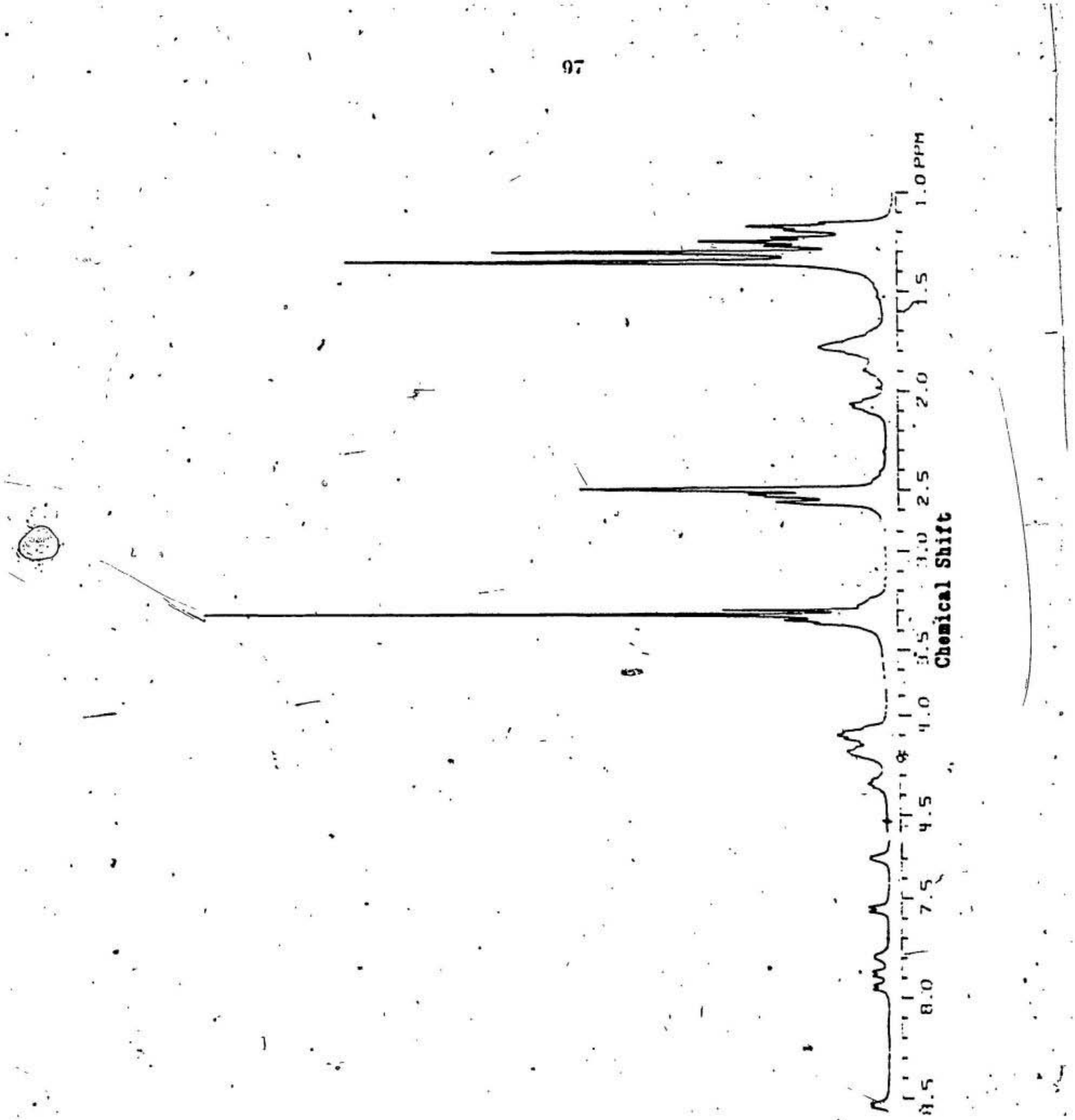

Figure 3-15: Proton NMR Spectrum of N^{α}*t*BocProDAlaAlaNHCH$_3$ in DMSO-d$_6$

Table 3-16: Proton NMR Peak Assignments of N^{α}*t*BocProDAlaAlaNHCH$_3$ in DMSO-d$_6$

Resonance	*t*Boc	Pro	DAla	Ala	NHCH$_3$
$(C\underline{H}_3)_3$-C-O	1.36^t 1.31^c	---	---	---	---
α-C$\underline{H}$	---	4.33	4.18	4.10	---
β-C$\underline{H}$	---	2.07	1.25	1.19	---
γ-C$\underline{H}$	---	1.81 1.90	---	---	---
δ-C$\underline{H}$	---	3.35	---	---	---
N$\underline{H}$	---	---	7.95^t 7.88^c	7.55^t 8.55^c	7.30^t 7.80^c
NHC$\underline{H}_3$	---	---	---	---	2.55

Chemical shift values in ppm, t = *trans* isomer, c = *cis* isomer

peptide. The *trans* conformer was determined to be the more abundant species through carbon-13 NMR (see section 3.2.3.1). Hence, in instances when the resonances due to the *cis* and *trans* isomers are resolved, the peak with the greatest relative area will be assigned to the *trans* conformer.

The NH protons resonate between 7.3 and 8.6 ppm. The expanded spectrum of this region is shown in Figure 3-16. Although splitting patterns (in this set of experiments) were less informative when compared with the proton NMR data on the glycine analogue in DMSO-d_6, the NH region was much better resolved and the decoupling experiments were much more successful and informative. The assignment of the NH resonances of the $NHCH_3$ was relatively straight forward. The $NHCH_3$ was expected to resonate as a quartet and therefore the two non-doublet resonances at 7.30 and 7.80 ppm were so assigned. The larger resonance at 7.30 ppm was assigned to the $NHCH_3$ corresponding to the *trans* conformer, the smaller to the *cis* conformer. Both the alanine enantiomer NHs were expected to resonate as doublets. Therefore, the remaining assignments had to rely heavily on the results of the decoupling experiments. Unfortunately, neither of the $NHCH_3$ resonances was coupled to any of the doublets. To begin with, one of the doublets had to be assigned. Hydrogen-bonded NHs tend to be shielded to a greater extent than non-hydrogen-bonded NHs and are expected to be farther upfield. An example is derived from the $NHCH_3$ resonances of the title peptide in DMSO-d_6. This need not, however, always be the case. One only has to look as far as the glycine analogue in DMSO-d_6 for a contradiction. In the postulated double β-turn model (see section 1.5), the NHs belonging to both the L-alanine

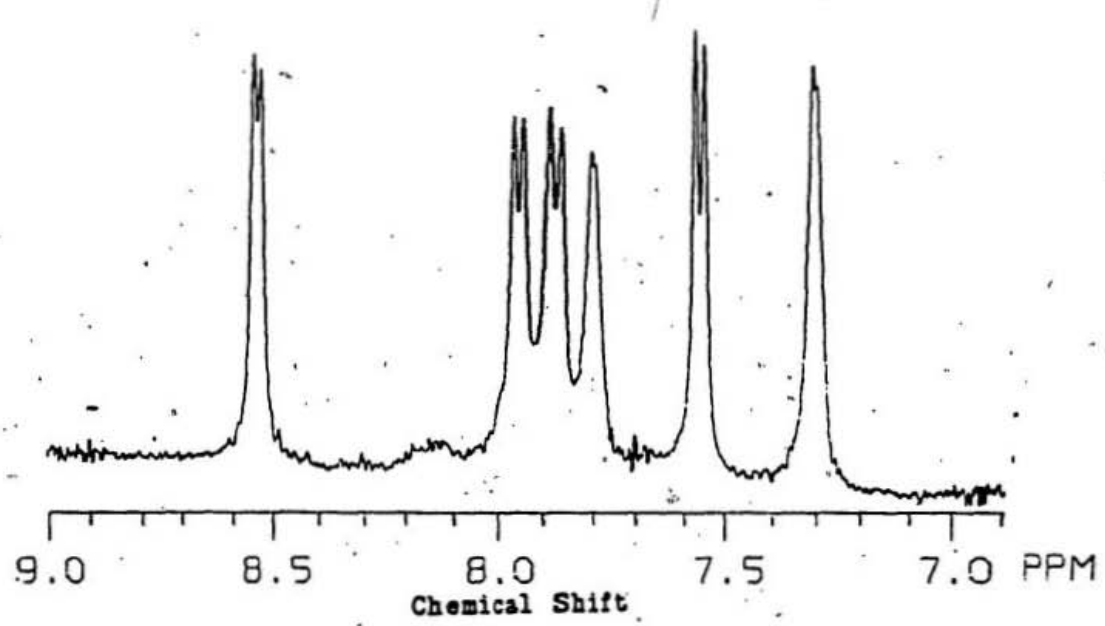

Figure 3-16: Expanded NH Region of the Proton NMR Spectrum of $N^{\alpha}t$BocProDAlaAlaNHCH$_3$ in DMSO-d_6

and the $NHCH_3$ of the *trans* peptide are expected to be hydrogen-bonded. The N<u>H</u> of the *trans* peptide $NHCH_3$ is already the farthest upfield of all the N<u>H</u> resonances. The next most upfield doublet resonated at 7.55 ppm and was tentatively assigned to the N<u>H</u> of the *trans* isomer's L-alanine. This resonance was strongly coupled to the doublet at 7.95 ppm and therefore the latter was assigned as the N<u>H</u> of the D-alanine belonging to the *trans* isomer. The two remaining doublets at 8.55 ppm and 7.88 ppm are strongly coupled to each other and are not coupled to any of the resonances previously assigned to the *trans* isomer. This, along with their relative intensity, indicate that both belong to the alanine enantiomers of the *cis* isomer. Which N<u>H</u> belongs to D-alanine and which to L-alanine requires more probing (see below).

The α-carbon proton resonances were found between 4.1 and 4.4 ppm. They were not resolved into *cis* and *trans* isomers. The α-carbon proton of proline was expected to resonate as a triplet. The triplet at 4.33 ppm was therefore assigned to the proline α-carbon proton. The prolyl α-C<u>H</u> was strongly coupled to the resonance at 7.88 ppm but not to the resonance at 8.55 ppm and therefore, since the D-alanine residue neighbours the proline residue, the resonance at 7.88 ppm was assigned to the D-alanine N<u>H</u> of the *cis* isomer and, through the process of elimination, the resonance at 8.55 ppm was assigned to the L-alanine N<u>H</u> of the *cis* isomer. The α-C<u>H</u> resonance at 4.10 ppm was coupled to the resonance at 8.55 ppm which had previously been assigned to the L-alanyl N<u>H</u> of the *cis* isomer and was therefore assigned to the L-alanine α-C<u>H</u>. Elimination and the fact that decoupling of the resonance at 4.18 ppm affects the resonances of both alanines (D

and L) of the *trans* peptide allows the assignment of that resonance to the D-alanine α-carbon proton.

The above assignments rely heavily on the assumption that the initial assignment of the resonance at 7.55 ppm to the L-alanyl NH of the *trans* isomer was correct. The relative areas of the coupled sets indicate that the *cis/trans* assignments were correct but it is possible that a C_7 ring can form with the tBoc carbonyl and the NH of the D-alanine.. The decoupling experiments could not rule this out, there being no contradiction if the resonance at 7.55 ppm is assigned to the NH of the D-alanine. However since the C_7 (γ-turn) has more conformational strain than the C_{10} (β-turn), especially with the proline residue in the middle, its existence is improbable. For the C_7 ring to form the proline carbonyl would have to be *cis* to the proline ring. Temperature-dependence and infrared studies add further support to the existence of the C_{10} ring as opposed to the C_7 (see sections 3.3.3.4 and 4.2).

The remaining assignments correlate very well with the glycine analogue. The reasoning remains the same. The multiplet at 3.35 ppm belongs to the proline δ-CH. In addition to the non-deuterated DMSO contamination at 2.49 ppm which was also found in the proton NMR spectrum of the Gly-peptide in DMSO-d_6, there is some H_2O contamination seen at 3.30 ppm (see Figure 3-15). The methyl protons of the $NHCH_3$ occur as a doublet at 2.55 ppm. The proline β-CHs are found at 2.07 ppm and those of the γ-CHs are found as a small peak at 1.90 ppm and a larger peak at 1.81 ppm. Both the latter peaks are broad, the edges of the former contributing to the size of the latter. As mentioned before, this

phenomenon is due to the non-equivalency of the proline ring γ protons; integration results support this interpretation. The resonances at 1.31 and 1.36 ppm correspond to the methyl group protons of the *t*Boc group of the *cis* and *trans* isomers, respectively. The most interesting thing about the region below the α-carbon protons is the assignment of the two triplets at 1.17 and 1.25 ppm. They are both due to the alanine β-carbon protons but cannot be accurately assigned to either the D or the L enantiomers with the data on hand. The fact that they were fairly well-resolved suggests that there is some difference in enviroments. The glycine analogue's L alanine β-carbon proton resonates at 1.19 ppm and therefore I would suggest that it is likely to be the L-alanine β-C<u>H</u> which resonates at 1.17 ppm and the D-alanine β-C<u>H</u> at 1.25 ppm. Confirmation would, however, require selective deuteration experiments.

3.3.3.2. Peak Assignments in $CDCl_3$

The proton NMR spectrum of N^{α}*t*BocProDAlaAlaNHCH$_3$ in $CDCl_3$ is shown in Figure 3-17. The peak assignments are listed in Table 3-17. The assignments of the proton NMR resonances of N^{α}*t*BocProDAlaAlaNHCH$_3$ in $CDCl_3$ were made through the position and splitting of peaks and through decoupling experiments, as outlined in previous sections (see above). As indicated in the section on carbon-13 NMR only the *trans* isomer of the DAla-peptide exists in chloroform (see section 3.2.3.2). As with the peptide in DMSO-d_6, one of the major problems was the existence of two enantiomers within the peptide. Because of this, splitting patterns would be less informative and problems with resolution may occur. Fortunately with this particular system the decoupling experiments were particularly successful.

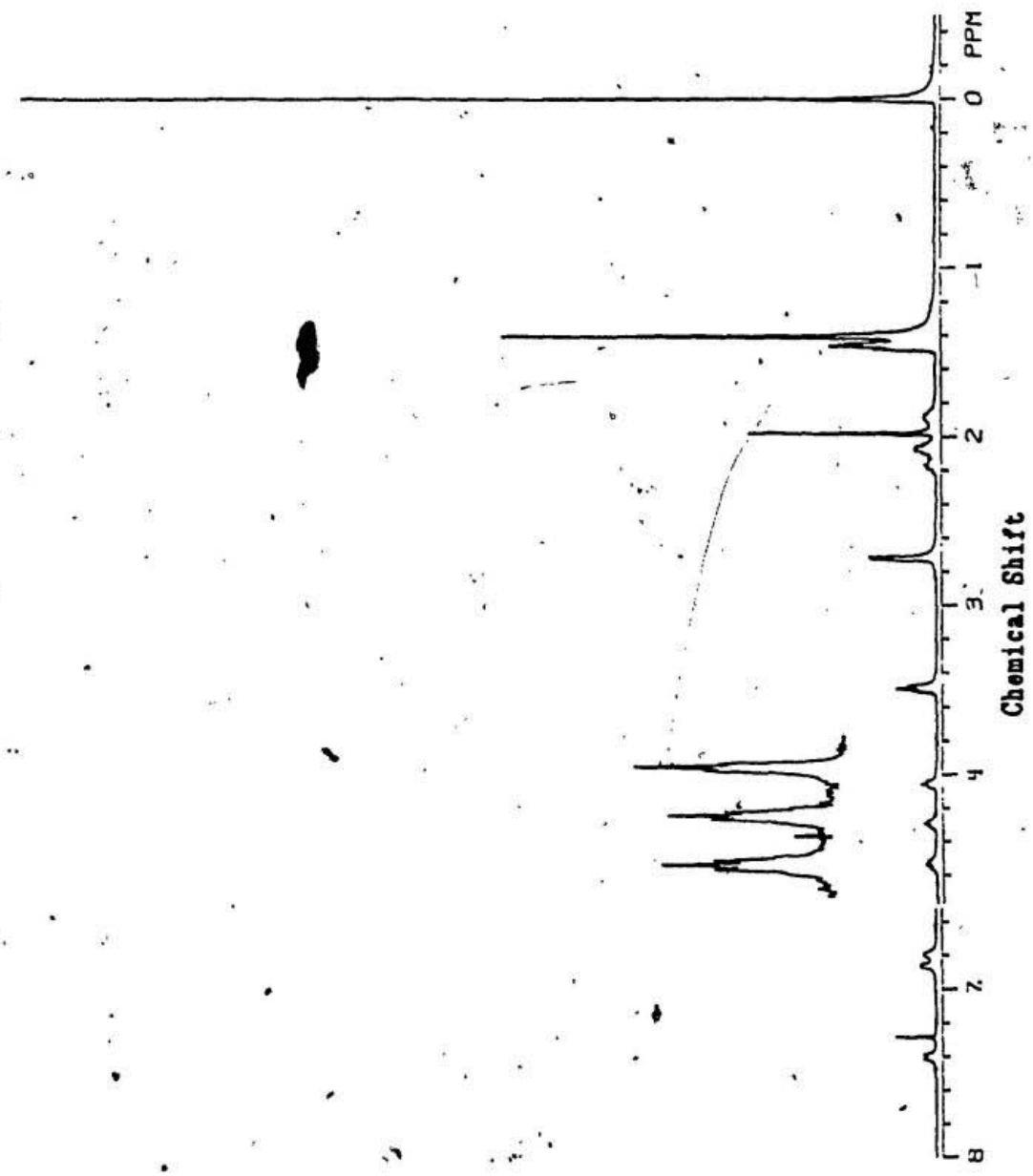

Figure 3-17: Proton NMR Spectrum of N^{α}tBocProDAlaAlaNHCH$_3$ in $CDCl_3$

Table 3-17: Proton NMR Peak Assignments of N^{α}*t*BocProDAlaAlaNHCH$_3$ in $CDCl_3$

Resonance	*t*Boc	Pro	DAla	Ala	$NHCH_3$
$(C\underline{H}_3)_3$-C-O	1.40	---	---	---	---
α-C$\underline{H}$	---	4.05	4.53	4.29	---
β-C$\underline{H}$	---	2.17	1.44*	1.48*	---
γ-C$\underline{H}$	---	2.07 1.88	---	---	---
δ-C$\underline{H}$	---	3.48	---	---	---
N$\underline{H}$	---	---	7.39	6.66	6.79
$NHC\underline{H}_3$	---	---	---	---	2.71

Chemical shift values in ppm
* Unsure of assignment

The NH protons resonate between 6.7 and 7.4 ppm. The expanded spectrum of this region is shown in Figure 3-18. The two alanine enantiomers, D and L, were expected to yield doublets in the NH region of the spectrum. Two such doublets are found at 7.39 ppm and at 6.66 ppm. The specific assignment of the doublets to either the D- or L- alanyl NH relied on the decoupling experiments. An ill-resolved quartet was found at 6.79 ppm and was attributed to the NH of the $NHCH_3$. The peak at 7.27 ppm was due to $CHCl_3$ contamination.

The α-carbon protons resonated between 4.0 and 4.6 ppm. A triplet was expected for the proline α-CH and therefore the well-resolved triplet at 4.05 ppm was assigned to the proline α-carbon proton. The alanine α-carbon protons was expected to resonate as quintets. The two quintets at 4.29 and 4.53 ppm were assigned to the D- and L- alanyl α-CH although, as with the corresponding NH resonances, the differentiation relied on the decoupling experiments.

The decoupling of one proton affects mainly those protons closest to it through the backbone of the peptide. The quartet at 6.79 ppm, attributed to the $NHCH_3$, was coupled to the doublet at 6.86 ppm and the α-CH resonance at 4.29 ppm. Both of those resonances were therefore assigned to the L-alanine. The resonance at 6.86 ppm was coupled to that at 4.29 ppm leaving little doubt that they belong to the same enantiomer. The other NH doublet at 7.39 ppm was coupled only to the quintet at 4.53 ppm and therefore both were assigned to the D enantiomer of alanine. The quintet at 4.53 ppm was also coupled to what had previously been assigned to the L-alanine α-carbon proton resonance. This indicated that they are neighbours and the initial assignment of the α-carbon protons was correct.

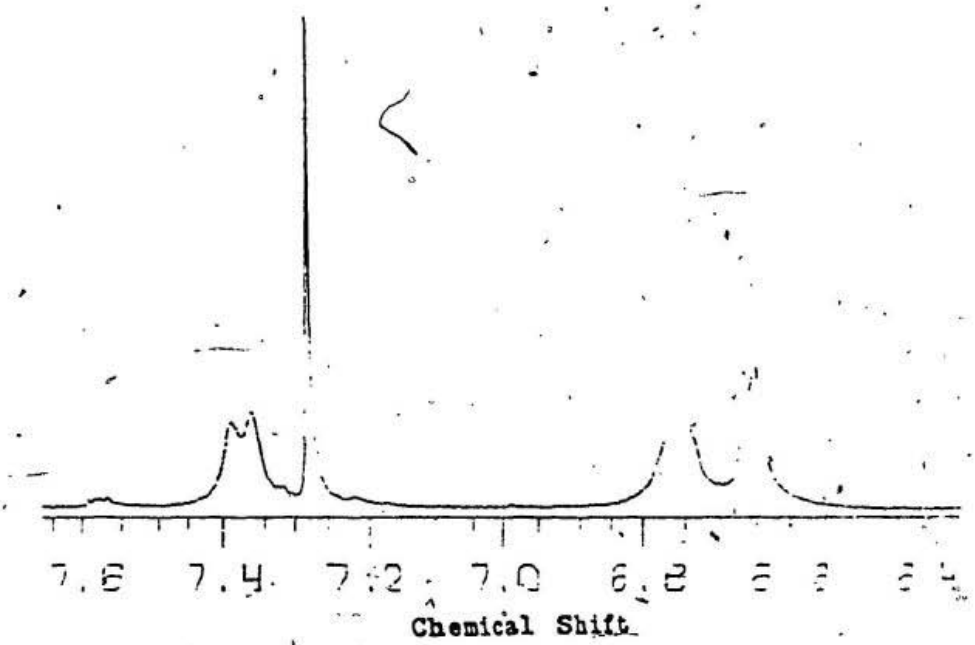

Figure 3-18: Expanded NH Region of Proton NMR Spectrum of N^{α}tBocProDAlaAlaNHCH$_3$ in $CDCl_3$

The remaining assignments were relatively straight forward and closely followed the pattern seen with both peptide analogues in the various solvents examined. The resonance at 3.48 were attributed to the proline ring δ-carbon protons. The doublet at 2.71 ppm belongs to the protons of the $NHCH_3$ methyl group. The peak at 1.40 ppm was due to the methyl protons of the *t*Boc and the cluster of peaks at 1.44, 1.46 and 1.48 ppm were due to the unresolved β-carbon protons of the two alanine enantiomers. The three broad multiplets at 2.17, 2.07 and 1.88 ppm are due to the proline ring β and γ protons. The pattern is representative of non-equivalent protons. Those peaks of the group farther downfield are due to the protons of the β-carbon because they are closer to, and hence more affected by, the deshielding carbonyl than those of the γ-carbon.

3.3.3.3. Peak Assignments in Acetone-d_6

The proton NMR spectrum of N^{α}*t*BocProDAlaAlaNHCH$_3$ in acetone-d_6 is shown in Figure 3-19. The peak assignments are listed in Table 3-18. The resonance assignments were made through the position and splitting of peaks as outlined in the previous section on NMR (see above). As with the peptide in DMSO-d_6 and $CDCl_3$, the assignment of NMR resonances was made difficult by the presence of two alanine enantiomers. Carbon-13 NMR indicated that only the *trans* isomer existed to any significant extent.

The NH protons resonate between 6.9 and 8.2 ppm. The expanded spectrum of this region is shown in Figure 3-20. The NH protons of the two alanyl residues (D and L) were expected to resonate as doublets and therefore, a well-resolved doublet found at 7.43 ppm was assigned to one of the alanyl NHs. Neither of the

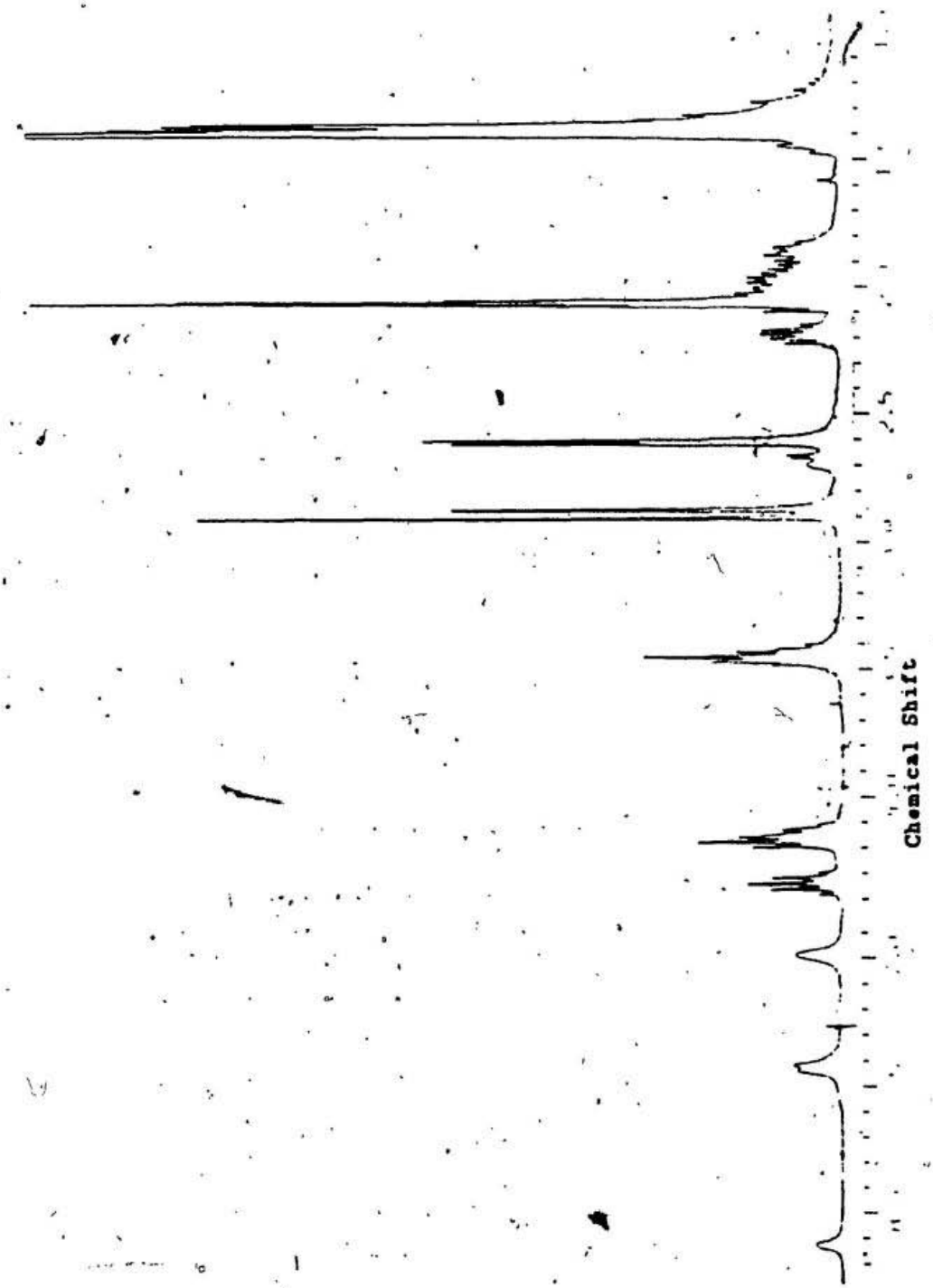

Figure 3-19: Proton NMR Spectrum of N^{α}tBocProDAlaAlaNHCH$_3$ in Acetone-d_6

Table 3-18: Proton NMR Peak Assignments of N^{α}*t*BocProDAlaAlaNHCH$_3$ in Acetone-d$_6$

Resonance	*t*Boc	Pro	DAla	Ala	$NHCH_3$
$(C\underline{H}_3)_3$-C-O	1.39*	---	---	---	---
α-C$\underline{H}$	---	4.17*	4.34	4.17*	---
β-C$\underline{H}$	---	2.18 2.00*	1.39*	1.39*	---
γ-C$\underline{H}$	---	2.00*	---	---	---
δ-C$\underline{H}$	---	3.44	---	---	---
N$\underline{H}$	---	---	8.12	7.43	6.98
$NHC\underline{H}_3$	---	---	---	---	2.61^{t} 2.68^{c}

Chemical shift values in ppm, t = *trans* isomer, c = *cis* isomer
* peaks with same chemical shift were unresolved from each other

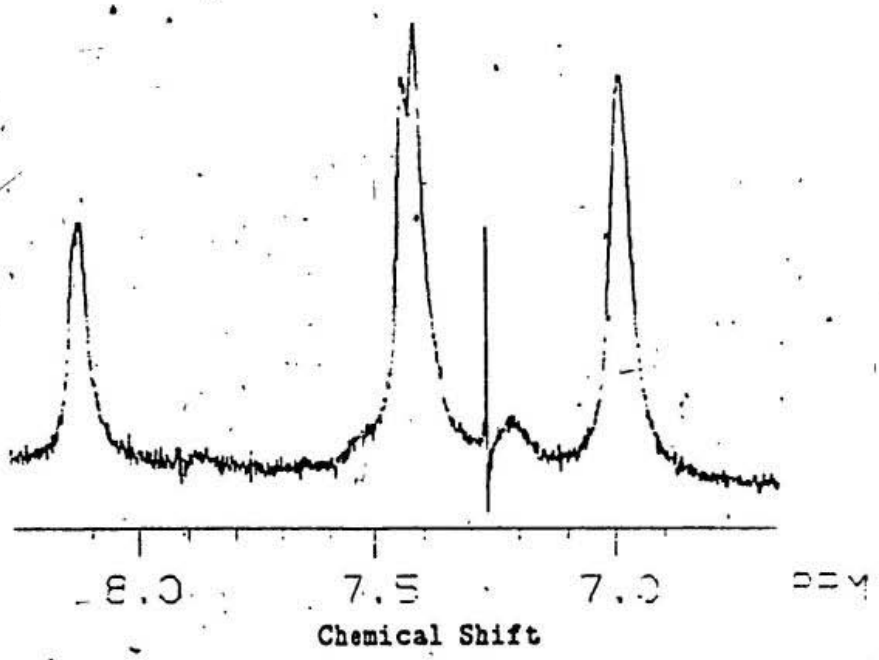

Figure 3-20: Expanded NH Region of the Proton NMR Spectrum of N^{α}*t*BocProDAlaAlaNHCH$_3$ in Acetone-d$_6$

two remaining NH resonances at 8.12 ppm and 6.98 ppm were resolved into a doublet nor a quartet which was expected for the NH of the $NHCH_3$. In both DMSO-d_6 and $CDCl_3$, the relative order, downfield to upfield, of the NH resonances was D-alanine, alanine and $NHCH_3$. Therefore, the resonance at 8.12 ppm was assigned to the D-alanyl NH, the doublet at 7.43 ppm was assigned to the alanyl NH and the peak at 6.98 ppm was assigned to the $NHCH_3$.

The α-carbon protons resonated between 4.1 and 4.4 ppm. The resonance centred at 4.34 ppm occurred as a quintet which was expected for an alanyl α-CH. The peaks centred around 4.17 ppm appeared to consist of the quintet expected for the other alanyl α-CH and the triplet expected for the prolyl α-CH. Based on the data in DMSO-d_6 and $CDCl_3$, where the D-alanyl α-CH resonance was downfield from the respective L-alanyl resonance, the quintet at 4.34 ppm was assigned to the α-CH of the D-alanyl and the peaks centred at 4.17 ppm were assigned to the α-CH of both the L-alanyl and prolyl residues.

The remaining peaks followed closely the pattern seen with both peptide analogues in various solvents (see above). There were, however, several unique features. The resonance at 3.44 ppm was assigned to the proline δ-carbon proton. The protons of the $NHCH_3$ methyl group were expected to resonate as a large doublet between 2.5 ppm and 2.8 ppm and therefore, the large doublet at 2.61 ppm was assigned to the $NHCH_3$ of the *trans* peptide. The very small doublet at 2.68 ppm appeared, with the exception of size, to be very similar to the doublet at 2.61 ppm and was therefore assigned to the $NHCH_3$ of the *cis* isomer. The amount of *cis* isomer was, as with the carbon-13 data, too low to quantify. The

peaks centred around 2.18 ppm were assigned to one of the proline β-carbon protons. The mass of peaks around 2.0 ppm were attributed to the other proline β-carbon proton, the γ-CHs and the non-deuterated acetone which was expected to resonate at 2.07 ppm (Jackman and Sternhell, 1969). The pattern is representative of non-equivalent protons. The resonances due to the *t*Boc methyl protons and both the alanyl β-carbon protons were not resolved from each other. They occurred as a large noisy multiplet centred around 1.39 ppm. The two peaks at 2.91 ppm and 2.88 ppm showed a marked solvent-dependency upon the addition of hydrated calcium perchlorate. Both peaks were shifted drasticly downfield to the point where, at a calcium to peptide ratio of five, they were found as a large peak at 4.33 ppm. Since the proton NMR resonances due to H_2O contamination are very solvent-dependent, the two peaks were attributed to H_2O contamination. The sharpness of the two signals indicated that there was a slow exchange between two populations. Elemental analysis indicated that the DAla-peptide crystallizes with one molecule of water (see section 2.2.4) and the peak at 2.91 ppm grows in intensity in relation to the peak at 2.88 ppm upon the addition of the hydrated calcium perchlorate. Therefore, the resonance at 2.88 ppm was attributed to water molecules hydrogen-bonded to the peptide and the resonance at 2.91 ppm was attributed to water molecules hydrogen-bonded to acetone.

3.3.3.4. Temperature-Dependence of NH Protons

Unlike the temperature-dependence data obtained with the glycine peptide the results with the D-alanine peptide were unambiguous. The results of the temperature dependence studies in DMSO-d_6 are plotted in Figure 3-21 and the slopes are listed in Table 3-19. Both the NH proton resonances assigned to the alanine and $NHCH_3$ of the *trans* isomer showed a large difference in the extents to which they were affected by temperature as compared to the other resonances. Both had slopes in the $-(2\text{-}3)\times10^{-3}$ ppm/° C range expected for hydrogen-bonded NH protons (Stimson *et al.*, 1977) The remaining NH proton resonances all had temperature-dependence slopes greater than -5×10^{-3} ppm/° C which was indicative of non-hydrogen-bonded NH protons (Stimson *et al.*, 1977). The NHs of the alanyl and $NHCH_3$ from the *trans* isomer were the two NHs expected to hydrogen bond if the peptide takes on a double β-turn character (see section 1.5). None of the *cis* isomer NHs nor the D-alanyl NH of the *trans* isomer were expected, or were found from the present data, to be hydrogen-bonded. The fact that there were two hydrogen-bonded NHs added further strength to the statement made earlier that the C_7 ring formed between the N^{α}*t*Boc C=O and the NH of the D-alanine was improbable (see section 3.3.3.1). If such a conformation did occur, the hydrogen bond between the NH of the $NHCH_3$ and the carbonyl of the proline could not have formed since the C=O would be pointing in the wrong direction (see sections 1.1 and 4.3) The peptide bond must remain in a planar *trans* configuration. This, however, was not proof since the second hydrogen bond could possibly have formed between the NH of the $NHCH_3$ and the carbonyl of the D-alanine thereby producing two hydrogen-bonded C_7

Table 3-19: Temperature-Dependence of NH Protons of N^{α}*t*BocProDAlaAlaNHCH$_3$ in DMSO-d$_6$

Residue	N	Slope (x10^3 ppm/° C)
D-Alanine-trans	11	-6.90
D-Alanine-cis	11	-6.06
Alanine-trans	12	-2.63
Alanine-cis	12	-7.69
$NHCH_3$-trans	12	-2.20
$NHCH_3$-cis	11	-5.14

N = the number of values used in the determination of slope

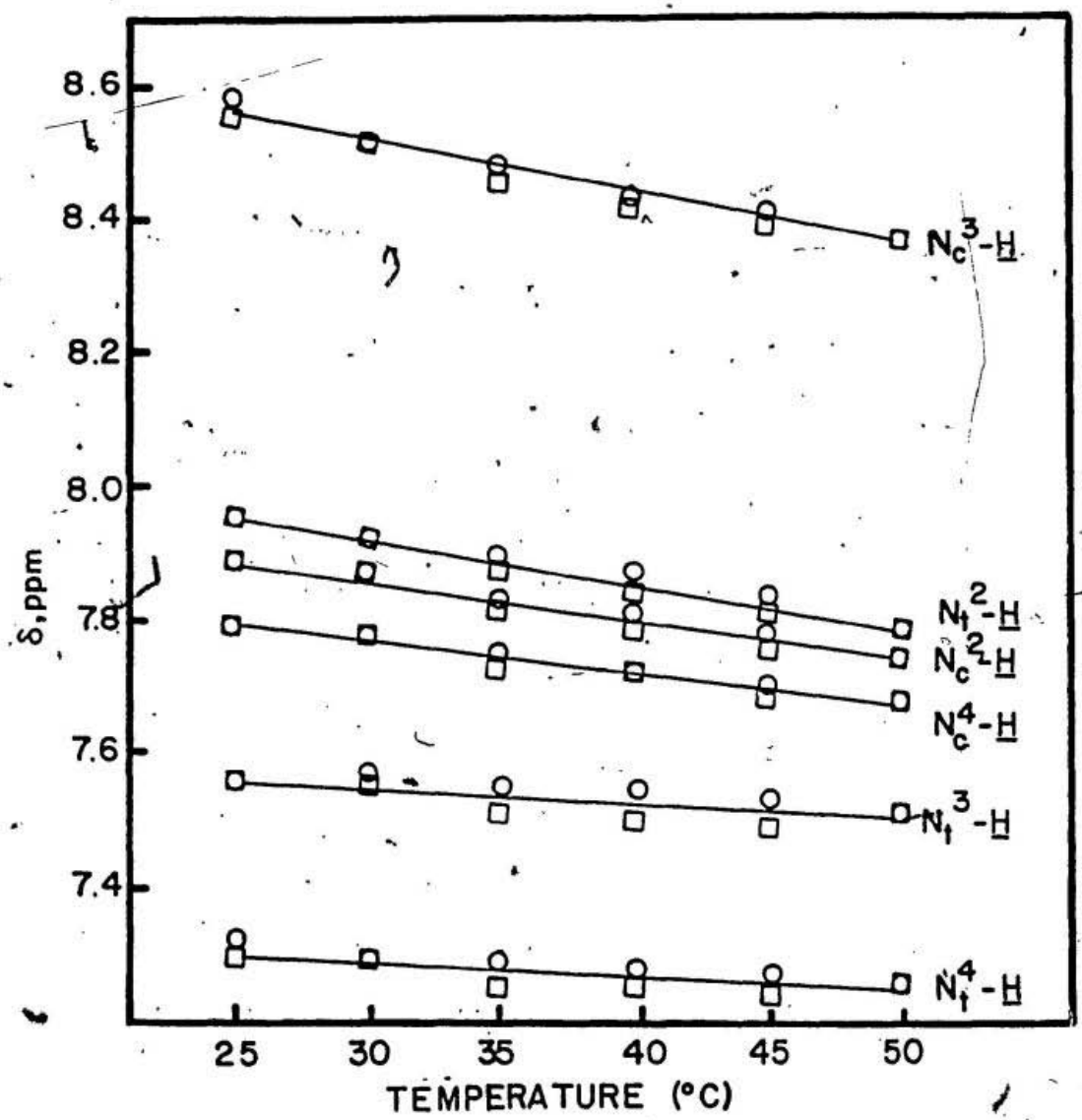

Figure 3-21: Temperature-Dependence of NH Protons of N^{α}tBocProDAlaAlaNHCH$_3$ in DMSO-d_6

rings. Although possible, this is highly unlikely, especially when one takes into account that the ProDAla sequence has been shown by both crystal and solution spectroscopic methods to contain a Type II β-turn configuration (Aubry *et al.*, 1977; Rao *et al.*, 1983; Ananthanarayanan and Cameron, to be published). The L-proline-D-alanine configuration provides enough steric hindrance to support the statement that the Type II β-turn configuration was maintained in the N^{α}*t*BocProDAlaAlaNHCH$_3$ peptide. The infrared data, to be discussed later (see section 4.2), will show that neither of the C_7 rings exist and therefore that the proton NMR peak assignments of the DAla-peptide in DMSO-d_6 are correct.

3.4. Conformational Information From Coupling Constants

3.4.1. Introduction

As stated in the introduction to proton NMR, the characteristic splitting patterns observed for individual N<u>H</u> protons can yield coupling constants which are related to the dihedral angle of the N-C^{α} bond (ϕ angle) and can be used to estimate a peptide's conformation. In an amino acid residue, the resonance of the N<u>H</u> proton is split due to spin-spin coupling with the proton(s) attached to the adjacent carbon atom(s). The coupling constant ($^3J_{N\underline{H}\text{-}C\underline{H}}$) donates the separation between the split resonance (measured in Hz) arising from the N<u>H</u>-C^{α}<u>H</u> coupling. The coupling constant can be related to the dihedral angle θ by a Karplus-type equation:

$$^3J_{N\underline{H}\text{-}C\underline{H}} = A\cos^2\theta + B\cos\theta + C\sin^2\theta$$

where A, B and C are constants. The coefficients depend upon the particular

model system used (Bystrov *et al.*, 1969, 1973; Ramachandran *et al.*, 1971). For the purposes here, the values of Bystrov *et al.* (1973) were used (A= 9.8, B= -1.1, C= 0.4). The resulting "Karplus-Type Curve" is shown in Figure 3-22. The conversion of θ to the Φ angles used in the description of peptides (see section 1.1) is achieved through θ+60 for L-amino acids and θ−60 for D-amino acids. The coupling constant cannot be derived directly from a triplet as observed with the NH resonance of a glycyl residue (ABX system) (see section 3.3.2). In such a case the separation between the two outside peaks of the triplet equals the sum of two coupling constants from which the Φ dihedral angle can be obtained directly through a modified Karplus-type equation (A= 6.0, B= -1.5, C= 12.5) (Wuthrich, 1976). The range for Φ and Ψ angles is -180° to 180° (Handbook of Biochemistry and Molecular Biology, 1976), all other values (*i.e.* 190°) are not permitted notations. The coefficients have been determined through experimental and theoretical studies and have to be expressed in terms of "permissible ranges" due to various effects such as electronegative side chain groups, rotational effects of the C^{α}-C' bond and deviations of the peptide bond from planarity (Wuthrich, 1976). The above $^{3}J_{NH\text{-}CH}$ values were in Hz and were converted from ppm by the equation J_{Hz}=360xJ_{ppm} since a 360 MHz instrument was used. Because of quadrupolar relaxation of the ^{14}N nucleus and, less frequently, to proton exchange the NH signals tend to be broad and can overlap. The overlap causes contraction of intercomponent spacing corrections for which are based on the peak-to-trough ratios of the doublets (Bystrov, 1976). The quoted coupling constants have been corrected with the exception of the glycine NH triplets. The derived Φ angles are accurate to ± 10°.

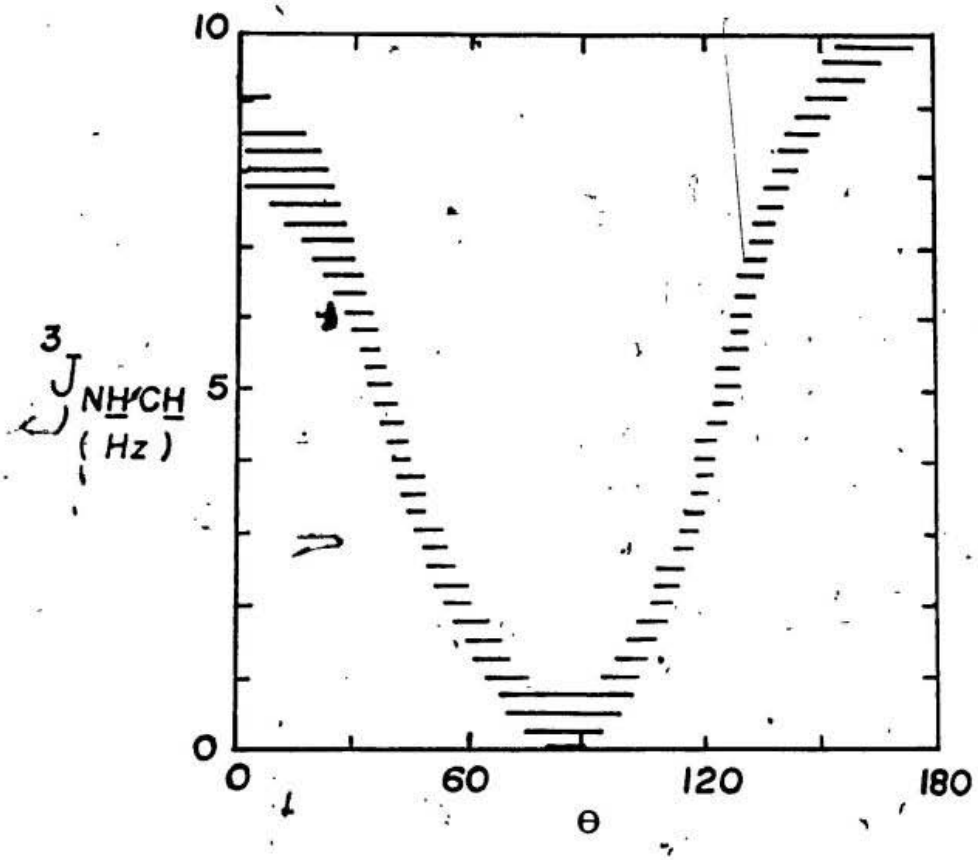

Figure 3-22: Relationship Between the NH-CH Coupling Constant and the ϕ Dihedral Angle

3.4.2. Conformation of N^{α}tBocProGlyAlaNHCH$_3$

In DMSO-d_6, the coupling constants from the NH resonances could only be obtained for the glycyl residue of both the *cis* and *trans* isomers, and the alanyl residue of the *trans* isomer. The other NH signals did not yield coupling constants because of the overlap or the ill-resolved nature of the quartet due to the $NHCH_3$ of the *cis* isomer (see section 3.3.2.1 and Figure 3-8). They were therefore not very helpful in structural determination. The ϕ angles, computed from the observed $^3J_{NH\text{-}CH}$ values, along with the actual coupling constants are shown in Table 3-20. The value of 194-202° for the ϕ angle of the alanyl residue is not permitted.

The tetrapeptide N^{α}tBocProGlyAlaNHCH$_3$ has been presumed to take on a double β-turn conformation in solution (see Chapter 4). The glycyl residue would act as the $(i+2)$th residue for the first β-turn and the $(i+1)$th residue for the second. The ϕ angle of the $(i+1)$th residue of a β-turn must be close to $\pm$ 60° (Venkatachalam, 1968). The value of 63° for the ϕ angle of the glycyl residue (see Table 3-20) is seen to provide the best fit. The positive value means the second β-turn could be either Type I', II' or III'. The proline ring restricts the prolyl residue ϕ angle to -60°. Therefore, with a ϕ angle of 63° for the $(i+2)$th residue and a proline at position $(i+1)$, the only possible conformation for the first β-turn is a Type II. Both solution and crystal studies have shown that ProGly containing β-turns tend to be Type II (Brahmachari *et al.*, 1979, 1981; Boussard *et al.*, 1979). Although 63° for the ϕ angle of the glycyl residue is close to the expected 60° of Type I' and Type III', both these conformations require a D

Table 3-20: N^{α}*t*BocProGlyAlaNHCH$_3$ ϕ Angles Derived from NH Resonance Coupling Constants in DMSO-d_6

Residue	$^3J_{NH\text{-}CH}$(Hz)	θ_1	θ_2	ϕ_1	ϕ_2
Gly-trans	5.22	--	--	63°	134°
Gly-cis	5.22	--	--	63°	134°
Ala-trans	7.56 (1.00)	8-25°	134-142°	68-85°	194-202°
Ala-cis	UR.	--	--	--	--
$NHCH_3$-trans	UR.	--	--	--	--
$NHCH_3$-cis	UR.	--	--	--	--

UR. ≒ unresolved (Correction Factor)
Coupling constant of glycine residue NH are uncorrected.

residue at the position occupied by the L-proline (Venkatachalam, 1968; Chandrasekaren *et al.*,1973) and hence, only the Type II β-turn for the first β-turn is compatible with the experimental data.

An examination of a Ramachandran map eliminates the Type II' β-turn as a potential second β-turn (Ramachandran and Sasisekharan, 1968) (see section 1.3.2). Only a Type I' or III' β-turn can follow and overlap a Type II β-turn. The alanine residue acts as the $(i+2)$th residue of the second β-turn. The computed range of 68-85° (see Table 3-20) is equally close to the ϕ angle of the $(i+2)$th residue of a Type I' β-turn (90°) as to that of a Type III' β-turn (60°). Therefore, a definitive statement cannot be made.

In $CDCl_3$, only the ϕ for the alanyl residue of the *trans* isomer could be derived (see Figure 3-10). As was mentioned earlier, the alanyl residue corresponds to the $(i+2)$th residue of the second β-turn. The observed coupling constant was 7.45 Hz (correction factor 1.15) which corresponds to θ_1 and θ_2 ranges of 9°-26° and 133°-141°. These translate into ϕ angles of 69°-86° and 193°-201degr, respectively. The latter set can be discounted, while the former set is in the range ascribed to either a Type I' or a Type III' β-turn.

The above data and discussion allow one to state fairly confidently that the peptide N^{α}tBocProGlyAlaNHCH$_3$ forms a Type II β-turn followed immediately by an overlapping Type I' or Type III' β-turn.

3.4.3. Conformation of N^{α}tBocProDAlaAlaNHCH$_3$

In DMSO-d_6, the well-resolved NH region of the D-Ala peptide allows a much more complete use of the coupling constant data than was possible with the glycine analogue (see Figure 3-16). The computed ϕ angles along with the actual coupling constants are shown in Table 3-21. As with the glycine analogue, the DAla-peptide was shown to take on a double β-turn conformation in solution (see section 3.3.3.4 and Chapter 4). The calculated ϕ angles of the D-alanine residue fit the required ϕ angles for the $(i+2)$th residue of β-turn types II, III and I' (Venkakachalam, 1968, Chandrasekaran *et al.*, 1973). However, the L-L and D-D nature of the latter two β-turns, respectively, and the presence of the sterically restrictive prolyl residue (ϕ angle of -60°) make the Type II β-turn ($\phi_{(i+2)}$=80°) the most likely conformation for the first β-turn. Solution and crystal studies have shown that β-turns which contain proline and D-alanine at positions $(i+1)$ and $(i+2)$, respectively, take on a Type II conformation (Aubry *et al.*, 1977; Ananthanarayanan and Shyamasundar, 1981; Rao *et al.*, 1983; Crisma *et al.*, 1984; Ananthanarayanan and Cameron, to be published).

The 80° - 89° D-alanine ϕ angle fits comfortably into the allowed region for the $(i+1)$th residue of the Type II, III' and I' β-turns (Venkatachalam, 1968; Chandrasekaran *et al.*, 1973). Therefore, the above three β-turn types are possible for the second β-turn. The alanyl residue acts as the $(i+2)$th residue of the second β-turn. Even with one set immediately discounted (195°-207°) the field of choice for the second β-turn is not narrowed. The 60°-81° range encompasses the ϕ angles of all three β-turn types. The Ramachandran plots

Table 3-21: N^{α}tBocProDAlaAlaNHCH$_3$ ϕ Angles Derived from NH Resonance Coupling Constants in DMSO-d_6

Residue	$^3J_{NH-CH}$(Hz)	Θ_1	Θ_2	Φ_1	Φ_2
DAla-trans	8.45 (1.03)	0-19°	140-149°	(-60)-(-41)°	80-89°
DAla-cis	5.75 (1.05)	29-35°	128-130°	-31-(-25)°	68-70°
Ala-trans	8.29 (1.05)	0-21°	135-147°	60-81°	195-207°
Ala-cis	5.97 (1.10)	29-35°	128-130°	89-95°	188-190°
NHCH$_3$-trans	UR.	--	--	--	--
NHCH$_3$-cis	UR.	--	--	--	--

UR. = unresolved (Correction Factor)

show that the Type II β-turn is most easily followed by a Type I' or a Type III' but not a Type II β-turn (Ramachandran and Sasisekharan, 1968) (see section 1.3.2). Therefore, of the three possible β-turns, only Type II can be discounted.

In $CDCl_3$, the proton NMR spectra of N^{α}*t*BocProDAlaAlaNHCH$_3$ yielded coupling constants for the NH resonances of both the L- and the D-alanines (see Figure 3-18). Only the *trans* form of the peptide was present. The coupling constants along with the calculated φ angles are shown in Table 3-22. The first β-turn had been shown previously to be a Type II β-turn. The φ angle of the (*i*+2)th residue of a Type II β-turn is expected to be 80° (Venkatachalam, 1968). The D-alanine being the (*i*+2)th residue of the first β-turn makes the -60° to -52° φ angle range impossible. The question which remained after the analysis of the coupling constants derived from the proton NMR data of the DAla-peptide in DMSO-d_6 was whether the second β-turn, was a Type I' or a Type III' β-turn. The φ angle of the D-alanine residue can fit either but the φ angle of the L-alanine can not. Of the two alanyl residue φ angles which present themselves, the 183°-191° range can be discounted immediately. The remaining range of 91°-98° is very much closer to the 90° expected for the (*i*+2)th residue of a Type I' β-turn than the expected Type III' value of 60°.

Based on the above considerations, the structure of the N^{α}*t*BocProDAlaA[ClaNHCH$_3$ peptide was assigned as a Type II β-turn followed by an overlapping Type I' β-turn.

The similarity between the two peptides favours the assignment of the second

Table 3-22: N^{α}tBocProDAlaAlaNHCH$_3$ Φ Angles Derived from N<u>H</u> Resonance Coupling Constants in $CDCl_3$

Residue	$^3J_{\underline{NH}\text{-}C\underline{H}}$(Hz)	Θ_1	Θ_2	Φ_1	Φ_2
D-Alanine	9.07 (1.05)	0-8°	146-158°	(-60)-(-52)°	86-98°
Alanine	5.78 (1.07)	31-38°	124-131°	91-98°	183-191°

(Correction Factor)

β-turn of N^{α}tBocProGlyAlaNHCH$_3$ as a Type I' β-turn. Since the $i+1$ ϕ angle of β-turn types I' and III' are identical (Venkatachalam, 1968), the coupling constants may reflect a minor distortion from ideal dimensions or a reflection of the presence of multiple conformations with the Gly-peptide.

Chapter 4

Circular Dichroism, Infrared and Model Building

4.1. Circular Dichroism Characterization

4.1.1. Introduction

As described in the introductory chapter, circular dichroism (CD) spectroscopy is a sensitive tool for examining changes in peptide conformations induced by the addition of perturbants. The use of CD in the study of the effect of the addition of metal ions will be examined in Chapter 5. What follows here is a study of the different types of spectra produced by the two tetrapeptides in a variety of solvents. This type of study can provide useful information about the structures and relative stabilities of the peptides in their uncomplexed states.

The CD spectra of the peptide $N^{\alpha}t$BocProGlyAlaNHCH$_3$ and its D-alanine analogue $N^{\alpha}t$BocProDAlaAlaNHCH$_3$ were obtained in water, methanol and acetonitrile at ambient temperature. In general, the CD spectrum of a peptide may be considered to be the sum of the spectra of individual conformations (Chang *et al.*, 1978). Hence, a particular spectrum would be represented by:

$$[\theta]^{obs}_{res} = f_1[\theta]^1_{res} + f_2[\theta]^2_{res} + f_3 \cdots$$

where $[\theta]_{res}$ is the mean residue ellipticity expressed in units of degrees cm^2 $dmol^{-1}$ and f refers to the fraction of a particular structure (i.e. Type I β-turn, Type II β-turn, random coil). The mean molar ellipticity was derived from the original spectrum through the formula:

$$[\theta]_{res} = X \times S \times MRW \times (c \times l \times 10)^{-1}$$

Where X equals the pen deflection in cm, S is the scale used in millidegrees per cm, c is concentration in mg ml^{-1}, and l refers to path length in cm. MRW or mean residue weight denotes the molecular weight of the peptide divided by the number of peptide bonds.

The peptide amide bond contains occupied non-bonding (n) and π orbitals. When excited, an electron in a n or π orbital can be promoted into a vacant antibonding π (π^*) orbital resulting in n-π^* and π-π^* transitions. With an asymmetric peptide molecule, the amount of energy absorbed because of these transitions differs between left- and right-handed circularily polarized light. The CD spectrum is derived from this difference over a wavelength range (Brown, 1980; Bayley, 1980). Woody (1974), using theoretical calculations based on the n to π^* and π to π^* transitions of the peptide group, assigned eight classes of β-turn spectra (A through D and their mirror images (A' through D'). Although his calculations were based *in vacuo* they offer a good initial reference point. By altering the peptide backbone dihedral angles by 10° at a time, he examined all possible β-turn types as defined by Lewis *et al.* (1973). Table 4-1 lists the maxima

and minima of the spectral classes A through D as defined by Woody (1974). The spectral classes A' through D' are mirror images and differ from their roots by a sign change.Table 4-2 correlates the β-turn types as defined by Lewis *et al* (1973) with each of Woody's spectral classes. A Class B spectrum can be representative of nearly all β-turn types and conversely the Lewis' Type I β-turn can give rise to either Woody's Class A or B spectra. This becomes important when one considers how similar β-turn types could give rise to different CD spectra.

4.1.2. N^{α}tBocProGlyAlaNHCH$_3$

4.1.2.1. Spectral Data

The spectra of the peptide in all three solvents are shown in Figure 4-1. The maxima and minima are listed in Table 4-3.In all three solvents, the spectra were characterized by a strong negative band. In water the band was found at 201.5 nm but with methanol and acetonitrile the peak was red shifted to 207.7 nm. The intensity of the band increased as the polarity of the solvent decreased with the greatest difference between that of methanol ($[\theta]_{res} = -1.91 \times 10^3$) and acetonitrile ($[\theta]_{res} = -2.81 \times 10^3$). The $[\theta]_{res}$ of the peak in water was -1.63×10^3. The acetonitrile spectrum exhibited a pronounced shoulder at 235 nm. This shoulder occurred at 229 nm but to a much lesser extent in methanol and was not observed in water. The CD spectra of the title peptide in methanol and acetonitrile shared a common crossover point at 203 nm, while the CD spectrum of the peptide in water crossed over at 197.5 nm.

Table 4-1: Maxima and Minima of β-Turn CD Spectral Classes as Defined by Woody (1974)

Class	Sign	Wavelength Range (nm)
A	-	210-220
	+	195-200
	-	<190
B	-	>220
	+	200-210
	-	<190
C	-	200-210
	+	180-190
D	-	>225
	+	210-220
	-	190-200
	+	<190

Table 4-2: Predicted CD Spectral Classes (Woody (1974)) for β-Turn Types as Defined by Lewis *et al.* (1973)

Lewis Types	A	B	C	D	A'	B'	C'	D'
I	*	*				*		
I'	*	*	*			*	*	*
II		*				*		
III	*	*	*	*				
III'	*	*	*	*	*	*	*	*
IV		*	*	*			*	

* indicates that the Lewis *et al* structure can be found as that particular spectral class.

Table 4-3: Circular Dichroism Spectra of N^{α}*t*BocProGlyAlaNHCH$_3$ in Various Solvents

Solvent	Maxima or Minima (nm)	$[\theta]_{res}$ x10^{-3}	Maxima or Minima (nm)	$[\theta]_{res}$ x10^{-3}
Water	---	---	201.5	-1.63
MeOH	229	-0.37	207.7	-1.01
Acn	235	+0.63	207.7	-2.81

$[\theta]_{res}$ = mean residue ellipticity in degrees cm^2 dmol^{-1}

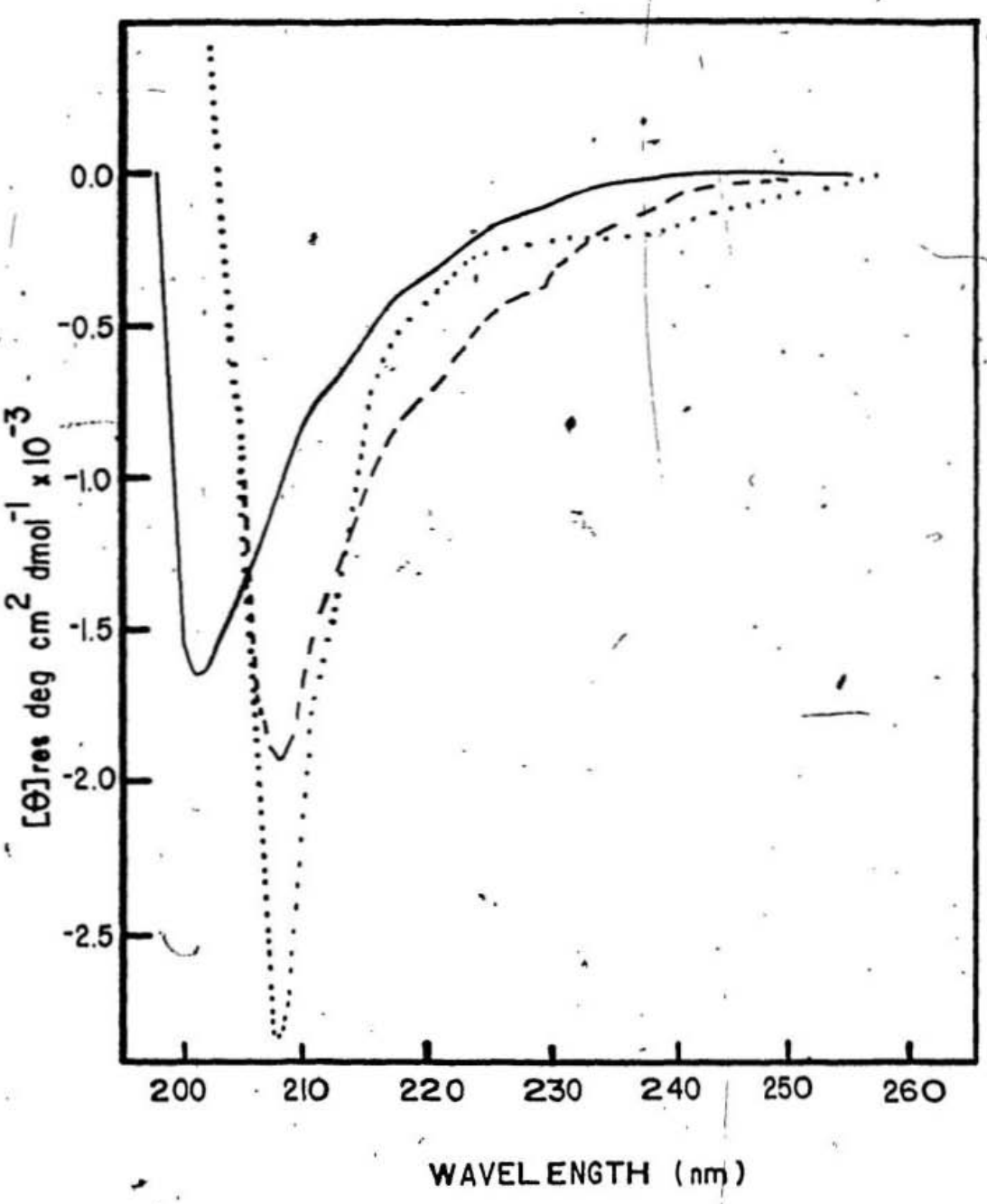

Figure 4-1: Circular Dichroism Spectra of N^{α}tBocProGlyAlaNHCH$_3$ in ——, water;- - - -, methanol; ·····, acetonitrile.

4.1.2.2. Analysis

The contributions of the various component parts of the spectra were elucidated from the results of Brahmachari *et al.* (1982). N^{α}AcProGlyAlaOH, studied by these authors, produced a Class B CD spectrum in TFE. Its analogue N^{α}AcProGlyLeuOH also produced a Class B spectrum (Woody, 1974) in TFE and had been shown to be nearly 100 percent Type II β-turn at low temperatures in TFE (Brahmachari *et al.*, 1979). Proton NMR coupling constants of N^{α}tBocProGlyAlaNHCH$_3$, presented in this thesis (see section 3.4.2) indicated that the first β-turn was a Type II. Therefore, it appeared to be reasonable to assume that the first β-turn of the tetrapeptide would produce a Class B spectrum. The second β-turn was characterized by NMR to be a Type I' (see section 3.4.2). According to Woody (1974) a Type I' β-turn is capable of producing a Class B spectrum similar to that produced by a Type II β-turn. The Class B spectrum produced by a Type I β-turn has a positive band which is slightly less intense and blue shifted in comparison to the positive band of the Class B spectrum produced by the Type II β-turn. The smaller negative band at 220 nm of the Class B spectrum produced by a Type I β-turn is also blue shifted and is twice as large in intensity as that of the Class B spectrum produced by a Type II β-turn (Woody, 1974). A Type I' β-turn would produce a mirror image spectrum to that of the Type I. These differences are greatly enhanced since the actual experimental values are often much greater or less than those predicted by the *in vacuo* calculations of Woody (1974) due to effects of the solvent. The magnitude of the positive band of N^{α}AcProGlyAlaOH in TFE, even at -20° C, was less then the theoretical value (Brahmachari *et al.*, 1982). In contrast, the magnitude of

the values of a Class B spectrum producing Type I β-turn was much larger than those predicted by Woody (Kawai and Fasman, 1978). If the values of Woody were used, the addition of a Class B producing Type II β-turn and a Class B' producing Type I' β-turn would effectively cancel each other out since their differences are relatively minor. By allowing for experimentally obtained variations the resultant spectrum would favour the contribution of the second β-turn. Adding the effect of random coil, one obtains a spectrum which would look like that obtained with N^{α}*t*BocProGlyAlaNHCH$_3$ in acetonitrile. The Gly-peptide was shown by carbon-13 NMR to be only 83.8 percent *trans* in acetonitrile (see section 3.2.2.1). The *cis* isomer (non-hydrogen-bonded) would be expected to contain random coil variations. None of Woody's other Type I' allowed classes would produce the observed spectrum.

In water, N^{α}*t*BocProGlyAlaNHCH$_3$ was found to be predominantly in the random coil form. The CD spectrum was similar to those seen with the ProGly-X tripeptides in water (Brahmachari *et al.*, 1982) which were considered representative of a random coil. Water is capable of forming intermolecular hydrogen bonds with the peptide and would be expected to disrupt any structure which is based primarily on *intra*molecular hydrogen bonds. Glycine, being conformationally very flexible, would not be expected to act as a β-turn stabilizer as would D-alanine.

The CD spectrum of the Gly-peptide in methanol appeared to have less of a contribution from the Type I' β-turn than the spectrum in acetonitrile with no parallel loss of the Type II β-turn. In other words, the second β-turn of the

tetrapeptide seemed to be disrupted more easily (i.e. was less stable) than the first β-turn. Also, the double β-turn conformation of the Gly-peptide (as described in section 3.3) appeared to be more stable in acetonitrile than in either methanol or water.

4.1.3. N^{α}tBocProDAlaAlaNHCH$_3$

4.1.3.1. Spectral Data

The CD spectra of N^{α}tBocProDAlaAlaNHCH$_3$ in all three solvents are shown in Figure 4-2 and the maxima and minima are listed in Table 4-4. The CD spectrum in water was characterized by a weak positive band centred at 236 nm ($[\theta]_{res}= 0.63x10^3$), a weak negative band around 223 nm ($[\theta]_{res}= 2.13x10^3$) and a strong positive band about 198 nm ($[\theta]_{res}= 12.7x10^3$). There was a relatively large change in the CD spectrum in going from water to methanol which was greater than the change observed with the transition from methanol to acetonitrile. With the change from water to methanol, the weak positive band disappeared, the negative band at 223 nm was significantly enhanced ($[\theta]_{res}= 14.95x10^3$) and the strong positive band decreased in intensity ($[\theta]_{res}= 5.70x10^3$) and exhibited a rather large red shift to 207.5 nm. In comparison, the change from methanol to acetonitrile was accompanied by a relatively small red shift of the negative band (from 223 to 225 nm) with no change in its intensity and a slight blue shift by about 1 nm of the positive band, with an increase in its intensity ($[\theta]_{res}= 6.35x10^3$).

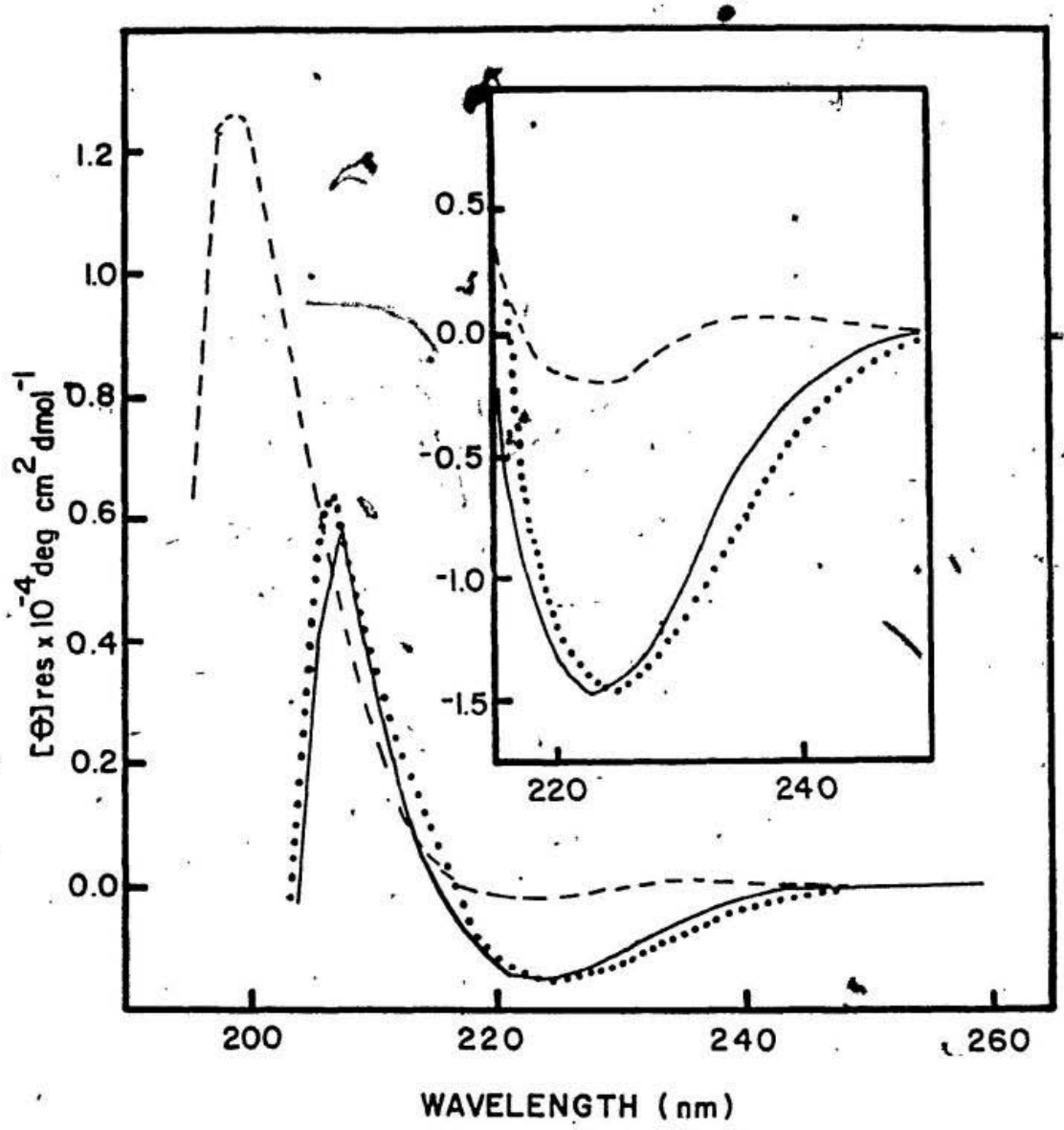

Figure 4-2: Circular Dichroism Spectra of $N^{\alpha}t$BocProDAlaAlaNHCH$_3$ in - - - - -, water; ——, methanol; · · · · ·, acetonitrile.

Table 4-4: Circular Dichroism Spectra of N^{α}tBocProDAlaAlaNHCH$_3$ in Various Solvents

Solvent	Maxima or Minima	$[\theta]_{res}$ x10^{-3}	Maxima or Minima	$[\theta]_{res}$ x10^{-3}	Maxima or Minima	$[\theta]_{res}$ x10^{-3}
Water	236	+0.63	223	-2.13	198.0	+12.70
MeOH			223	-14.95	207.5	+5.70
Acn			225	-14.95	206.5	+6.35

Maxima and Minima values in nm

$[\theta]_{res}$ = mean residue ellipticity in degrees cm^2 dmol^{-1}

4.1.3.2. Analysis and Comparison

The CD spectral contribution of the individual β-turns was elucidated along the same lines as with the glycine analogue (see section 4.1.2.2). The contribution of the first β-turn was derived from the work of Crisma *et al.* (1984). Several interesting features were observed in their CD studies of PivProDAlaNHCH$_3$. The CD spectrum in MeOH was characterized by two maxima, a minor one at 230 nm and a large one at 202nm. The spectrum does not become negative between 195 and 260 nm. Addition of water up to a water:methanol ratio of 9:1 did not alter the spectrum to any significant extent. The importance of this observation is that the Type II β-turn structure was maintained in water. This effect was also seen with the peptide N$^{\alpha}$*t*BocProDAlaAlaOH whose CD spectra in water and in the β-turn stabilizing solvent TFE at 5° C showed no appreciable difference (Ananthanarayanan and Attah-Poku, to be published). In both these cases, as with the peptide N$^{\alpha}$*t*BocProDALaAlaOCH$_3$ in water, the CD spectra showed the same type of positivity as was seen with PivProDAlaNHCH$_3$. The spectrum of N$^{\alpha}$*t*BocProDAlaAlaNHCH$_3$ in water, (Figure 4-2) was very similar to that of PivProDAlaNHCH$_3$. It, too, showed a hump (236 nm), but crossed over the base line to give rise to the weak minima at 224 nm. Proton NMR coupling constants had shown that the β-turn due to the ProDAla sequence of N$^{\alpha}$*t*BocProDAlaAlaNHCH$_3$ was a Type II (see section 3.4.3). None of the above mentioned ProDAla containing β-turns could be placed into any of the spectral classes of Woody (1974). The large difference seen between the CD spectra of N$^{\alpha}$*t*BocProDAlaAlaNHCH$_3$ upon changing the solvent from methanol to water was most likely due to the destabilization of the second β-turn while maintaining

the structure of the first. Unlike the glycine peptide, the first β-turn does not rely primarily on the formation of hydrogen bonds but is "forced" into the conformation by the steric restrictions of the D-alanine and hence is likely to be maintained even in water. The preferential destabilization of the second β-turn over the first was also seen with the glycine analogue.

The CD spectra of N^{α}*t*BocProDAlaAlaNHCH$_3$ in methanol and acetonitrile were very similar (see Figure 4-2). It appeared that only a small proportion of the second β-turn was destabilized with the change in solvent. This was in sharp contrast to the relatively large change that was seen with the glycine analogue (see Figure 4-1). The spectral contribution of the Gly-peptide's second β-turn appeared to collapse entirely with a change in solvent from acetonitrile to methanol (see section 4.1.2.2). This suggested that the second β-turn of the D-alanine analogue was more stable than that of the glycine analogue. The D-alanine thus appears to force the entire peptide into a more "compact" structure. This assertion was further borne out through observations in the NMR (see section 3.3.2.4) and the IR (see section 4.2) spectra.

The minima seen at 224 nm in the spectrum of the title peptide in water was not due to the random coil contribution of the sequence responsible for forming the second β-turn in the more non-polar solvents. The only difference between the title peptide and N^{α}*t*BocProDAlaAlaOH, which produces a completely positive CD spectrum in water, is a methylamide attached to the C-terminal end of the peptide sequence. It was more likely due to a small population of the second β-turn which may still exist in an equilibrium heavily shifted to the denatured form in water.

In order to produce the observed spectrum of the title peptide in either acetonitrile or methanol, the spectral contribution of the second β-turn would require a negative band around 225 nm, a small positive band around 210 nm and a large negative band at wavelengths less than 205 nm. This pattern was found with the Class D spectrum, which, according to Woody (1974), can represent a Type I' β-turn. The Type I' was shown through proton NMR coupling constants to be the most likely conformation of the DAla-peptide's second β-turn (see section 3.4.3). None of the other classes, as described by Woody (1974), could produce the desired effect. The observed difference seen between the CD spectra of the DAla-peptide and its glycine analogue (see Figures 4-1 and 4-2) is therefore most likely due to the different spectral contributions of the Type I' β-turn.

4.2. Infrared Studies

Peptides and proteins produce IR spectra which contain a number of characteristic absorption bands. There are nine "amide bands" (A, B, I to VII) of which only the two highest frequency bands (A and B) are due to N-H stretching (Thomas and Kyogoku, 1977). The length and geometry of a hydrogen bond effect the parameters of the Amide A band which occurs in the range 3300 to 3500 cm^{-1} (Parker, 1983). Hence, not only can the Amide A band be used to differentiate between NHs which are hydrogen-bonded and those which are not, but it can also be used to infer the particular type of bonded structure. Although other amide bands have been used to detect the presence of β-turns, most notably I and III and to a lesser extent II and V (Krimm and Bandekar, 1980; Fox *et al.*, 1981), the Amide A band is by far the most useful. Free NH stretching

frequencies occur around 3430 cm^{-1} while the C_{10} (β-turn) hydrogen-bonded NH frequencies are found near 3300 cm^{-1}. The C_5 and C_7 hydrogen-bonded conformers are observed at 3420 cm^{-1} and 3340 cm^{-1}, respectively (Avignon *et al.*, 1969; Rao *et al.*, 1980). Their reduced shift relative to the frequency of the free NH as compared to that seen with the C_{10} conformer was attributed to the lower stability of the C_5 and C_7 structures. Because of their size, they are less able to form a linear hydrogen bond as with the β-turn (Nemethy and Printz, 1972). Although general frequency ranges can be attributed to certain types of hydrogen-bonded structures, these ranges can be large and overlapping. For example, frequencies in the range expected for the C_7 conformer have been attributed to the C_{10} conformer (Ananthanarayanan and Shyamasundar, 1981).

Infrared spectra of both N^{α}*t*BocProGlyAlaNHCH$_3$ and its D-alanine analogue N^{α}*t*BocProDAlaAlaNHCH$_3$ were taken at room temperature in dry $CHCl_3$ in order to determine what type of hydrogen-bonding occurred. Peptides at concentrations 10 mg ml^{-1} to 0.625 mg ml^{-1} were run to determine which bands if any were due to *inter*molecular hydrogen-bonding. Up to 2.5 mg ml^{-1} there appeared to be no *inter*molecular hydrogen-bonding. The spectra of the Amide A region of both peptides at 2.5 mg ml^{-1} in dry $CHCl_3$ are shown in Figure 4-3. The peaks are listed in Table 4-5, the resolution is 3 cm^{-1}. The glycine spectrum showed some interesting facets. The Amide A region contained three peaks. The first at 3445 cm^{-1} was attributed to the free NH, the one at 3330 cm^{-1} was representative of a C_{10} (β-turn) structure. The third peak at 3385 cm^{-1} was attributed to a weaker *intra*molecular hydrogen-bonded structure. Although in

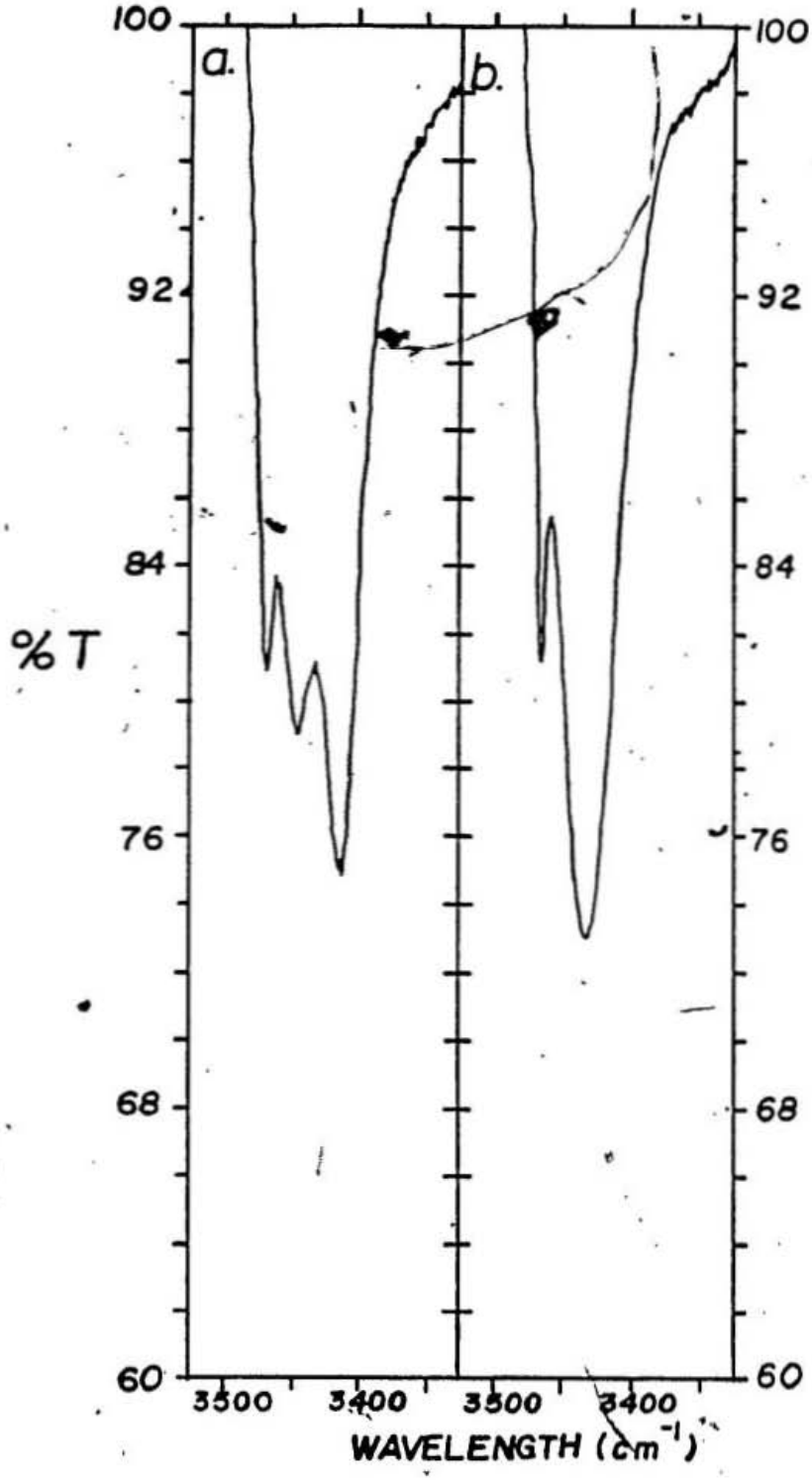

Figure 4-3: Infrared Spectrum Amide A Band of
(a) $N^{\alpha}t$BocProGlyAlaNHCH$_3$ and
(b) $N^{\alpha}t$BocProDAlaAlaNHCH$_3$ in $CHCl_3$

Table 4-5: Infrared Spectroscopy Amide A and Carbonyl Bands of (a) N^{α}*t*BocProGlyAlaNHCH$_3$ and (b) N^{α}*t*BocProDAlaAlaNHCH$_3$ in $CHCl_3$

Band (cm^{-1})	Gly-peptide	DAla-peptide
Amide A1	3445 cm^{-1}	3432 cm^{-1}
Amide A2	3385 cm^{-1}	3368 cm^{-1}
Amide A3	3330 cm^{-1}	
Carbonyl	1670 cm^{-1}	1668 cm^{-1}

Resolution of peaks is 3 cm^{-1}

the frequency range attributed to the C_7 conformer, the observation can also be explained on the basis of a weaker β-turn. The CD spectral data indicated that the second β-turn of both peptides was less stable than the first (see section 4.1). Model building (section 4.3) will provide more insight into the phenomenon. The DAla-peptide spectrum was simpler with the peak at 3432 cm^{-1} attributed to the free NH and that at 3368 cm^{-1} as belonging to the β-turn hydrogen-bonded NH. The frequency was relatively high which may reflect the presence of a less-stable hydrogen-bonded species. N^{α}*t*BocProDAlaValOH in chloroform has an IR band at 3340 cm^{-1} as does N^{α}*t*BocProDAlaLeuOH. These values are also fairly high but were assigned to a C_{10} hydrogen-bonded NH (Ananthanarayanan and Shyamasundar, 1981). The appearance of a single band at 3368 cm^{-1} with the DAla-peptide suggests that the two hydrogen bonds are more similar in the DAla-peptide than in the Gly-peptide which shows two bands. This had previously been alluded to in the sections on NMR (section 3.3.2.4) and CD (section 4.1). There was no indication of a C_7 conformer with the D-Ala peptide. Although the stretching band was in the C_7 region, X-ray, NMR, CD and other IR data all add up against the possibility.

Although carbonyl shifts have occasionally been used to determine the presence of *intra*molecular hydrogen-bonding (Kopple *et al.*, 1975; Boussard *et al.*, 1974), this was not possible with the two peptides studied here. The carbonyl peaks are shown in Figure 4-4 and listed in Table 4-5. The carbonyl peak at 1670 cm^{-1} for the Gly-peptide and 1668 cm^{-1} for the DAla-peptide were not resolved into bound and unbound carbonyls although their breadth suggests the presence of both species.

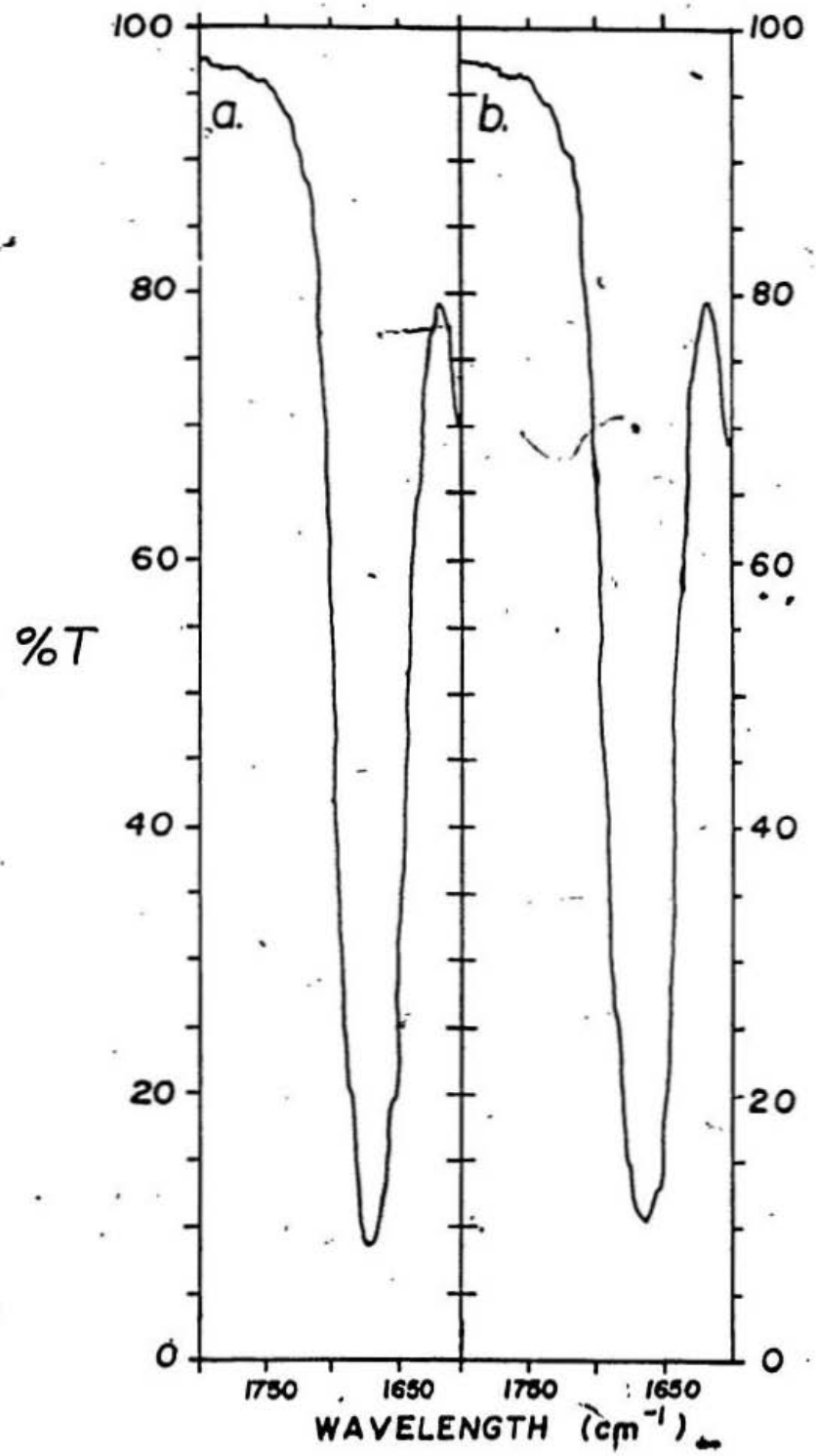

Figure 4-4: Infrared Spectrum Carbonyl Region of
(a) N^{α}*t*BocProGlyAlaNHCH$_3$ and
(b) N^{α}*t*BocProDAlaAlaNHCH$_3$ in $CHCl_3$

4.3. Summary of Uncomplexed Peptide Data and Model Building

This section summarizes the data obtained by NMR (see chapter 3), CD and IR (see sections 4.1 and 4.2) spectroscopy on N^{α}*t*BocProGlyAlaNHCH$_3$ and its D-alanine analogue N^{α}*t*BocProDAlaAlaNHCH$_3$ in the absence of metal ions. The data obtained on N^{α}*t*BocProDAlaAlaNHCH$_3$ were much more definitive than that obtained on the glycine analogue and will be summarized first.

4.3.1. N^{α}tBocProDAlaAlaNHCH$_3$

The N^{α}*t*BocProDAlaAlaNHCH$_3$ peptide forms two overlapping $4 \rightarrow 1$ *intra*molecular hydrogen bonds. The first hydrogen bond is formed between the carbonyl of the *t*Boc group and the NH of the alanyl residue. The second hydrogen bond is formed between the carbonyl of the prolyl residue and the NH of the N-methylamide. The existence and pattern of the *intra*molecular hydrogen bonds was determined through IR (see section 4.2) and proton NMR temperature-dependence studies (see section 3.3.3.4). Data derived from the coupling constants of the NH resonances indicated that the peptide conformation is a Type II β-turn followed by an overlapping Type I' β-turn (see section 3.4.3). A schematic drawing of the peptide is shown in Figure 4-5. Figure 4-6 shows a CPK model of the N^{α}*t*BocProDAlaAlaNHCH$_3$ peptide. The ϕ,ψ angles used in the construction of the CPK model were as defined by Venkatachalam (1968) for the various β-turn types with minor alterations dependent on the coupling constants of the NH resonances and are listed in Table 4-6.

The most interesting point, which was easily observed with the CPK model, is

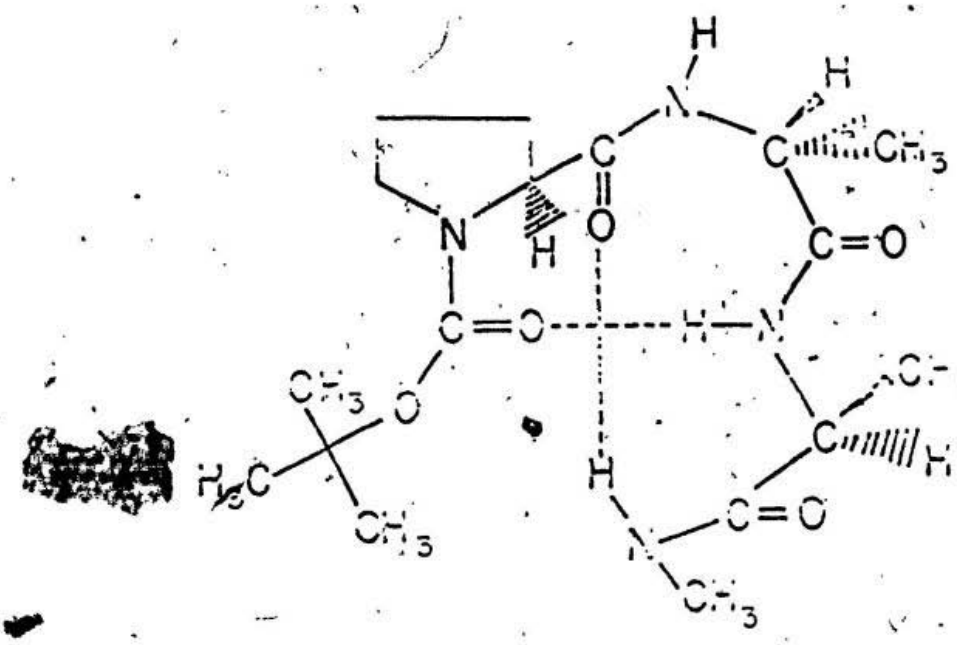

Figure 4-5: Schematic Diagram of Uncomplexed N^{α}*t*BocProDAlaAlaNHCH$_3$.

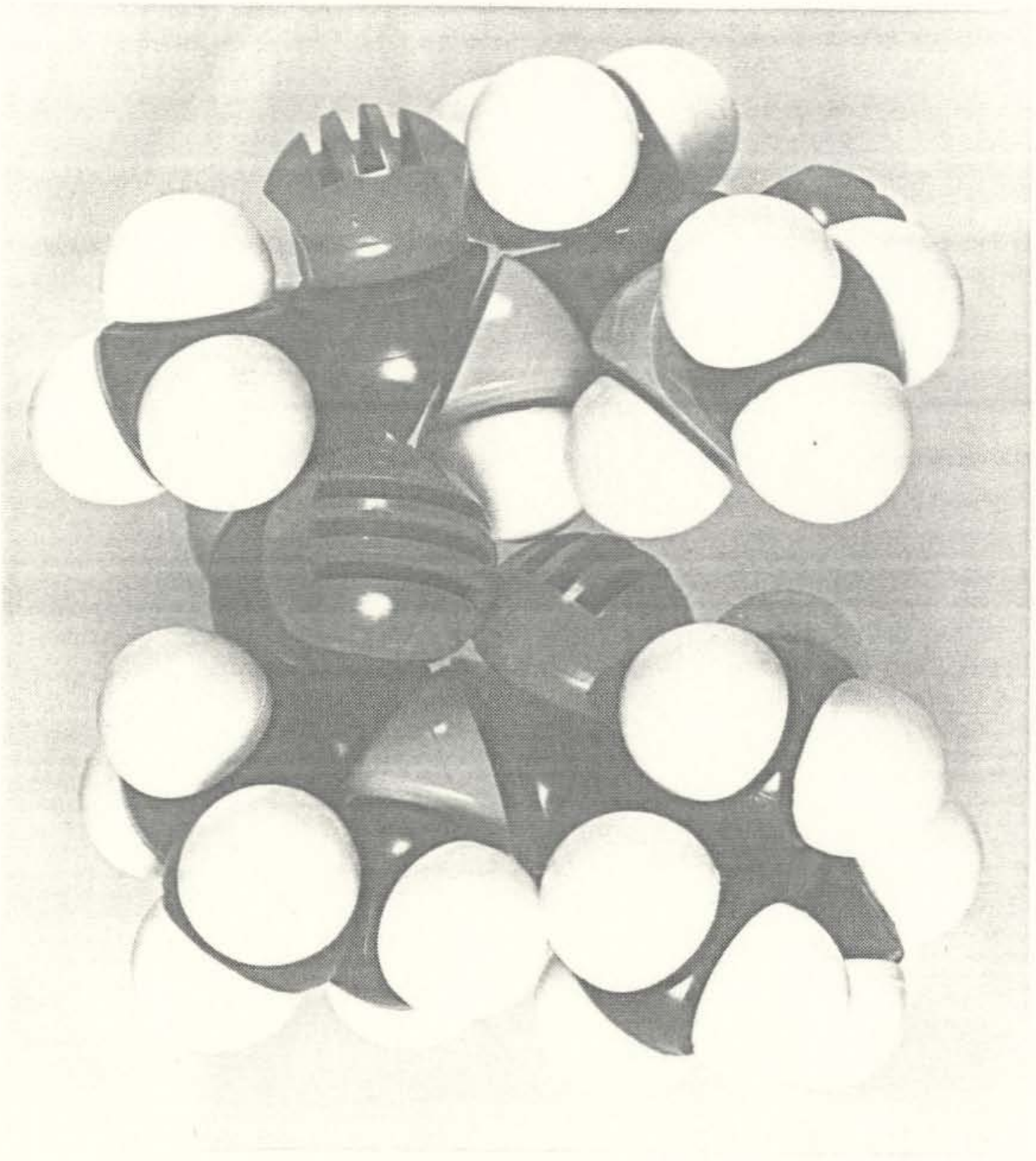

Figure 4-6: CPK Model of Uncomplexed N^{α}*t*BocProDAlaAlaNHCH$_3$

Table 4-6: ϕ,ψ Angles Used in the Construction of CPK Models of $N^{\alpha}t$BocProDAlaAlaNHCH$_3$

Residue	Position in First β-Turn	Position in Second β-Turn	ϕ	ψ
Proline	$i+1$	i	-60°	120°
D-Alanine	$i+2$	$i+1$	80°	0°
Alanine	$i+3$	$i+2$	60°	30°

the almost linear nature of the first hydrogen bond as compared to the second hydrogen bond. The second hydrogen bond has been shown through CD spectroscopy to be less stable than the first hydrogen bond (see section 4.1.3). In water, the first β-turn was maintained while the second β-turn was nearly completely disrupted. Water, being strongly polar, would be expected to disrupt hydrogen bonds. Hence, the first β-turn is shown to be stabilized by steric constraints in addition to the formation of an *intra*molecular hydrogen bond.

4.3.2. N^{α}tBocProGlyAlaNHCH$_3$

The hydrogen-bonding patterns of the N^{α}*t*BocProGlyAlaNHCH$_3$ peptide were not as clear as those of the DAla-peptide. The replacement of D-alanine with glycine would be expected to result in a peptide with more steric freedom and hence an increase in the number of potential conformations available in solution. With the D-alanine analogue in DMSO-d$_6$, the majority of the *trans* isomer of the peptide was in the double hydrogen-bonded conformation. This was made apparent by the well defined hydrogen-bonding patterns of the DAla-peptide as determined through temperature-dependence studies. On the other hand, the glycine analogue's temperature-dependence results were much more diffuse (see section 3.3.2.4). The higher *cis/trans* ratio of N^{α}*t*BocProGlyAlaNHCH$_3$ in DMSO-d$_6$ (1.13) compared with the D-alanine analogue (0.75) is a further indicator of the lowered ability of the Gly-peptide to form *intra*molecular hydrogen bonds. IR spectroscopy (see section 4.2) and solvent-dependent carbonyl shifts followed by carbon-13 NMR (see section 3.2.4.2) indicate that *intra*molecular hydrogen bonds do form. The ϕ angles of the various residues

derived from the coupling constants of the NH resonances suggest that, as with N^{α}*t*BocProDAlaAlaNHCH$_3$, the Gly-peptide takes on a Type II β-turn followed by an overlapping Type I' β-turn conformation although a Type III' β-turn is also possible for the second β-turn (see section 3.4.2).

The different CD curves of the two peptide analogues in identical solvents indicate that there are some differences between them (see section 4.1). The CD data also reveal information on the relative stabilities of the various β-turns. As expected, the ProGly containing β-turn is less stable than the ProDAla containing β-turn. The first β-turn of the glycine analogue did not form in water while that of the DAla-peptide did. The second β-turn of the DAla-peptide was more stable than the second β-turn of the glycine analogue. The majority of the second β-turn of N^{α}*t*BocProDAlaAlaNHCH$_3$ remained after changing the solvent from acetonitrile to methanol while the same change in solvents resulted in an almost total loss of the second β-turn of N^{α}*t*BocProGlyAlaNHCH$_3$. The lower stability was also alluded to by the IR data; only one type of hydrogen-bonded conformer was seen in the amide A region with the DAla-peptide but two well-resolved hydrogen-bonded NHs were found with the Gly-peptide (see section 4.2). The two hydrogen bonds of N^{α}*t*BocProDAlaAlaNHCH$_3$ were considered to be similar to each other, more so than the hydrogen bonds of the glycine analogue were to each other. As with the first β-turn of the two peptides, the greater stability of the DAla-peptide as compared to the Gly-peptide was due to the presence of D-alanine. Both D-alanine and glycine act as the (i+1)th residue of the second β-turn of their respective peptides.

Although the N^{α}tBocProGlyAlaNHCH$_3$ is found in a greater number of conformations in solution and is less stable than its D-alanine analogue, the double hydrogen-bonded conformation of the two peptides is essentially identical. Hence, the schematic diagram and CPK model seen in Figures 4-5 and 4-6, respectively, can represent the backbone conformation of the N^{α}tBocProGlyAlaNHCH$_3$ peptide as well.

Chapter 5

Ion-Binding

5.1. Introduction

Both carbon-13 and proton NMR and CD spectroscopy have been used to follow ion-binding by peptides. Vishwanath and Easwaran (1982) used these techniques to examine the complexing of valinomycin with calcium ion. Pease and Watson (1978) also used the above techniques to examine the conformational changes upon ion-binding to cyclo-(GlyProGlyDAlaPro). The peptides studied by the above authors, although cyclic, were similar to the linear N^{α}tBocProDAlaAlaNHCH$_3$ and its glycine analogue N^{α}tBocProGlyAlaNHCH$_3$ in that the only available ligands for cation-binding are backbone carbonyls. Therefore, the techniques and reasoning used in the delineation of the conformational changes induced on both the Gly- and DAla-peptide by the addition of calcium ion will follow closely those presented in the papers by Vishwanath and Easwaran (1982) and Pease and Watson (1978).

Nuclear magnetic resonance is capable of following the change in environment around a particular nucleus. By observing the chemical shifts of assigned NH resonances by proton NMR or assigned carbonyl resonances by carbon-13 NMR of a peptide one can follow the making and/or breaking of hydrogen bonds. The

coordination of the carbonyls to metal ions can also affect their carbon-13 NMR chemical shift. The main problem with NMR is the determination of whether the observed changes are due to the change in hydrogen bond status, solvent effect, metal-binding or a combination of the above. Circular dichroism is a very sensitive technique for following changes in the conformation of the peptide backbone. Although incapable of defining the exact conformational change, its advantage over NMR is that it follows the conformational change of the entire peptide. Hence, it is affected to a lesser extent than NMR by the peculiarities of environment around a particular atom.

As mentioned in the section summarizing chapters 3 and 4, the D-alanine is more effective than glycine in "locking" the uncomplexed peptide into a defined conformation (see section 4.3). Therefore, the effect of calcium ion on the conformation of N^{α}*t*BocProDAlaAlaNHCH$_3$ will be examined first.

5.2. N^{α}tBocProDAlaAlaNHCH$_3$

5.2.1. Circular Dichroism Studies

5.2.1.1. Studies Using Water as Solvent

The titration with calcium chloride of N^{α}*t*BocProDAlaAlaNHCH$_3$ and various of its precursors in water was followed by CD spectroscopy. The CD spectra of N^{α}*t*BocProDAlaAlaNHCH$_3$ in aqueous solvents of various [Ca^{2+}]/[peptide] ratios are shown in Figure 5-1. The spectra became increasingly positive as the concentration of calcium ion was increased to the point where at a [Ca^{2+}]/[peptide] ratio of 2000:1 it became completely positive. This was in

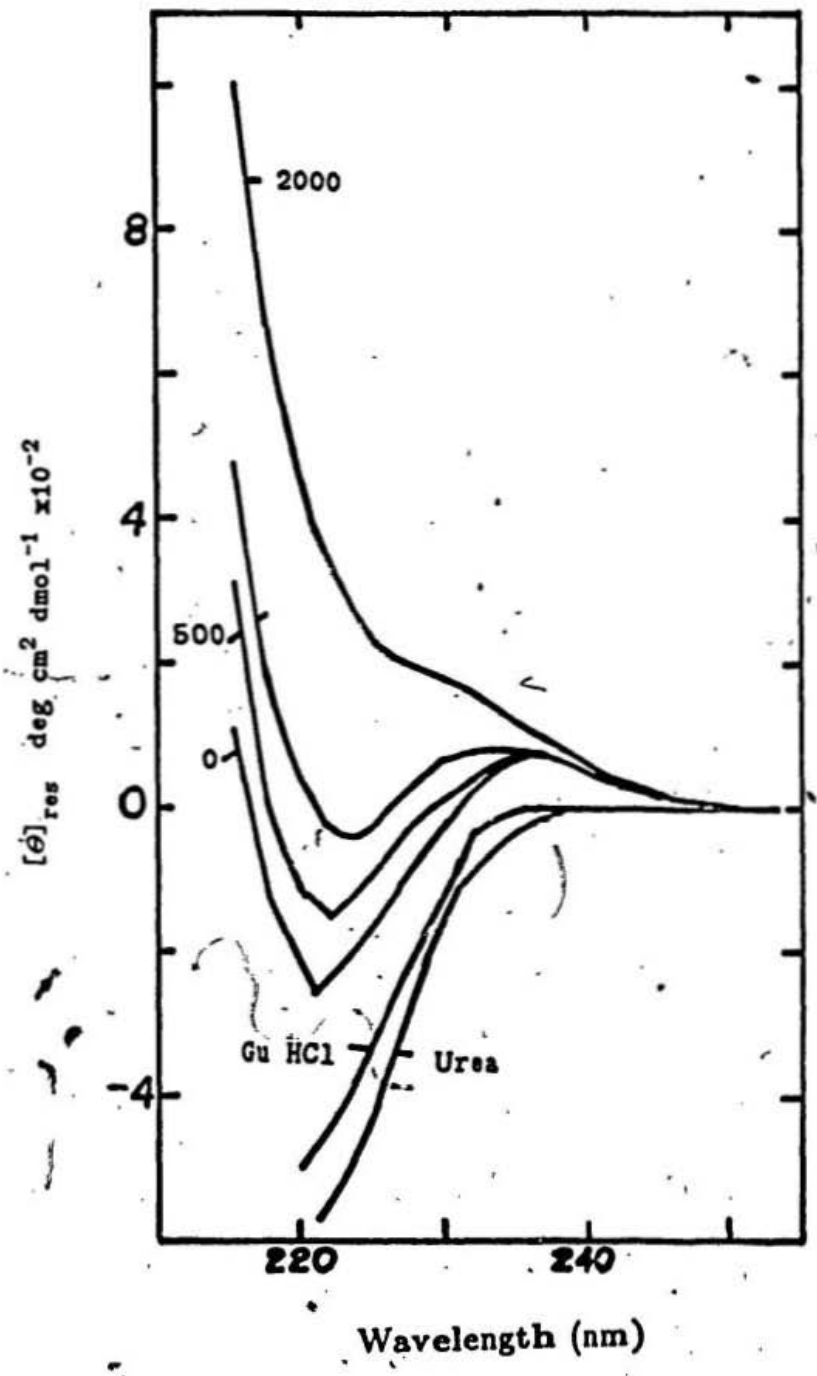

Figure 5-1: Circular Dichroism Spectra of N^{α}tBocProDAlaAlaNHCH$_3$ at Various Calcium Chloride to Peptide Ratios in Water and in the Presence of 6M GuHCl and 8M Urea

marked contrast to the effect of denaturants such as 6M guanidine hydrochloride and 8M urea which caused a collapse of the CD spectrum. In other words, the change observed through the addition of calcium ion was not due to a disruption of the peptide structure but a conformational change induced by calcium-binding. If a collapse of peptide structure did occur it would be extremely unlikely for a sign change to have occurred. A plot of the mean residue ellipticity at 220 nm *versus* ion to peptide molar ratio (shown in Figure 5-2) indicates that a "plateau" is reached at a $[Ca^{2+}]$/[peptide] ratio of 300:1. There are two possible reasons for the high ratio required for the binding curve to level off. Analysis of the CD data of the uncomplexed peptide showed that, in water, only a small portion of the peptide in solution has both β-turns formed. Secondly, water is capable of forming hydrogen bonds with the peptide carbonyls and hence compete with the coordination of carbonyls to calcium ion. The importance of the formation of the second β-turn was demonstrated by the total collapse of the CD spectrum of the peptide N^{α}*t*BocProDAlaAlaOCH$_3$ with a $[Ca^{2+}]$/[peptide] ratio of 4000:1 (see Figure 5-3). This spectrum is representative of a random coil structure. The same sort of collapse was seen with N^{α}*t*BocProDAlaAlaOH. The removal of the unrestrained terminal alanine allows greater access of the calcium ion to the peptide. This was inferred from the observed calcium ion titrated spectra of N^{α}*t*BocProDAlaOH and N^{α}*t*BocProDAlaNHCH$_3$ in water. There was no collapse of the spectra and at very high concentrations of calcium ion the bands became slightly more positive. Under these conditions, any binding that did occur was not significant as compared to that obtained with N^{α}*t*BocProDalaAlaNHCH$_3$. The spectra of the latter three peptides in water, with and without calcium ion,

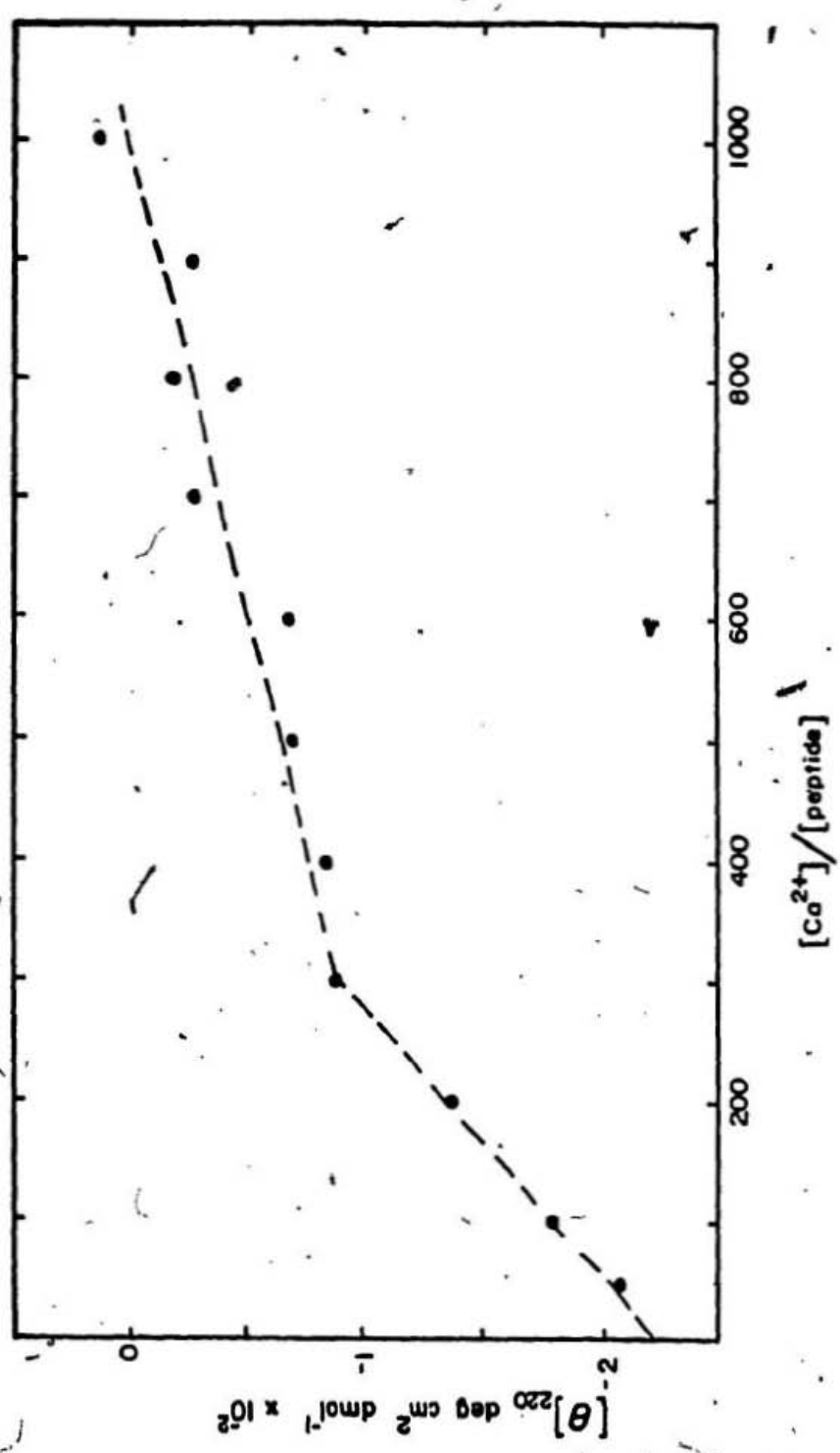

Figure 5-2: $[\theta]^{220}_{res}$ *vs.* $[Ca^{2+}]/[Peptide]$ of N^{α}*t*BocProDAlaAlaNHCH$_3$ in Water

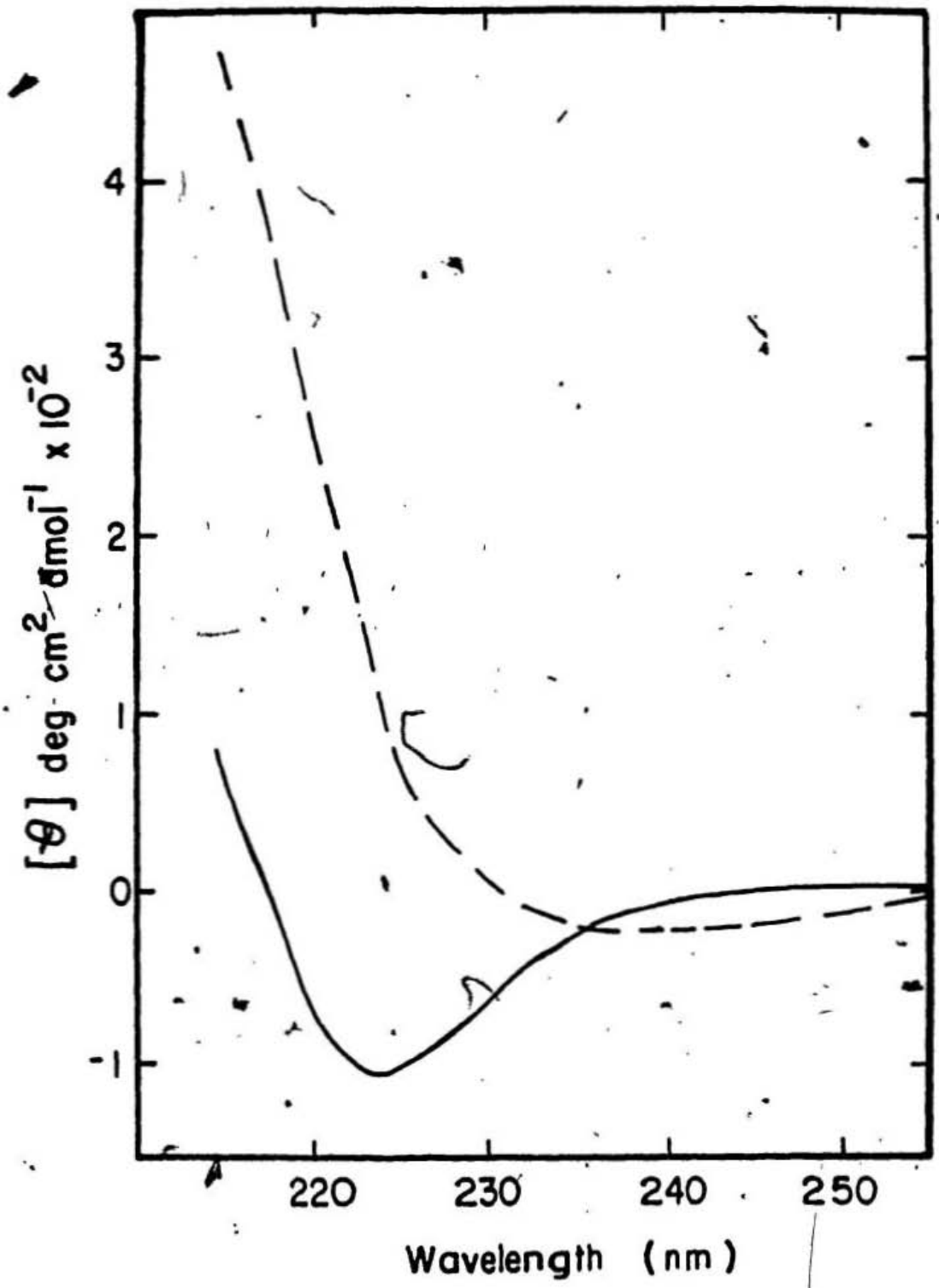

Figure 5-3: Circular Dichroism Spectra of N^{α}*t*BocProDAlaAlaOCH$_3$ With and Without Calcium Ion in Water

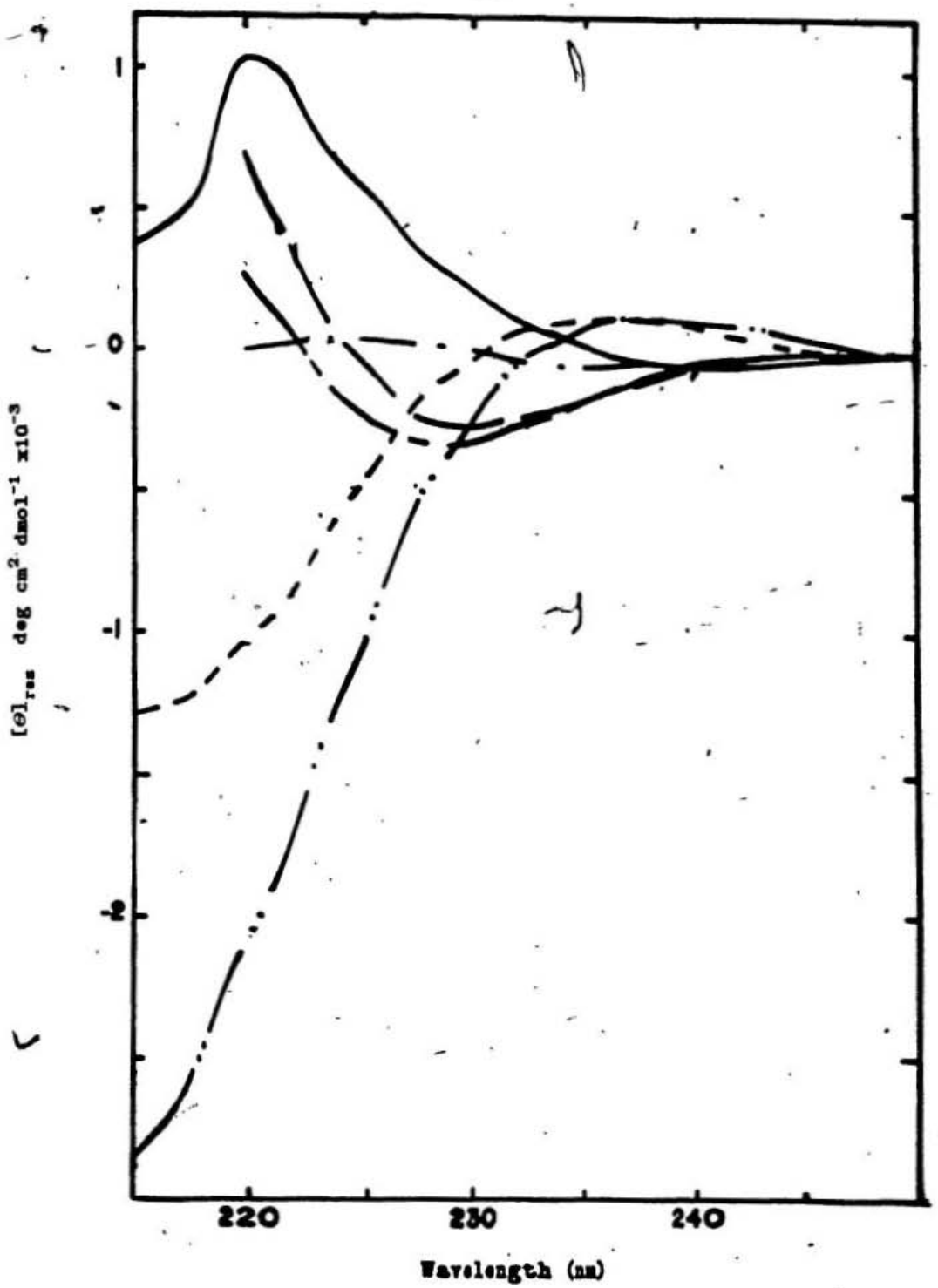

Figure 5-4: Circular Dichroism Spectra of N^{α}*t*BocProDAlaAlaOH alone——, 2000xcalcium—·—; N^{α}*t*BocProDAlaNHCH$_3$ alone- - - -, 2000xcalcium—··—; N^{α}*t*BocProDAlaOH alone——, 2000xcalcium— — —.

are shown in Figure 5-4. These short peptides all have carbonyls which are capable of coordinating to the calcium ion. However, it appears that a peptide requires the minimum number of residues to form a double β-turn for effective binding to occur. How effective is a binding which requires 300 molar equivalents of calcium ion to peptide to reach the "plateau"? Further binding studies would have to be performed in a solvent which did not disrupt the hydrogen-bonding patterns and which was unlikely to compete with the calcium ion for the carbonyls.

5.2.1.2. Studies Using Acetonitrile as Solvent

CD spectroscopy demonstrated that the double β-turn conformer of N^{α}*t*BocProDAlaAlaNHCH$_3$ was stabilized in acetonitrile (see 4.1.3). Acetonitrile would not form strong hydrogen bonds with the peptide carbonyls and is therefore less likely to interact with the peptide than water. Therefore the binding would be expected to reach a maximum at a lower $[Ca^{2+}]/[peptide]$ ratio than that required in water. The results were much more dramatic than expected. The CD spectra of N^{α}*t*BocProDAlaAlaNHCH$_3$ in acetonitrile at various $[Ca^{2+}]/[peptide]$ ratios is shown in Figure 5-5. The portion of the spectrum due to the $n \rightarrow \pi^*$ transition (215-235 nm) becomes increasingly negative until a calcium to peptides ratio of 3:1 and thereafter slowly becomes more positive. Figure 5-6 plots the mean residue ellipticity at 221 nm *versus* the $[Ca^{2+}]/[peptide]$ ratio. Extrapolation of the points indicate that a maximum is achieved at a calcium to peptide ratio of 1.2:1. The binding of the peptide to calcium ion appears to be strongly favoured when acetonitrile is the solvent as opposed to when water was used as solvent. The observed effect is not due to non-specific binding or a salt-

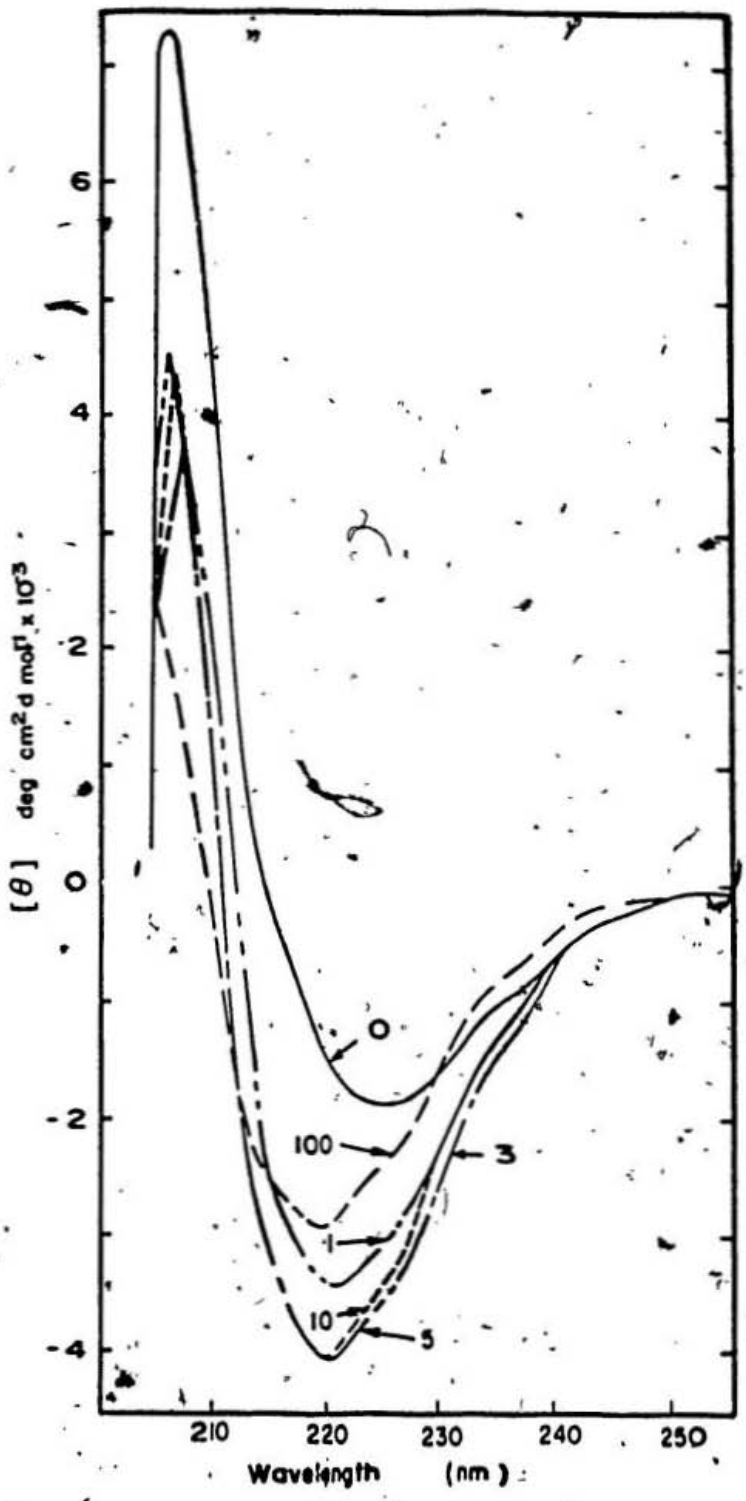

Figure 5-5: Circular Dichroism Spectra of N^{α}tBocProDAlaAlaNHCH$_3$ at Various Calcium to Peptide Ratios in Acetonitrile

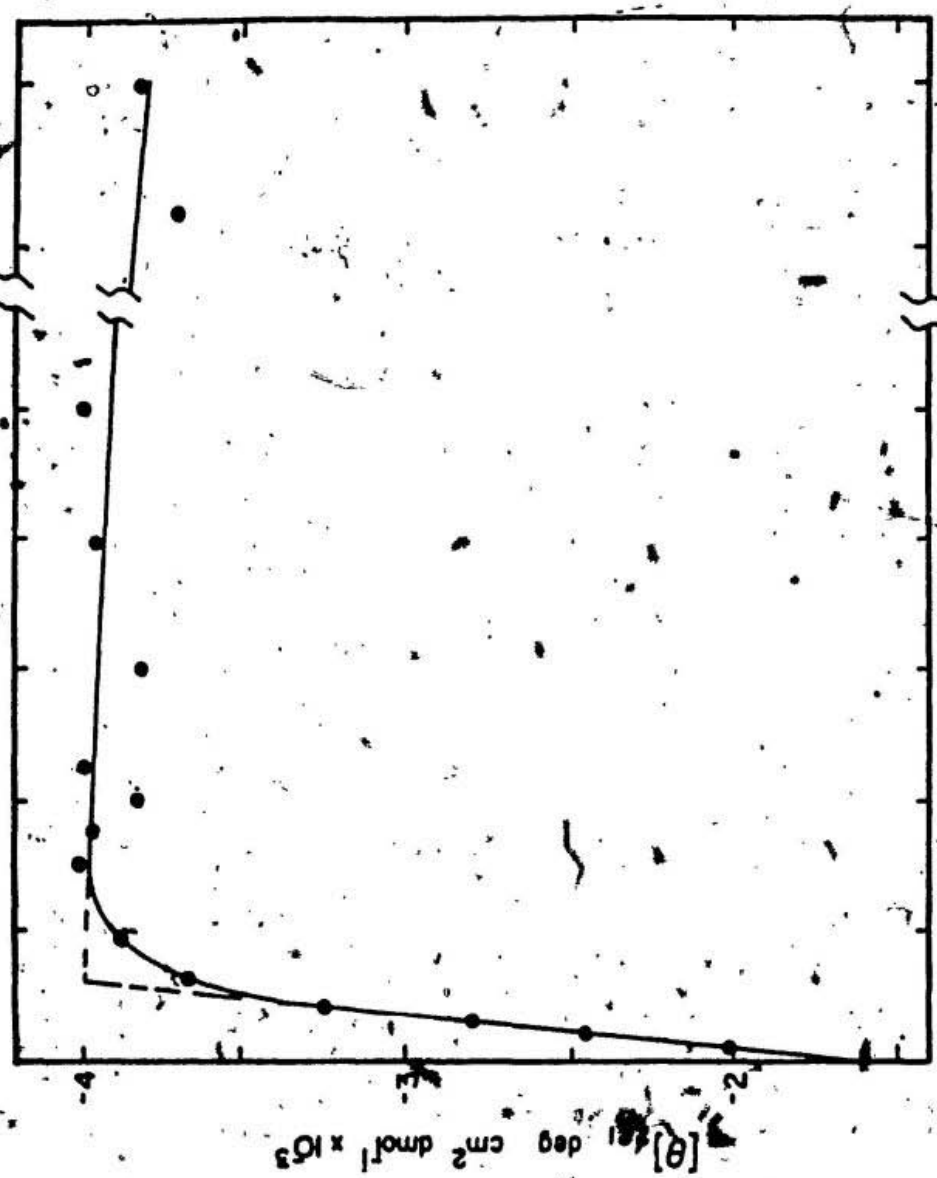

Figure 5-6: $[\theta]^{221}_{res}$ *vs.* $[Ca^{2+}]/[Peptide]$ of N^{α}*t*BocProDAlaAlaNHCH$_3$ in Acetonitrile

effect since if the latter were the case, one would not observe such a distinctive curve. The plot of $[\theta]_{res}^{221}$ *vs.* $[Ca^{2+}]$/[peptide] would in both cases be expected to remain linear from zero to a much higher calcium to peptide ratio. The shape of the plot represents a specific saturable conformational change upon the addition of calcium ion. After a $[Ca^{2+}]$/[peptide] ratio of 3 the mean residue molar ellipticity at 221 nm slowly becomes more positive. A similar effect was seen with the peptide in water after a $[Ca^{2+}]$/[peptide] ratio of 300. This represents non-specific binding or the general "salt-effect" on the system.

5.2.2. NMR Studies

Nuclear magnetic resonance can be used to follow changes of the environment surrounding a particular nucleus. Proton NMR allows one to follow the fate of the NH protons while carbon-13 can be used for the same purpose with respect to the peptide carbonyls. The titration with calcium perchlorate of N^{α}*t*BocProDAlaAlaNHCH$_3$ by both carbon-13 and proton NMR was done in acetone-d_6 since the peptide was not soluble to the extent required for NMR particularly the carbon-13. The uncomplexed peptide was found to be predominantly in the *trans* form in acetone-d_6 (see section 3.2.3.3) and hence the consecutive β-turn structure was deemed to be stabilized in that solvent.

The change in the chemical shift of the NH protons *versus* calcium to peptide ratio is shown in Figure 5-7. The peak assignments of the proton NMR of N^{α}*t*BocProDAlaAlaNHCH$_3$ in acetone-d_6 without added calcium ion were made in section 3.3.3.3. The NH protons belonging to the L-alanine and the NHCH$_3$ showed a significantly greater change in chemical shift, upon calcium ion addition,

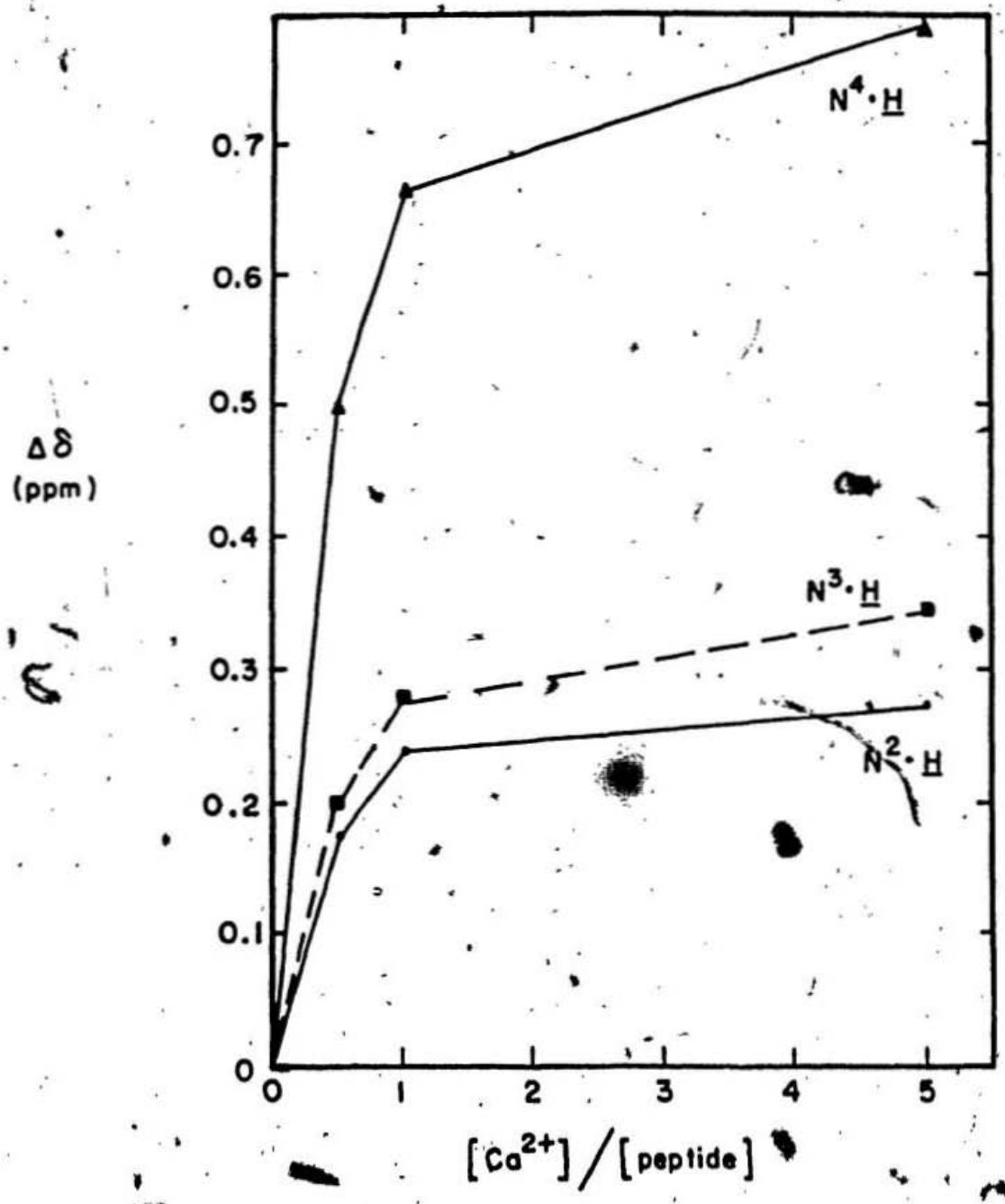

Figure 5-7: Change in Chemical Shift of NH Resonances *vs.* $[Ca^{2+}]/[Peptide]$ Ratio of N^{α}*t*BocProDAlaAlaNHCH$_3$ in Acetone-d_6

when compared to the NH resonance corresponding to the D-alanine. The NH protons of the L-alanine and the $NHCH_3$ were found to be hydrogen-bonded while the NH of the D-alanyl residue was not (see chapter 3 and section 4.3). Therefore, the large change in chemical shift was taken to be indicative of the breaking of hydrogen-bonds.

The change in chemical shift of the carbonyl resonances *versus* the calcium to peptide ratio is shown in Figure 5-8.The carbon-13 resonance assignments of the uncomplexed peptide in acetone-d_6 had been made previously (see section 3.2.3.3). The carbonyls belonging to the *t*Boc group and the prolyl residue ($C{=}O^1$ and $C{=}O^2$, respectively in Figure 5-8) showed significantly less change in chemical shift, upon calcium ion addition, than the carbonyls corresponding to the D- and L-alanyl residues ($C{=}O^3$ and $C{=}O^4$, respectively). The prolyl and *t*Boc carbonyls were determined to be hydrogen-bonded while those of the two alanine enantiomers were not (see chapter 3 and section 4). The change was not attributed, as in the case of the NH resonances, to the breaking of hydrogen bonds but to the coordination of the carbonyls to the calcium ion. The environment surrounding the carbonyl changes little whether the carbonyl is involved in hydrogen-bonding or coordination to calcium ion. However, in the case of those carbonyls not previously involved in hydrogen-bonding, the change in surrounding environment upon coordination to calcium ion is much greater and hence the change in chemical shift is larger.

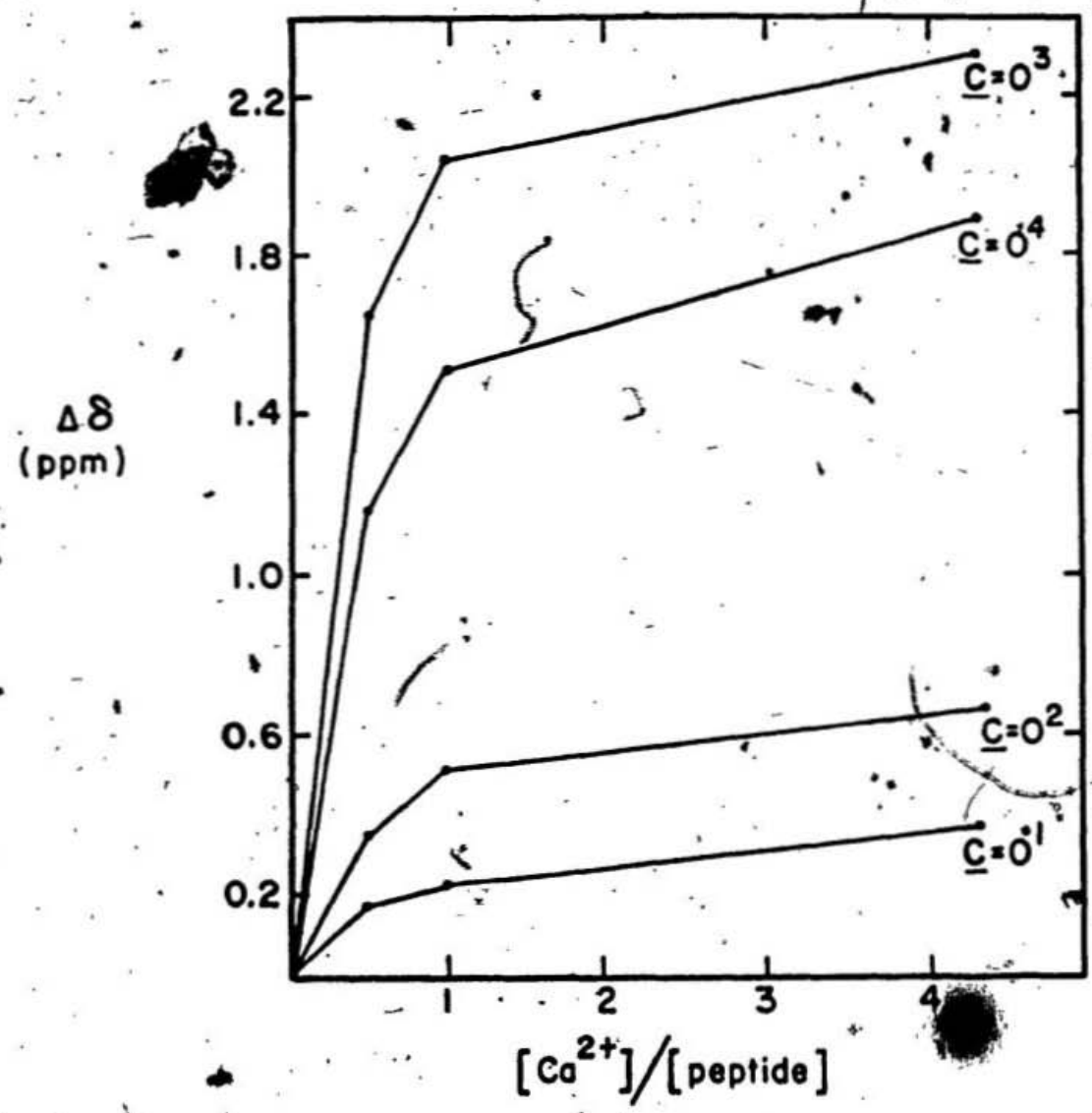

Figure 5-8: Change in Chemical Shift of Carbonyl Resonances *vs.* $[Ca^{2+}]/[Peptide]$ Ratio of N^{α}*t*BocProDAlaAlaNHCH$_3$ in Acetone-d_6

5.3. N^{α}tBocProGlyAlaNHCH$_3$

5.3.1. Circular Dichroism Studies

As with the N^{α}*t*BocProDAlaAlaNHCH$_3$ peptide, the titration of the Gly-peptide with calcium ion was followed by CD spectroscopy. The CD spectra of N^{α}*t*BocProGlyAlaNHCH$_3$ in acetonitrile at various [Ca^{2+}]/[peptide] ratios is shown in Figure 5-9. Unlike the DAla-peptide the $n \rightarrow \pi^*$ portion of the spectra became increasingly positive with the addition of calcium ion until saturation at which point it slowly became more negative. The differences in the relative shape of the spectra and the trend upon the titration with calcium ion between the Gly- and the DAla-peptide is not a major problem since the CD spectra of the uncomplexed peptide is also different. The plot of the mean residue ellipticity *versus* [Ca^{2+}]/[peptide] ratio is a better indicator of the similarity of the effect of calcium ion on the two peptides. The plot of the mean residue ellipticity at 220 nm *versus* the calcium to peptide ratio is shown in Figure 5-10. The Gly-peptide reaches calcium ion saturation at a lower calcium to peptide ratio than the DAla-peptide. This may indicate that N^{α}*t*BocProGlyAlaNHCH$_3$ is more capable of binding calcium ion than N^{α}*t*BocProDAlaAlaNHCH$_3$. The possible reasons for this will be discussed in section 5.4. The less than 1:1 ratio of peptide to calcium required to reach a "plateau" with N^{α}*t*BocProGlyAlaNHCH$_3$ in acetonitrile (0.6:1) indicates that a simple 1:1 binding does not exist. This aspect of binding will be dealt with in section 5.5.

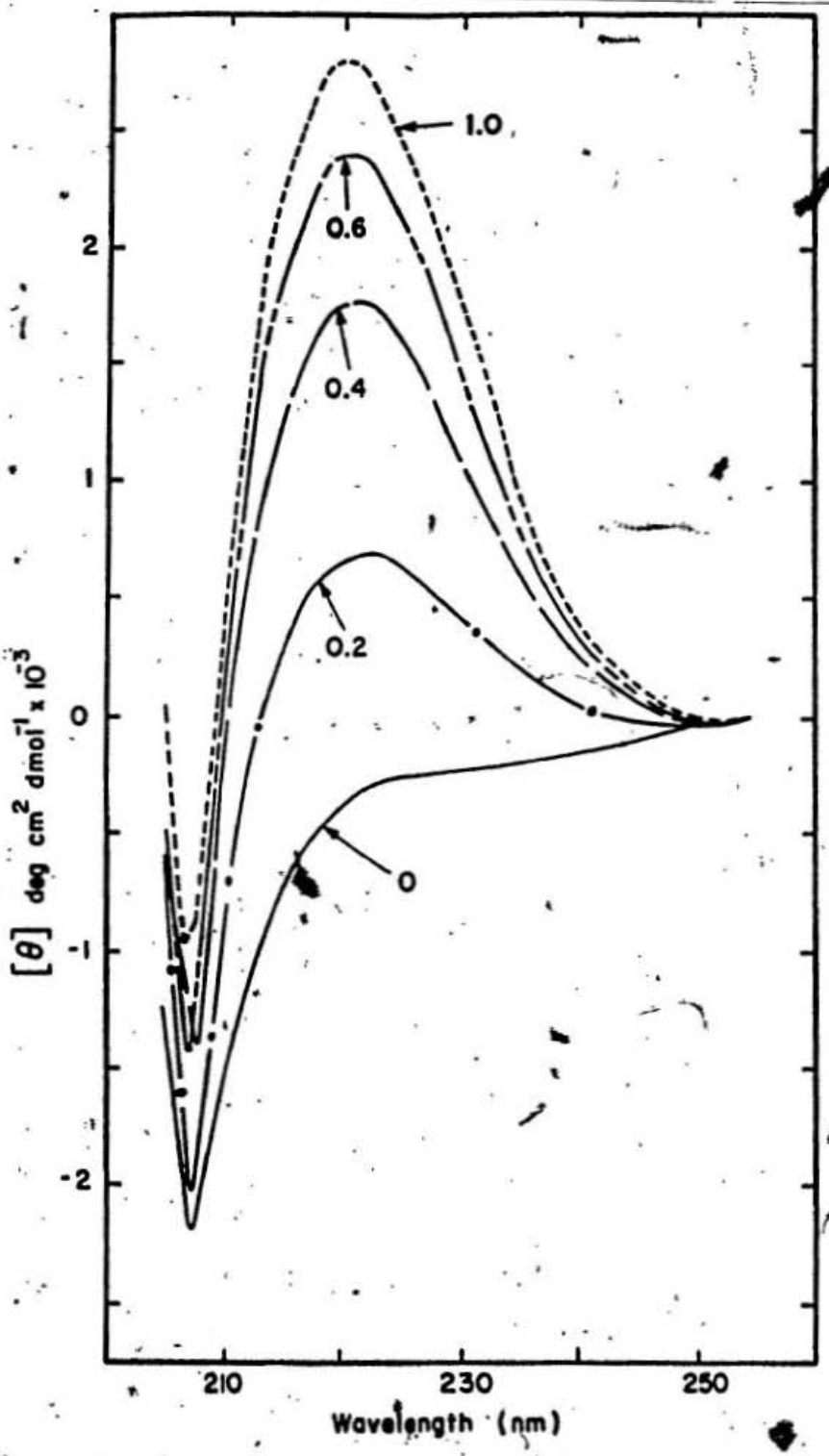

Figure 5-9: Circular Dichroism Spectra of N^{α}tBocProGlyAlaNHCH$_3$ at Various Calcium to Peptide Ratios in Acetonitrile

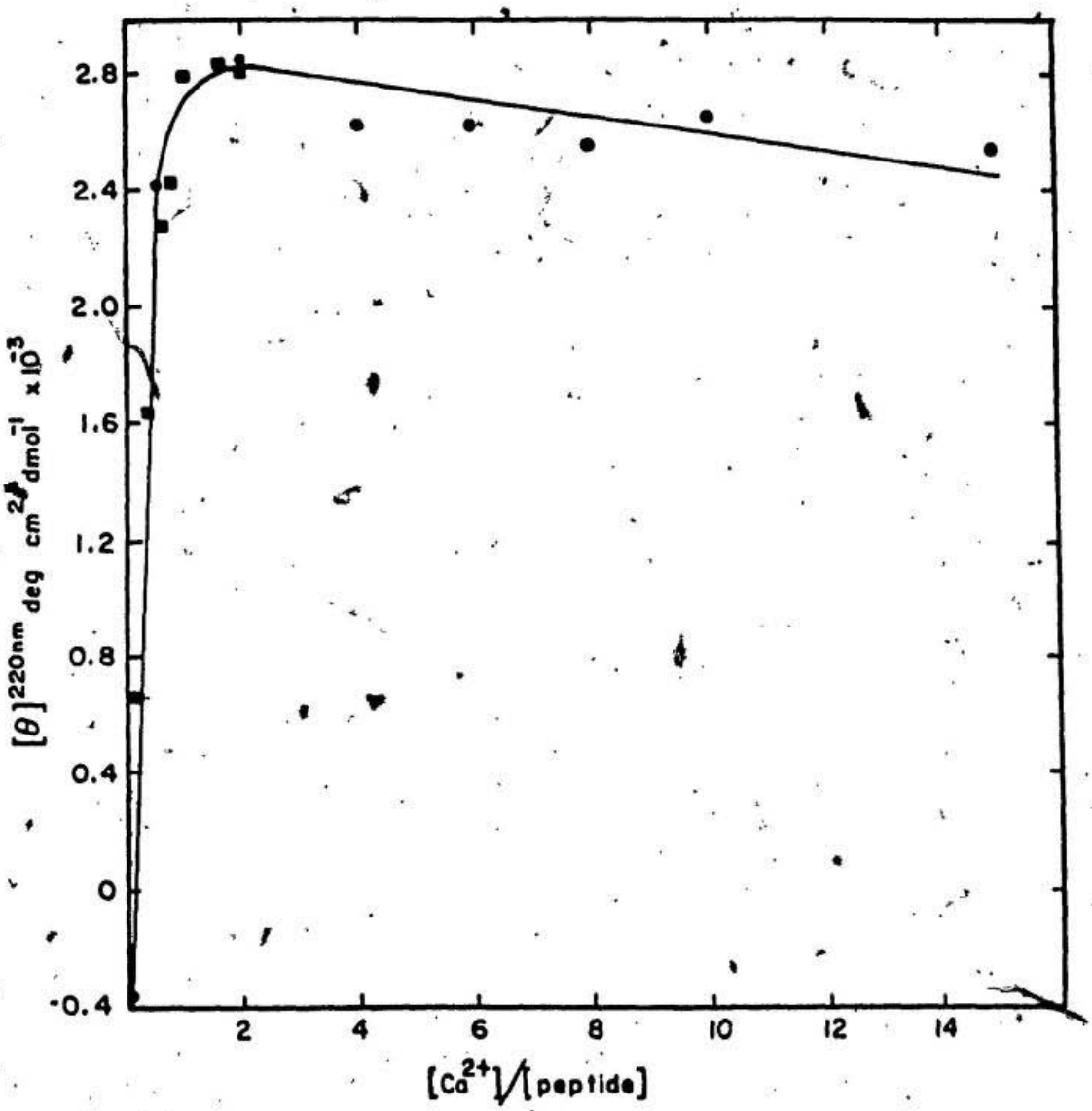

Figure 5-10: $[\theta]^{220}_{res}$ *vs.* [Ca^{2+}]/[Peptide] of N^{α}tBocProGlyAla[redacted]$NHCH_3$ in Acetonitrile

5.3.2. NMR Studies

As with the N^{α}*t*BocProDAlaAlaNHCH$_3$ peptide, NMR spectroscopy was used to follow the change in environment surrounding the NH proton and carbonyl carbons. The N^{α}*t*BocProGlyAlaNHCH$_3$ peptide was more soluble in acetonitrile-d_3 than the DAla-peptide and hence the NMR studies were able to be preformed in that solvent. The change in the chemical shift of the NH protons *versus* the calcium to peptide ratio as followed by proton NMR is shown in Figure 5-11. The results are not as clear as those achieved with the DAla-peptide. The NH proton resonance which showed the largest change in chemical shift corresponds to the glycine NH which had previously been postulated not to have been hydrogen-bonded (see section 4.3). With the DAla-peptide, the NH proton which was postulated not to have been hydrogen-bonded, showed the smallest change in chemical shift when compared to the other, hydrogen-bonded, NH protons. However, the NH corresponding to the L-alanyl residue, which was hydrogen-bonded in the uncomplexed species, had a change in chemical shift only slightly greater than the non-hydrogen-bonded D-alanine NH. The shape of the titration curves is similar for all NH protons whether or not they are hydrogen-bonded and therefore the shape of the plot cannot be used as a criteria for the elucidation of hydrogen-bonding patterns.

The effect of the addition of calcium ion on the chemical shift of the carbonyl resonances as followed by carbon-13 NMR is shown in Figure 5-12. As with the DAla-peptide, the plot of the chemical shift *versus* the calcium to peptide ratio had less of an initial slope with the carbonyls corresponding to the *t*Boc group and

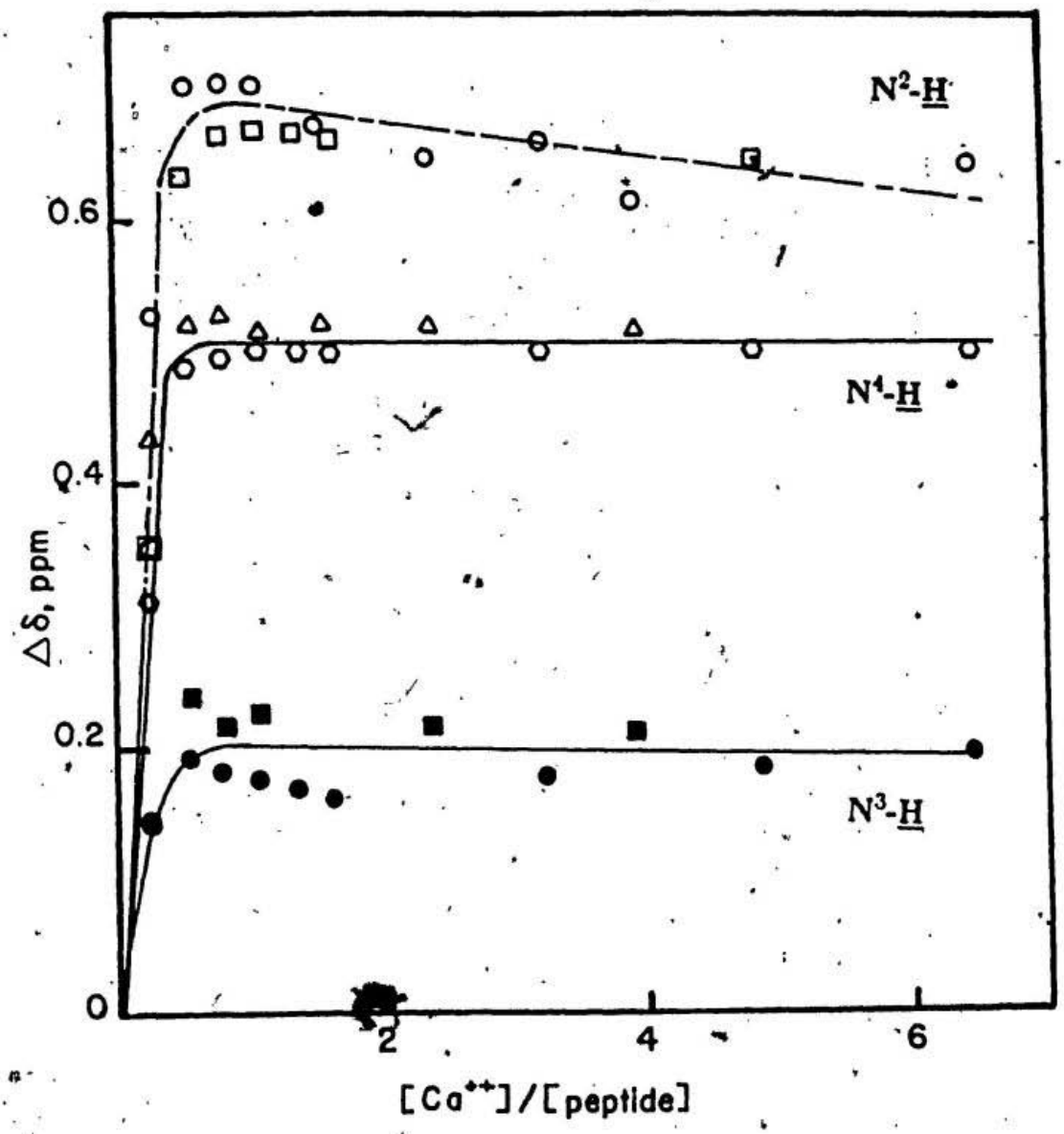

Figure 5-11: Change in Chemical Shift of NH Resonances *vs.* $[Ca^{2+}]/[Peptide]$ Ratio of N^{α}*t*BocProGlyAlaNHCH$_3$ in Acetonitrile-d_3

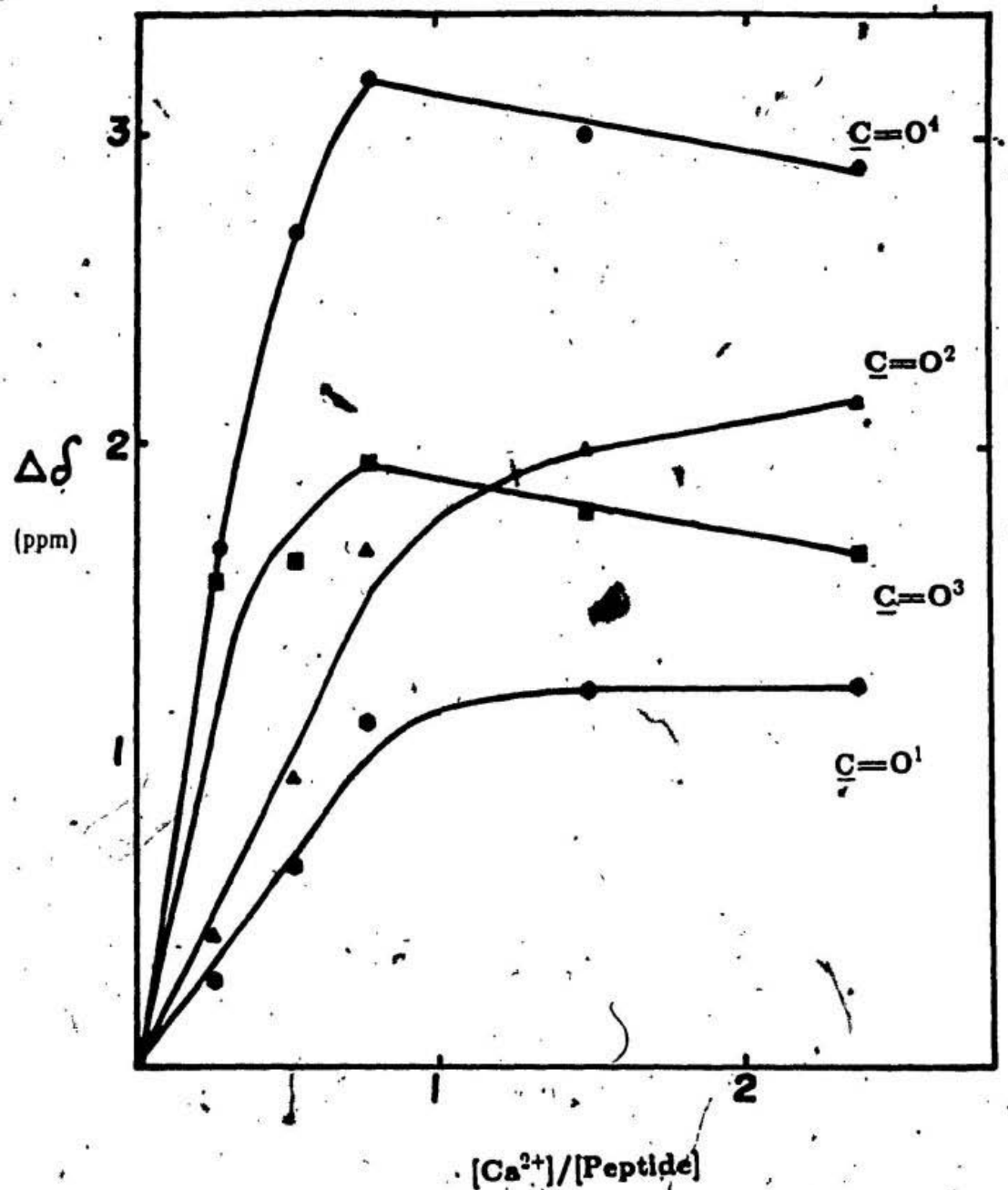

Figure 5-12: Change in Chemical Shift of Carbonyl Resonances *vs.* $[Ca^{2+}]/[Peptide]$ Ratio of N^{α}-BocProGlyAlaNHCH$_3$ in Acetonitrile-d_3

prolyl residue than with L- and D-alanyl carbonyls. The hydrogen-bonding patterns of the uncomplexed peptide were determined to be the same with the N^{α}*t*BocProGlyAlaNHCH$_3$ peptide and the N^{α}*t*BocProDAlaAlaNHCH$_3$ peptide (see chapter 3 and section 4.3) and therefore the interpretation of the effect of the addition of calcium ion on the carbonyls of the two peptides was considered to be the same.

The apparent contradiction between the proton and carbon-13 NMR data, in the case of the Gly-peptide although unfortunate, is not unique to this system. Vishwanath and Easwaran (1982) stated that in instances of such contradiction, the reliance on the carbonyl shifts is more reasonable in the elucidation of hydrogen-bonding patterns than the NH proton signals. The changes in NH proton chemical shift could be the combined effect of the state of two types of hydrogen bonds. In addition to the *intra*molecular hydrogen bonds between a carbonyl and an amide, one can also have *inter*molecular hydrogen bonds involving the NH and either the N of acetonitrile-d_3 (CD_3CN) or the O of H_2O. Since the calcium perchlorate is a hydrated molecule , there is an addition of water into the system which parallels the addition of calcium ion.

Therefore, based primarily on the carbon-13 NMR data, the N^{α}*t*BocProGlyAlaNHCH$_3$ peptide undergoes an analogous conformational change to that observed with the N^{α}*t*BocProDAlaAlaNHCH$_3$ peptide. The four peptide carbonyls coordinate to the calcium ion and the two *intra*molecular hydrogen bonds that exist in the uncomplexed species are broken.

5.4. Ion-Specificity Studies

To determine whether either of the two peptides are ion-selective, the effect of the addition of various cations was followed by CD spectroscopy in acetonitrile and compared to the effect observed with calcium ion. Solutions with [ion]/[peptide] ratios of 2 were prepared and in the case of the monovalent cations, a second set of solutions were prepared with ionic strength equal to that of the divalent cations. Figures 5-13 and 5-14 compare the effect of the perchlorate salts of calcium, magnesium, sodium and lithium on the mean residue ellipticity of the Gly-peptide and DAla-peptide, respectively. The binding of potassium ion to peptide was not explored since the perchlorate salt was not soluble in acetonitrile. In both peptides, the monovalent sodium ion binds weakly if at all. The binding of lithium to both peptides is greater than that of the sodium ion but still very much less than the calcium ion. The enhanced binding of lithium over sodium is expected due to its higher charge to size ratio. Even at twice molar concentrations, the sodium and lithium ions bind weakly when compared to the calcium ion. The major difference between the two peptides is in the ability to bind magnesium ion. The binding of magnesium ion to the $N^{\alpha}t$BocProDAlaAlaNHCH$_3$ is at the level of the monovalent cations while with the $N^{\alpha}t$BocProGlyAlaNHCH$_3$ peptide the level of binding, although not as high as with the calcium ion, is significant. With calcium-binding, saturation is reached much more quickly with the Gly-peptide than with the DAla-peptide (see above). Both phenomena can be attributed to the enhanced flexiblity of the peptide chain with the glycine analogue as opposed to the DAlanine analogue. The ionic radius of the magnesium ion is smaller than the ionic radius of calcium

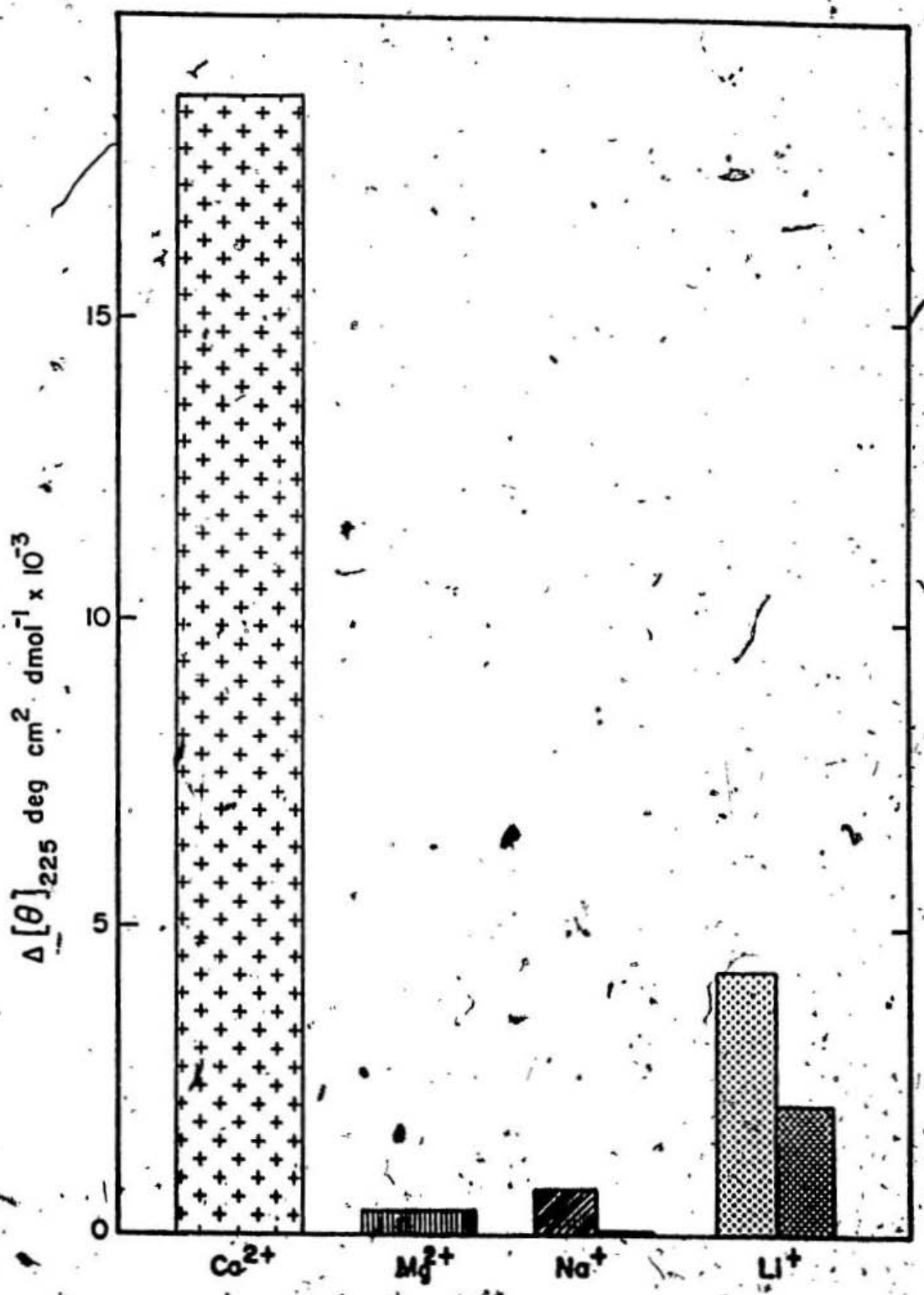

Figure 5-13: Ion-Specificity of N$^{\alpha}$*t*BocProGlyAlaAlaNHCH$_3$

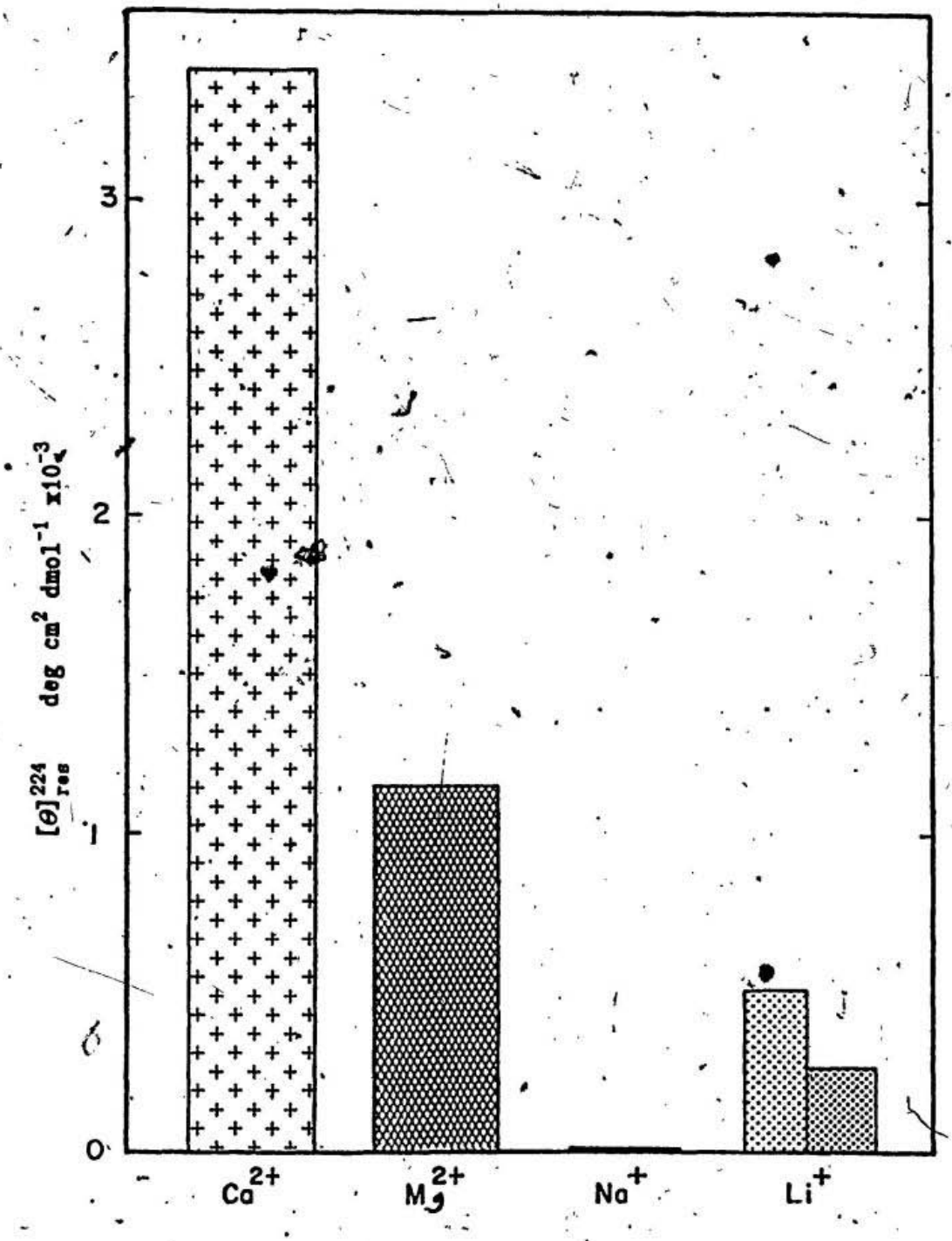

Figure 5-14: Bar graph of Ion-Specificity of N^{α}tBocProDAlaAlaNHCH$_3$ in acetonitrile. Bars corresponding to monovalent ions are split in two; bar on the right is equimolar to a [Ca^{2+}]/[peptide] ratio of 2, bar on the left is adjusted for equal ionic strength to a [Ca^{2+}]/[peptide] ratio of 2. Both calcium and magnesium are at [ion]/[peptide] ratios of 2.

ion. The calcium ion also requires more coordination sites to be filled (7 or 8) than the magnesium ion (6). The range of distances for Ca-O in the primary coordination sphere are 0.229 to 0.265 nm and for Mg-O, the much narrower range of 0.200 to 0.216 nm (Campbell, 1983). This in conjunction with the more regular stereochemistry required by a coordination number of six compared to seven and eight would explain why a more flexible molecule is required to bind magnesium. "The pocket is altered to fit the change."

It is possible that the types of binding and the associated conformational changes are different. If this were the case, the change in CD spectra would be expected to be different and hence, the comparison of the effect at one wavelength would be meaningless. To examine whether or not the mode of binding was the same, the $N^{\alpha}t$BocProGlyAlaNHCH$_3$ peptide was titrated over a range of magnesium to peptide ratios. The mean molar ellipticity at 224 nm was plotted against the $[Mg^{2+}]$/[peptide] ratio. The plot, shown in Figure 5-15, indicates that a higher concentration of magnesium ion is required to reach saturation. However, the effect does not appear to be due to a different mode of binding. The spectrum of the Gly-peptide at a magnesium to peptide ratio of 2 is similar to the spectra of the Gly-peptide at calcium to peptide ratios lower than 2.

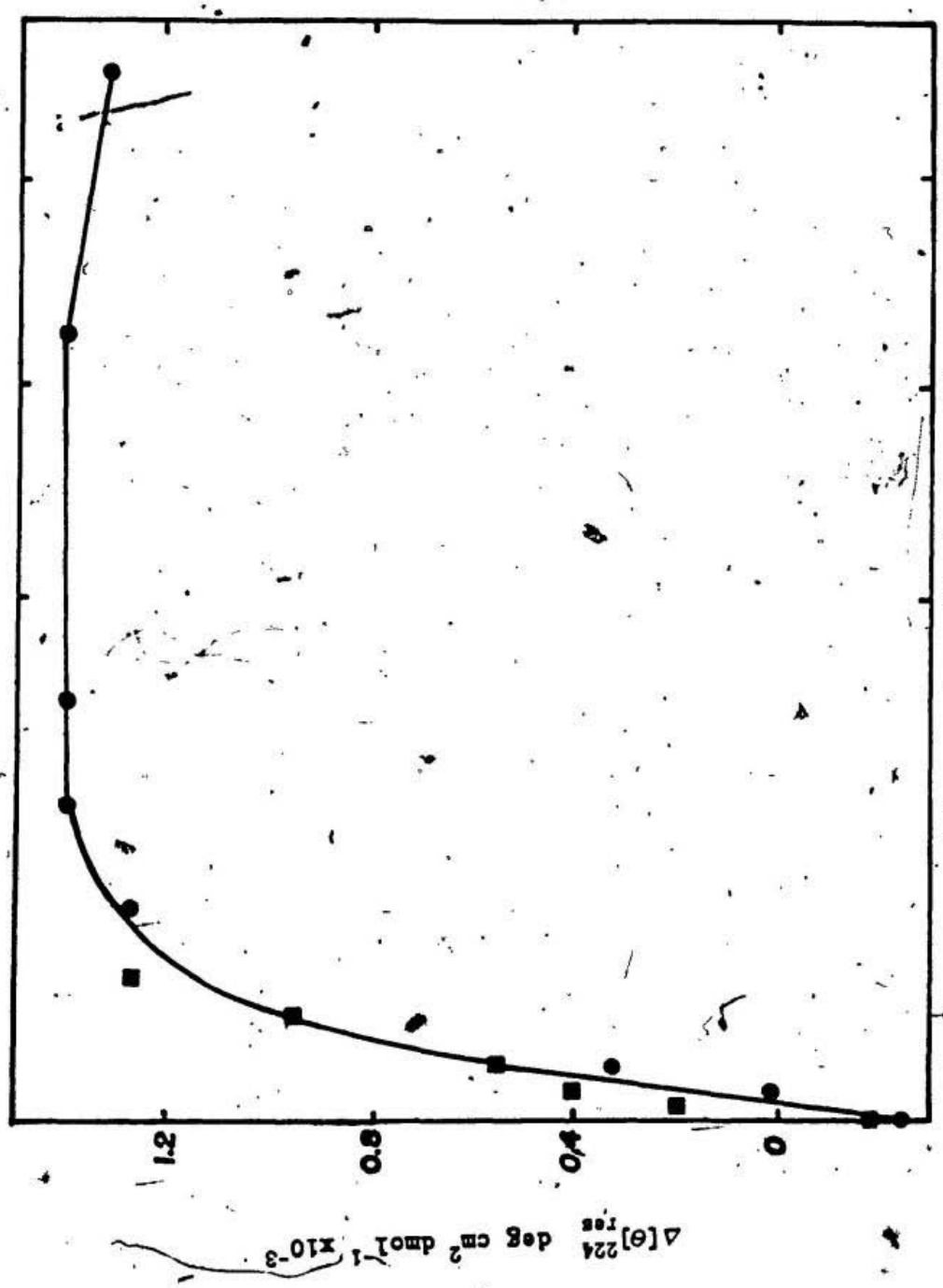

Figure 5-15: $[\theta]^{224}_{res}$ *vs.* $[Mg^{2+}]/[Peptide]$ of $N^{\alpha}t$BocProGlyAlaNHCH$_3$ in Acetonitrile

5.5. Ion-Binding Constants

The binding curves, as determined by CD spectroscopy, of the calcium ion titration of N^{α}tBocProGlyAlaNHCH$_3$ were analyzed for binding constants and stoichiometries. The peptide molecule has at most four ligands capable of coordinating to the metal ion and the calcium ion requires seven to eight coordination sites to be filled by either solvent or peptide carbonyls. Therefore, it is possible that a system of multiple equilibria could exist. With a peptide to ion ratio of 1:1 the remaining coordination sites could be filled by either perchlorate ions or water molecules. With a 2:1 peptide:ion complex, all eight calcium ion coordination sites could be filled by peptide carbonyls. In this case, there would be a "sandwich" configuration similar to that seen with the calcium ion complex of valinomycin (Vishwanath and Easwaran, 1982) where the calcium ion lies between two peptide molecules. The two equilibria and their association constant are described below:

$$P+M=PM \qquad K_1=\frac{[PM]}{[P][M]}$$

$$PM+M=P_2M \qquad K_2=\frac{[P_2M]}{[PM][M]}$$

where P, M, PM, P_2M, K_1 and K_2 stand for the peptide, cation, the 1:1 peptide-cation complex, the 2:1 peptide-cation complex, the stability constant for the 1:1 peptide-cation complex and the stability constant for the 2:1 peptide-cation complex, respectively. The stoichiometry and stability constants were calculated by Dr. Sastri by fitting the titration curve to various combinations of equilibrium

using the proceedure of Reuben (1973). The analysis indicated the coexistence of two equilibria and yielded the stability constants of K_1=9.09x10^{3}M^{-1} and K_2=5x10^{4}M^{-1}. Up to a [Ca^{2+}]/[peptide] ratio of 0.5:1, the 2:1 complex is formed; beyond that point a 1:1 complex begins to predominate. Stability constants can also be derived from a Scatchard plot of the experimental data, but these plots were found to be biphasic and non-linear.

5.6. Conclusions and Model Building

The peptides N^{α}*t*BocProDAlaAlaNHCH$_3$ and its glycine analogue N^{α}*t*BocProGlyAlaNHCH$_3$ were shown by proton and carbon-13 NMR, CD and IR spectroscopy to take on a conformation in solution characterized by a Type II β-turn followed by an overlapping Type I' β-turn (see sections 3.4.1 and 4.3). Using NMR, all four carbonyls of both peptides, were shown to coordinate to the calcium ion resulting in the breaking of the *intra*molecular hydrogen bonds found with the uncomplexed species. A schematic diagram of the complexed DAla-peptide alongside the uncomplexed DAla-peptide is shown in Figure 5-16.

Figures 4-6, 5-17 and 5-18 show the CPK models of the uncomplexed DAla-peptide, the calcium-complexed DAla-peptide, and the calcium-complexed DAla-peptide with the calcium ion removed for clarity. Note that the carbonyls are orientated above the plane. The binding data revealed that at lower concentrations, the peptide forms a 2:1 peptide to ion complex resulting in potentially eight coordination sites of the calcium ion being filled from above and below the plane. The first and second β-turns of the Gly-peptide were shown to be less stable than the corresponding β-turns of the DAla-peptide (see chapter 4).

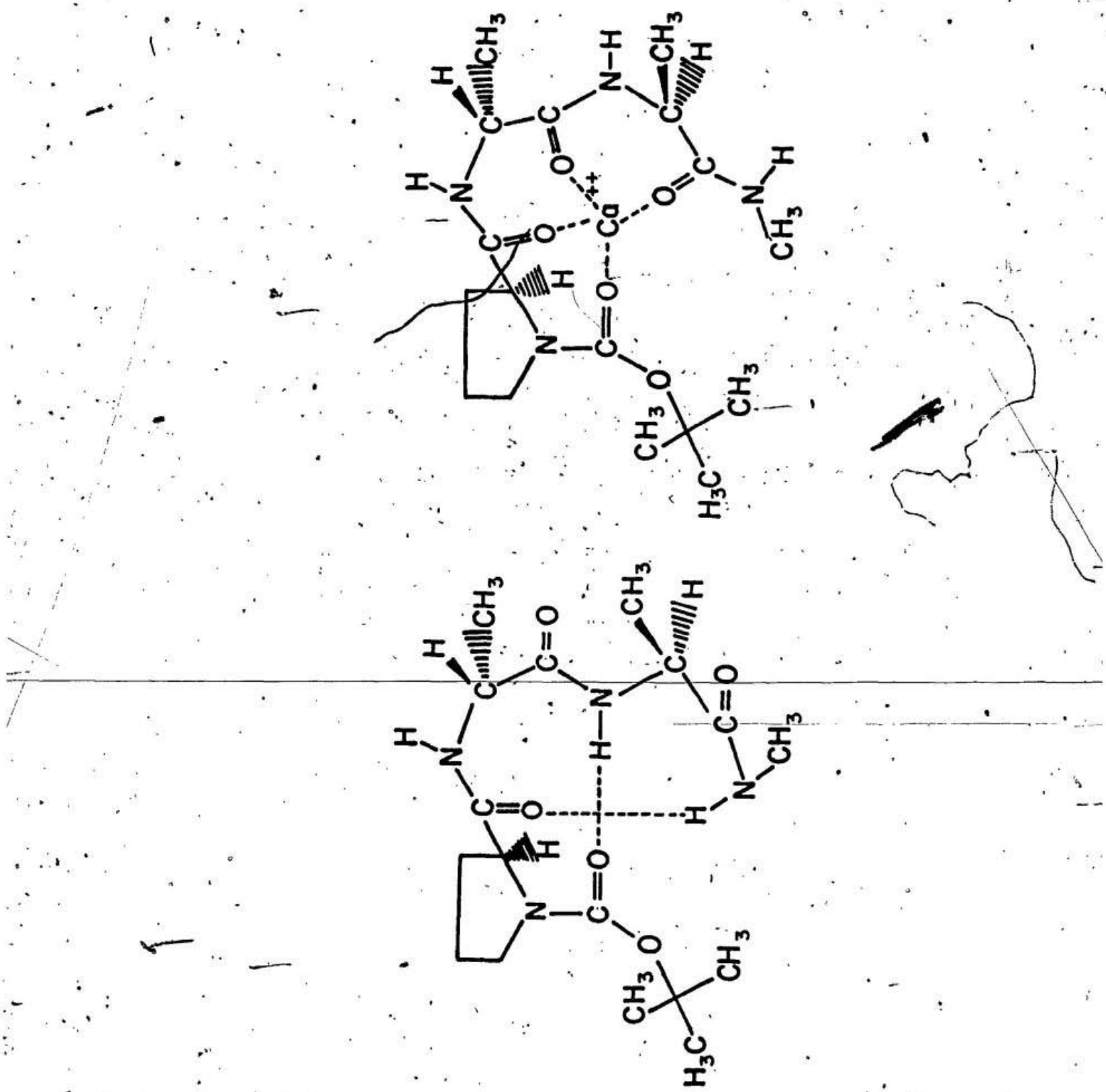

Figure 5-16: Schematic Diagram of N^{α}*t*BocProDAlaAlaNHCH$_3$ in a) Uncomplexed Form and b) Calcium-Complexed Form

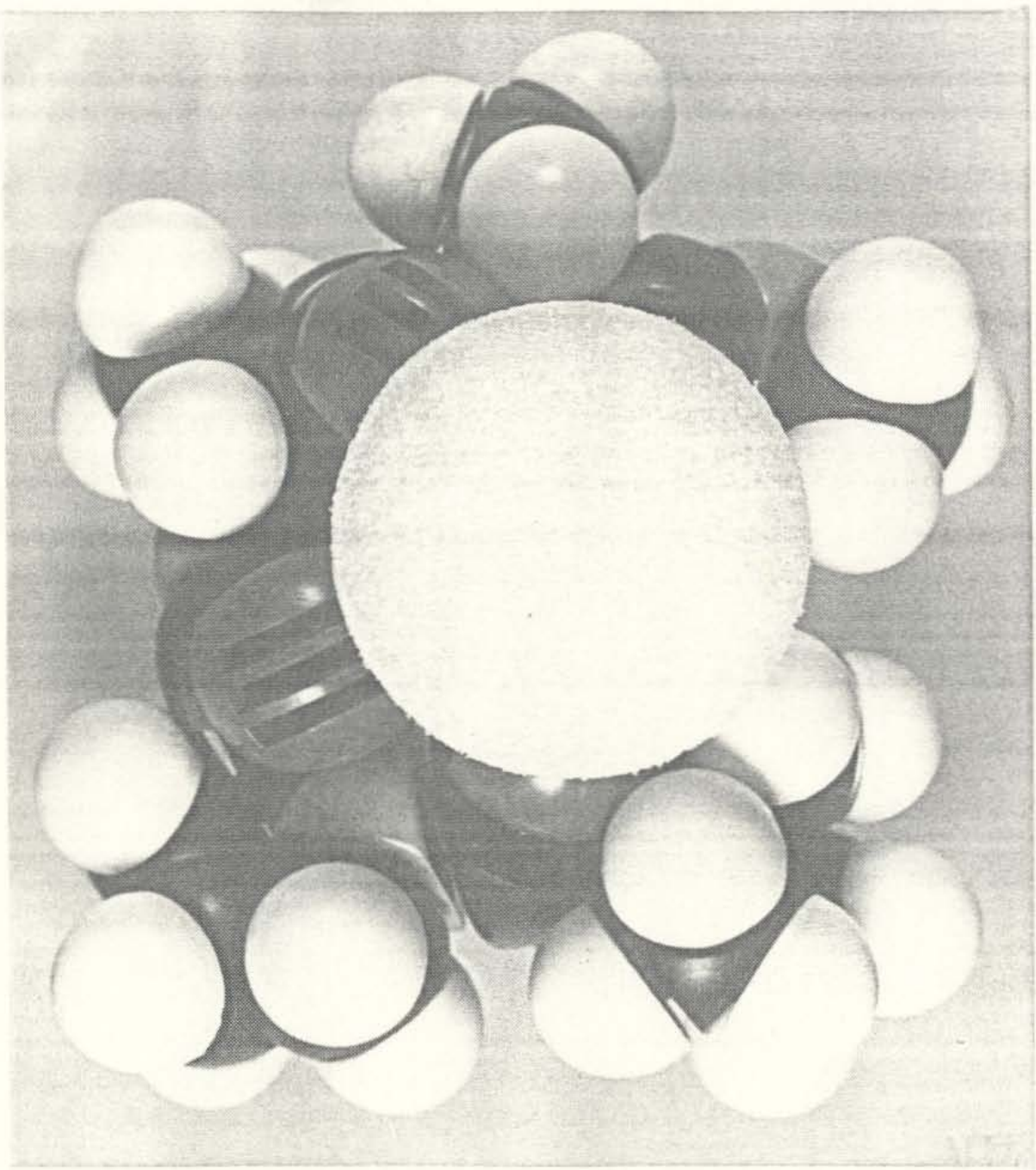

Figure 5-17: CPK Models of N^{α}*t*BocProDAlaAlaNHCH$_3$ in Calcium-Complexed Form

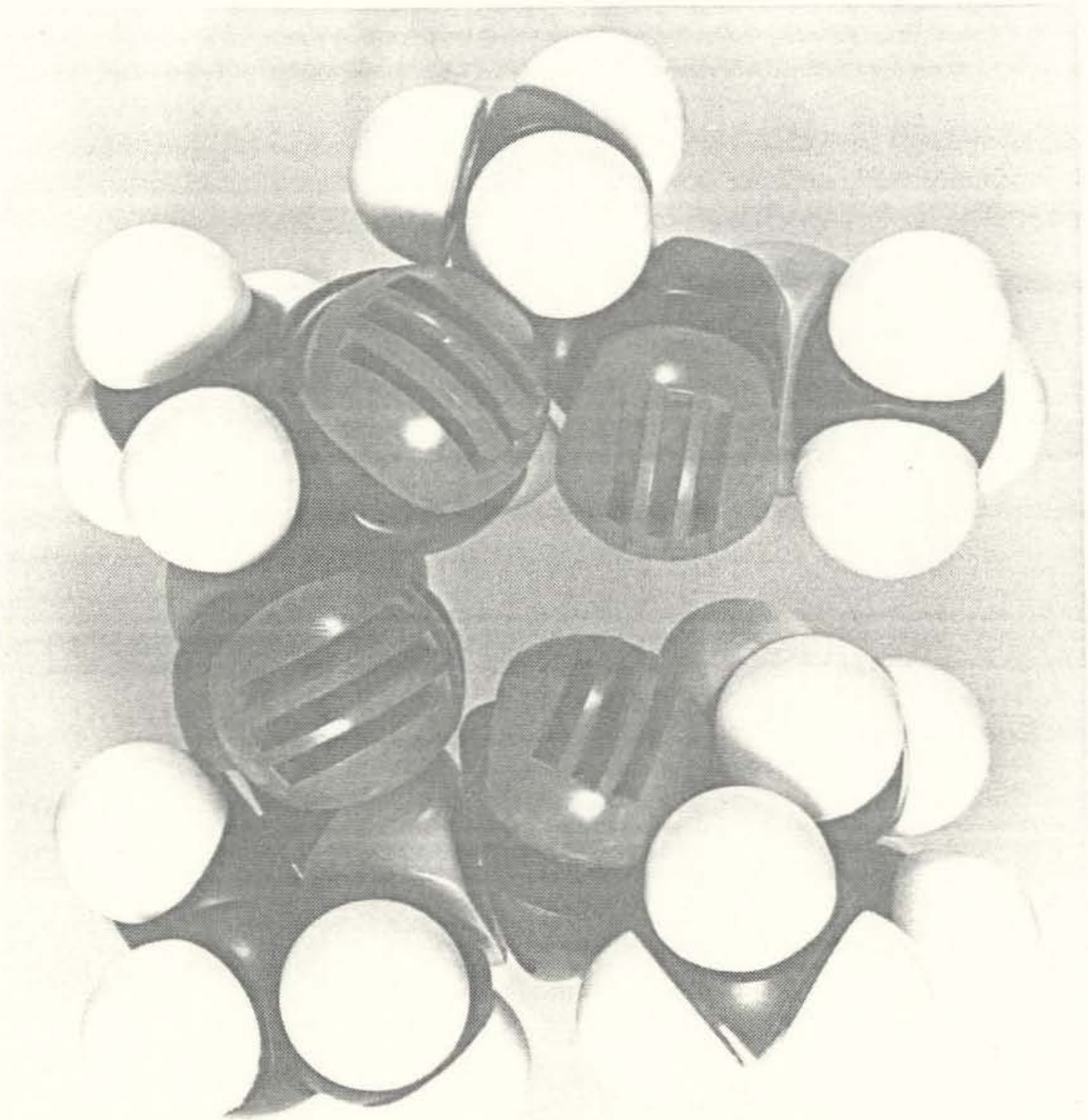

Figure 5-18: CPK Models of N^{α}*t*BocProDAlaAlaNHCH$_3$ in Calcium-Complexed Form Without Calcium Ion

This decreased stability was attributed to an increased flexibility of the peptide because of the replacement of D-alanine with glycine. The N^{α}*t*BocProGlyAlaNHCH$_3$ peptide is not restricted to as narrow a range of conformations as its D-alanine analogue, and hence, is more able to "fit" to the metal ion. Because of this increased "fit", the Gly-peptide is able to bind a wider range of metal ions. This is demonstrated by the significant binding of the Gly-peptide to magnesium as opposed to the DAla-peptide and the fact that the N^{α}*t*BocProGlyAlaNHCH$_3$ requires a lower concentration of calcium ion than N^{α}*t*BocProDAlaAlaNHCH$_3$ to reach saturation.

CD spectroscopy was also used to demonstrate that the double β-turn structure was the minimal structural frame work needed for the binding of calcium ion. The N^{α}*t*BocProDAlaAlaNHCH$_3$ peptide and its glycine analogue N^{α}*t*BocProGlyAlaNHCH$_3$ are the shortest peptides yet to be shown to bind calcium ion. Of greater significance is the requirement of only the backbone carbonyls and the absence of ligands more commonly associated with cation complexing (*i.e.* carboxyls and hydroxyls). There appears to be a relationship between the ability of the peptide to form overlapping β-turns and its ability to bind calcium ion. The occurrence of consecutive tetrapeptides of high β-turn forming potential corresponding to the calcium-binding site of homologous calcium-binding proteins and the predominance of β-turns at postulated calcium-binding sites of protein and peptide ionophores in general (see section 1.4) suggests that the relationship is more than just an interesting phenomenon. This strong correlation, along with the demonstrated ion-selectivity of the tetrapeptides

discussed in this thesis, suggest to the author that the consecutive β-turn forming ability of a sequence plays an integral part in the binding of calcium ion to the homologous calcium-binding proteins. The fact that the final complex of calcium ion with these proteins involves carboxyl and hydroxyl groups in addition to carbonyls does not rule out the above mentioned relationship. The overlapping β-turn may act as an initial requirement for binding which once accomplished is stabilized by the preferred coordination of carboxyl and hydroxyl groups over carbonyls. The later statement is pure conjecture and must be viewed with extreme caution. Its purpose was to point out that the two views on calcium-binding are not necessarily contradictory. The comparison of the calcium-binding capability of peptides with appropriately placed hydroxyl and carboxyl groups that cannot form consecutive β-turns with those peptides that can is the next logical step in the delineation of the involvement of supersecondary structure in ion-binding.

The work presented in this thesis has reinforced the relationship between structure and function of peptide and protein molecules. It has also produced a simplified model of ionophore action and the conformational change associated with ion-binding. That a relationship between consecutive β-turn forming ability and calcium-binding exists has been demonstrated, however, whether each is mutually inclusive or not remains to be seen.

References

1. Ananthanarayanan, V.S. (1983) *J. Biomolecular Strucure and Dynamics* **1**, pp843-855.

2. Ananthanarayanan, V.S., Brahmachari, S.K. and Pattabiraman, N. (1984) *Arch. Biochem. Biophys.* **232**, pp482-495.

3. Ananthanarayanan, V.S. and Shyamasundar, N. (1981) *Biochem. Biophys. Res. Commun.* **102**, pp295-301.

4. Aubert, J.-P., Biserte, G. and Loucheux-Lefebvre, M.H. (1976) *Arch. Biochem. Biophys.* **175**, pp410-418.

5. Aubry, A., Protas, J., Boussard, G. and Marraud, M. (1977) *Acta Cryst.* **B33**, pp2399-2406.

6. Avignon, M., Huong, P.V., Lascombe, J., Marraud, M. and Neel, J. (1969) *Biopolymers* **8**, pp69-89.

7. Babu, Y.S., Sack, J.S., Greenhough, T.J., Bugg, C.E., Means, A.R. and Cook, W.J. (1985) *Nature* **315**, pp37-40.

8. Ballardin, A., Fischman, A.J., Gibbons, W.A., Roy, J., Schwartz, I.L., Smith, C.W., Walter, R. and Wyssbrod, H.R. (1978) *Biochemistry* **17**, pp4443-4454.

9. Bayley, P. (1980) in *An Introduction to Spectroscopy for Biochemists* (Brown, S.B., ed.) Academic Press, London, p177.

10. Benedetti, E., Pavone, V., Toniolo, C., Bonora, G.M. and Palumbo, M. (1977) *Macromolecules* **10**, pp1350-1356.

11. Bodanszky, M., Klausner, Y.S. and Ondetti, M.A. (1976) in *Peptide Synthesis, 2nd edition* (G.A. Olah, ed.) John Wiley and Sons, New York.

12. Bonora, G.M., Mapelli, C., Toniolo, C., Wilkening, R.R. and Stevens, E.S. (1984) *Int. J. Biol. Macromol.* **6**, pp179-188.

13. Boussard, G., Marraud, M. and Aubry, A. (1979) *Biopolymers* **18**, pp1297-1331.

14. Boussard, G., Marraud, M. and Neel, J. (1974) *J. Chim. Phys.* **71**, pp1081-1091.

15. Boussard, G. and Marraud, M. (1985) *J. Am. Chem. Soc.* **107**, pp1825-1828.

16. Bovey, F.A. (1969) in *Nuclear Magnetic Resonance Spectroscopy*, Academic Press, New York, p233.

17. Blaha, K. and Budesinsky, M. (1973) *Int. J. Peptide Protein Res.* **5**, pp309-403.

18. Brahmachari, S.K. and Ananthanarayanan, V.S. (1978) *Curr. Sci.* **47**, pp107-108.

19. Brahmachari, S.K. and Ananthanarayanan, V.S. (1979) *Proc. Natl. Acad. Sci. U.S.A.* **76**, pp5119-5123.

20. Brahmachari, S.K., Ananthanarayanan, V.S., Brahms, S., Brahms, J., Rapaka, R.S. and Bhatnagar, R.S. (1979) *Biochem. Biophys. Res. Commun.* **86**, pp605-612.

21. Brahmachari, S.K., Bhat, T.N., Sudhakar, V., Vijayan, M., Rapaka, R.S., Bhatnagar, R.S. and Ananthanarayanan, V.S. (1981) *J. Am. Chem. Soc.* **103**, pp1703-1708.

22. Brahmachari, S.K., Rapaka, R.S., Bhatnagar, R.S. and Ananthanarayanan, V.S. (1982) *Biopolymers* **21**, pp1107-1125.

23. Brown, S.B. (1980) in *An Introduction to Spectroscopy for Biochemists* (Brown S.B., ed.) Academic Press, London, pp17-18.

24. Bystrov, V.F. (1976) *Prog. in NMR Spectroscopy* **10**, pp41-81.

25. Bystrov, V.F., Ivanov, V.T., Portnova, S.L., Balashova, T.A. and Ovchinnikov, Y.A. (1973) *Tetrahedron* **29**, pp873-877.

26. Bystrov, V.F., Portnova, S.L., Tsetlin, V.I., Ivanov, V.T. and Ovchinnikov, Y.A. (1969) *Tetrahedron* **25**, pp493-515.

27. Campbell, A.K. (1983) in *Intracellular Calcium, Its Universal Role as Regulator* (Gutfreund, H. ed.) John Wiley and Sons, New York, pp117-119.

28. Chandrasekaran, R., Lakshminarayanan, A.V., Pandya, U.V. and Ramachandran, G.N. (1973) *Biochim. Biophys. Acta.* **303**, pp14-27.

29. Chang, C.T., Wu, C.C. and Yang, J.T. (1978) *Analytical Biochemistry* **91**, pp13-31.

30. Chopra, R.K. and Ananthanarayanan, V.S. (1982) *Proc. Natl. Acad. Sci. U.S.A.* **79**, pp7180-7184.

31. Chou, P.Y., Adler, A.J. and Fasman, G.D. (1975) *J. Mol. Biol.* **96**, pp29-45.

32. Chou, P.Y. and Fasman, G.D. (1977) *J. Mol. Biol.* **115**, pp135-175.

33. Chou, P.Y. and Fasman, G.D. (1978) *Adv. Enzymology* **47**, pp45-148.

34. Chou, P.Y. and Fasman, G.D. (1978) *Annu. Rev. Biochem.* **47**, pp251-276.

35. Christl, M. and Roberts, J.D. (1972) *J. Am. Chem. Soc.* **94**, pp4565-4573.

36. Creighton, T.E. (1983) in *Proteins: Structures and Molecular Properties* W.H. Freeman and Co., New York.

37. Crawford, J.L., Lipscomb, W.N. and Schellman, C.G. (1973) *Proc. Natl. Acad. Sci. U.S.A.* **70**, pp538-542.

38. C.R.C. Handbook of Biochemistry and Molecular Biology, 3rd edition (1976) Volume II, Proteins (Fasman, G.D., ed.), pp64-72.

39. Crisma, M., Fasman, G.D., Balaram, H. and Balaram, P. (1984) *Int. J. Peptide Protein Res.* **23**, pp411-419.

40. Deber, C.M., Bartman, B. and Blout, E.P. (1975) in *Peptides: Chemistry, Structure and Biology* (Meienhofe, J. and Walter, R., eds.), Ann Arbor Science, Michigan.

41. Degelaen, J.P., Pham, P. and Blout, E.R. (1984) *J. Am. Chem. Soc.* **106**, pp4882-4890.

42. Deslauriers, R., Komoroski, R.A., Levy, G.C., Paiva, C.M. and Smith, I.C.P. (1976) *FEBS Lett.* **62**, pp50-56.

43. Deslauriers, R., Smith, I.C.P. and Walter R. (1974) *J. Biol. Chem.* **249**, pp7006-7010.

44. Dorman, D.E. and Bovey, F.A. (1973) *J. Org. Chem.* **38**, pp2379-2383.

45. Duax, W.L. and Smith, G.D. (1981) in *Biomolecular Stereodynamics, Volume II* (Sarma, R.H., ed.) Adenine Press, New York, pp311-322.

46. Fermandjian, S., Tran-Dinh, S., Savrda, J., Sala, E., Mermet-Bouvier, R., Bricas, E. and Fromageot, P. (1975) *Biochim. Biophys. Acta.* **399**, pp313-338.

47. Fossel, E.T., Easwaran, K.R.K. and Blout, E.R. (1975) *Bioploymers* **14**, pp927-935.

48. Fox, J.A., Tu, A.T., Hruby, V.J. and Mosberg, H.I. (1981) *Arch. Biochem. Biophys.* **211**, pp628-631.

49. Grathwohl, C. and Wuthrich, K. (1974) *J. Magn. Res.* **13**, pp217-225.

50. Herzberg, O. and James, M.N.G. (1985) *Nature* **313**, pp653-659.

51. Higashijima, T., Tasumi, M. and Miyazawa, T. (1977) *Biopolymers* **16**, pp1259-1270.

52. Howarth, O.W. and Lilley, D.M.J. (1978) *Prog. in NMR Spectroscopy* **12**, pp1-40.

53. Isogai, Y., Nemethy, G., Rackovsky, S., Leach, S.J. and Scheraga, H.A. (1980) *Biopolymers* **19**, pp1183-1210.

54. Jackman, L.M. and Sternhell, S. (1969) in *Applications of Nuclear Magnetic Resonance Spectroscopy in Organic Chemistry, 2nd edition*, Pergamon Press, Oxford, pp124-128 and p164.

55. Jung, G., Bosch, R., Katz, E., Schmitt, H., Voges, K.-P. and Winter, W. (1983) *Biopolymers* **22**, pp241-246.

56. Karle, I.L. (1984) *Int. J. Peptide Protein Res.* **23**, pp32-38.

57. Kawai, M. and Fasman, G. (1978) *J. Am. Chem. Soc.* **100**, pp3630-3632.

58. Khaled, M.A., Renugopalakrishnan, V. and Urry, D.W. (1976) *J. Am. Chem. Soc.* **98**, pp7547-7553.

59. Kimura, S. and Imanishi Y. (1983) *Biopolymers* **22**, pp2383-2395.

60. Kopple, K.D. (1971) *Biopolymers* **10**, pp1139-1152.

61. Kopple, K.D., Go, A. and Pilipauskas, D.R. (1975) *J. Am. Chem. Soc.* **97**, pp6830-6838.

62. Kopple, K.D., Go, A. and Schamper, T.J. (1978) *J. Am. Chem. Soc.* **100**, pp4289-4295.

63. Kretsinger, R.H. (1976) *Annu. Rev. Biochem.* **45**, pp239-266.

64. Kretsinger, R.H. (1980) *C.R.C. Crit. Rev. Biochem.* **8**, pp119-174.

65. Kretsinger, R.H. and Nockolds, C.E. (1973) *J. Biol. Chem.* **248**, pp3313-3326.

66. Krimm, S. and Bandekar, J. (1980) *Biopolymers* **19**, pp1-29.

67. Kumar, N.G., Izumiya, N., Miyoshi, M., Sugano, H. and Urry, D.W. (1975) *J. Am. Chem. Soc.* **97**, pp4105-4114.

68. Levy, G.C., ed. (1976) in *Topics in Carbon-13 N.M.R. Spectroscopy* **2**, Wiley-Interscience, New York.

69. Lewis, P.N., Momany, F.A. and Scheraga, H.A. (1971) *Proc. Natl. Acad. Sci. U.S.A.* **68**, pp2293-2297.

70. Lewis, P.N., Momany, F.A. and Scheraga, H.A. (1973) *Biochim. Biophys. Acta.* **303**, pp211-229.

71. London, R.E., Matwiyoff, N.A., Stewart, J.M. and Cann J.R. (1978) *Biochemistry* **17**, pp2277-2283.

72. Lyerla Jr., J.R., Barber, B.H., Freedman, M.H. (1973) *Can. J. Biochem.* **51**, pp460-464.

73. Lynn, T.E. and Kushick, J.N. (1984) *Int. J. Peptide Protein Res.* **23**, pp601-609.

74. Maxfield, F.R., Bandekar, J., Krimm, S., Evans, D.J., Leach, S.J.,

Nemethy, G. and Scheraga, H.A. (1981) *Macromolecules* **14**, pp997-1003.

75. Moews, P.C. and Kretsinger, R.H. (1975) *J. Mol. Biol.* **91**, pp201-228.

76. Moon, R.B. and Richards, J.H. (1972) *Proc. Natl. Acad. Sci. U.S.A.* **69**, pp2193-2197.

77. Nair, C.M., Vijayan, M., Venkatachalapathi, Y.V. and Balaram, P. (1979) *J.C.S. Chem. Comm.* **24**, pp1183-1184.

78. Nagaraj, R., Shamala, N. and Balaram, P. (1979) *J. Am. Chem. Soc*, **101**, pp16-20.

79. Nagaraj, R. and Balaram, P. (1981) *Biochemistry* **20**, pp2828-2835.

80. Nemethy, G., McQuie, J.R., Pottle, M.S. and Scheraga, H.A. (1981) *Macromolecules* **14**, pp975-985.

81. Nemethy, G. and Printz, M.P. (1972) *Macromolecules* **5**, pp755-758.

82. Okamoto, K. and Urry, D.W. (1976) *Biopolymers* **15**, pp2337-2351.

83. Parker, F.S. (1983) in *Applications of Infrared, Raman, and Resonance Raman Spectroscopy in Biochemistry*, Plenum, New York.

84. Pease, L.G. and Watson, C. (1978) *J. Am. Chem. Soc.* **100**, pp1279-1286.

85. Prasad, B.V.V., Balaram, H. and Balaram, P. (1982) *Biopolymers* **21**, pp1261-1273.

86. Ramachandran, G.N., Chandrasekaran, R. and Kopple, K.D. (1971) *Biopolymers* **10**, pp2113-2131.

87. Ramachandran, G.N., Lakshminarayanan, A.V. and Kolaskar, A.S. (1973) *Biochim. Biophys. Acta.* **303**, pp8-13.

88. Ramachandran, G.N. and Mitra, A.K. (1976) *J. Mol. Biol.* **107**, pp85-92.

89. Ramachandran, G.N. and Sasisekharan, V. (1968) *Adv. Prot. Chem.* **23**, pp283-437.

90. Ramaprasad, S., Shekar, S.C. and Easwaran, K.R.K. (1981) *Curr. Sci.* **50**, pp662-668.

91. Rao, B.N.N., Kumar, A., Balaram, H., Ravi, A. and Balaram, P. (1983) *J. Am. Chem. Soc.* **105**, pp7423-7428.

92. Rao, Ch.P., Nagaraj, R., Rao, C.N.R. and Balaram, P. (1980) *Biochemistry* **19**, pp425-431.

93. Reuben, J. (1973) *J. Am. Chem. Soc.* **95**, pp3534-3540.

94. Richarz, R. and Wuthrich, K. (1978) *Biopolymers* **17**, pp2133-2141.

95. Schimmel, P.R. and Flory, P.J. (1968) *J. Mol. Biol.* **34**, pp105-120.

96. Schwyzer, R., Tun-kyi, A., Caviezel, M. and Moser, P. (1970) *Helv. Chim. Acta.* **53**, pp15-27.

97. Sibanda, B.L. and Thornton, J.M. (1985) *Nature* **316**, pp170-174.

98. Small, D., Chou, P.Y. and Fasman, G.D. (1977) *Biochem. Biophys. Res. Commun.* **79**, pp341-346.

99. Smimizu, T. and Fujishige S. (1980) *Biopolymers* **19**, pp2247-2265.

100. Smith, I.C.P., Deslauriers, R., Saito H., Walter, R., Garrigou-Lagrange, C., McGregor, H. and Sarantakis, D. (1973) *Ann. N.Y. Acad. Sci.* **222**, pp597-627.

101. Smith, G.D., Pletnev, V.Z., Duax, W.L., Balasubramanian, T.M., Bosshard, H.E., Czerwinski, E.W., Kendrick, N.E., Mathews, F.S. and Marshall, G.R. (1981) *J. Am. Chem. Soc.* **103**, pp1493-1501.

102. Smith, J.A. and Pease, L.G. (1980) *C.R.C. Crit. Rev. Biochem.* **8**, pp315-399.

103. Somorjai, R.L., and Deslauriers, R. (1976) *J. Am. Chem. Soc.* **98**, pp6460-6467.

104. Stimson, E.R., Zimmerman, S.S. and Scheraga, H.A. (1977) *Macromolecules* **10**, pp1049-1060.

105. Sughihara, T., Imanishi, Y. and Higashimura, T. (1976) *Biopolymers* **15**, pp1529-1542.

106. Sundaralingam, M., Bergstrom, R., Strasburg, G., Rao, S.T., Roychowdhury, P., Greaser, M. and Wang, B.C. (1985) *Science* **227**, pp945-948.

107. Szebenyi, D.M.E., Obendorf, K. and Moffat, K. (1981) *Nature* **294**, pp327-332.

108. Ptitsyn, O.B. (1981) *FEBS Lett.* **131**, pp197-202.

109. Tamburro, A.M., Guantieri, V. and Scatturin, A. (1984) *Int. J. Biol. Macromol.* **6**, pp241-248.

110. Torchia, D.A., di Corato, A., Wong, S.C.K., Deber, C.M. and Blout, E.R. (1972) *J. Am. Chem. Soc.* **94**, pp609-615.

111. Thomas, G.J.Jr. and Kyogoku, Y. (1977) in *Infrared and Raman Spectroscopy* Part C (Brame, E.G.Jr. and Grasselli, J.G., eds.) Marcel Dekker, New York, pp743-775.

112. Thomas, W.A. and Williams, M.K. (1972) *J.C.S. Chem. Comm.*, p994.

113. Tufty, R.M. and Kretsinger, R.H. (1975) *Science* **187**, pp167-169.

114. Urry, D.W. and Long, M.M. (1976) *C.R.C. Crit. Rev. Biochem.* **4**, pp1-45.

115. Urry, D.W. and Mitchell, L.W. (1976) *Biochem. Biophys. Res. Commun.* **68**, pp1153-1160.

116. Urry, D.W., Mitchell, L.W. and Ohnishi, T. (1974) *Biochem. Biophys. Res. Commun.* **59**, pp62-69.

117. Urry, D.W., Mitchell, L.W. and Ohnishi, T. (1974) *Biochemistry* **13**, pp4083-4090.

118. Urry, D.W., Mitchell, L.W. and Ohnishi, T. (1974) *Proc. Natl. Acad. Sci. U.S.A.* **71**, pp3265-3269.

119. Urry, D.W., Mitchell, L.W. and Ohnishi, T. (1975) *Biochim. Biophys. Acta.* **393**, pp296-306.

120. Urry, D.W., Mitchell, L.W., Ohnishi, T. and Long, M.M. (1975) *J. Mol. Biol.* **96**, pp101-117.

121. Urry, D.W. and Walter, R. (1971) *Proc. Natl. Acad. Sci. U.S.A.* **68**, pp956-958.

122. Van Roey, P., Smith, G.D., Balasubramanian, T.M., Czerwinski, E.W., Marshall, G.R. and Mathews, F.S. (1983) *Int. J. Protein Peptide Res.* **22**, pp404-409.

123. Venkatachalam, C.M. (1968) *Biopolymers* **6**, pp1425-1436.

124. Vishwanath, C.K. and Easwaran, K.R.K. (1982) *Biochemistry* **21**, pp2612-2621.

125. Vogt, H.-P., Strassburger, W., Wollmer, A., Fleischhauer, J., Bullard, B. and Mercola, D. (1979) *J. Theor. Biol.* **76**, pp297-310.

126. Weeds, A.G. and McLachlan, A.D. (1974) *Nature* **252**, pp646-649.

127. Woody, R.W. (1974) in *Peptides Polypeptides and Proteins* (Blout, E.R., Bovey, F.A., Goodman, M. and Lotan, N., eds.) John Wiley and Sons, New York, pp338-350.

128. Wuthrich, K. (1976) in *NMR in Biological Research: Peptides and Proteins*, North-Holland, Amsterdam.

129. Wuthrich, K., Tun-Kyi, A. and Schwyzer, R. (1972) *FEBS Lett.* **25**, pp104-108.

130. Young, P.E. and Deber, C.M. (1975) *Biopolymers* **14**, pp1547-1549.

131. Zimmerman, S.S. and Scheraga, H.A. (1977) *Biopolymers* **16**, pp811-843.

132. Zimmerman, S.S. and Scheraga, H.A. (1977) *Proc. Natl. Acad. Sci. U.S.A.* **74**, pp4126-4129.

133. Zimmerman, S.S., Shipman, L.L. and Scheraga, H.A. (1977) *J. Phys. Chem.* **81**, pp614-622.